TOWARD RESOLVING THE HUMAN NEOCORTEX EPILEPTIC PROTEOME

by

Gal Keren-Aviram

A dissertation submitted in partial fulfillment
of the requirements for the degree

of

Doctor of Philosophy

in

Biochemistry

MONTANA STATE UNIVERSITY
Bozeman, Montana

November 2013

APPROVAL

of a dissertation submitted by

Gal Keren-Aviram

This dissertation has been read by each member of the dissertation committee and has been found to be satisfactory regarding content, English usage, format, citation, bibliographic style, and consistency and is ready for submission to The Graduate School.

Dr. Edward A. Dratz

Approved for the Department of Chemistry and Biochemistry

Dr. Mary J. Cloninger

Approved for The Graduate School

Dr. Ronald W. Larsen

STATEMENT OF PERMISSION TO USE

In presenting this dissertation in partial fulfillment of the requirements for a doctoral degree at Montana State University, I agree that the Library shall make it available to borrowers under rules of the Library. I further agree that copying of this dissertation is allowable only for scholarly purposes, consistent with "fair use" as prescribed in the U.S. Copyright Law. Requests for extensive copying or reproduction of this dissertation should be referred to ProQuest Information and Learning, 300 North Zeeb Road, Ann Arbor, Michigan 48106, to whom I have granted "the right to reproduce and distribute my dissertation in and from microform along with the non-exclusive right to reproduce and distribute my abstract in any format in whole or in part."

Gal Keren-Aviram

November 2013

ACKNOWLEDGEMENTS

I would like to thank my mentor, Dr. Edward Dratz, who first planted the idea of a biochemistry Ph.D in my mind and then gave me the opportunity to accomplish it under his guidance, for his unlimited patience and support and for allowing me the time and space to do it my way. I would like to thank Dr. Jeffrey Loeb, the head of the Systems Biology of Epilepsy Project, for the opportunity to be a part of this amazing project, for his great enthusiasm and encouragement along the way, his lab members, for a great collaboration and friendship and the project's patients who made it all possible. I would like to thank my committee members, Drs. Martin Teintze, Brian Bothner, Frances Lefcort and Mark Nelson for their encouragement and advice. I would like to thank the Dratz lab members, past and present, especially Britt, Scott and Duane for years of heated discussions, laughter and great friendship. I would like to thank my friends and family for their love and support. To Dr. Ilai Keren, my husband and private statistician, for his invaluable contribution to this work in both professional and personal domains and to our children Neta and Noy for just being wonderful.

TABLE OF CONTENTS

TABLE OF CONTENTS – CONTINUED

LIST OF TABLES

Table Page

LIST OF FIGURES

Figure Page

LIST OF FIGURES – CONTINUED

Figure Page

GLOSSARY OF ABBREVIATIONS

2D-DIGE – two dimensional differential in-gel electrophoresis

AED - anti-epileptic drugs

AJ - adherens junction

BBB - blood brain barrier

CNS – central nerve system

CRMP - collapsin response mediator protein

CSF - cerebrospinal fluid

DRE - drug resistant epilepsy

EAAT – excitatory amino acid transporter

EC – endothelial cell

ECM - extra cellular matrix

ECP - extra cellular proteins

EEG - electroencephalography

EZ – epileptogenic zone

FC - fold change

GABA – gamma aminobutyric acid

GFAP - glial fibrillary acidic protein

IED – interictal epileptiform discharge

ILAE - international league against epilepsy

LC-MS/MS - liquid-chromatograph tandem mass-spectrometry

LMW – lower molecular weight

GLOSSARY OF ABBREVIATIONS - CONTINUED

mGluR – metabotropic glutamate receptor

POI – protein of interest

PTE – posttraumatic epilepsy

PTM – post translational modification

RBC - red blood cell

SBEP – systems biology of epilepsy project

SOI - spot of interest

TBI – traumatic brain injury

TLE - temporal lobe epilepsy

ABSTRACT

Epilepsy is a common and often devastating neurological disorder, which is not well understood at the molecular level. Exactly why some brain regions produce epileptic discharges and others do not is not known. Patients who fail to respond to antiseizure medication can benefit from surgical removal of brain regions that produce epileptic activities. The tissue removed in these surgeries offers an invaluable resource to uncover the molecular and cellular basis of human epilepsy. Here, we report a proteomic study, as part of a Systems Biology of Epilepsy Project, which utilizes *in vivo* electrophysiologically-characterized human brain samples from the neocortex of 6 patients with refractory epilepsy, to determine whether there are common proteomic patterns in human brain regions that produce epileptic discharges. This study is unique in that comparison of protein expression was made within same patient, between nearby epileptic and non-epileptic (or less epileptic) brain regions, as defined by their interictal (between seizure) spike frequencies. Protein spots were resolved from three subcellular fractions, using two-dimensional differential-in-gel-electrophoresis, revealing 31 spots that changed significantly and were identified by liquid-chromatography tandem mass-spectrometry. Interestingly, glial fibrillary acidic protein was found to be consistently down regulated in high spiking brain tissue and glial fibrillary acidic protein levels showed strong negative correlation with spiking frequency. We next developed a two-step analysis method to select for frequently changing spots among the patients and identified 397 of those proteins. Spots of interest were clustered by protein expression patterns across all samples. This analysis predicted proteomic changes due to both histological differences and molecular pathways by examination of gene ontology clusters. Our experimental design and proteomic data analysis predicts novel glial and vascular changes and changes in cytoskeleton and neuronal projections that provide new insights into the structural and functional basis of neocortical epilepsy.

INTRODUCTION

Clinical Epilepsy

Epilepsy is a common neurological disorder that affects the life of millions of people in the United States and throughout the world. The following epidemiological and clinical overview is intended to describe the condition, current practice and limitations.

Definitions

Epileptogenesis is "the process by which a normal brain becomes epileptic" (McNamara et al 2006). An epileptic seizure is "a transient occurrence of signs and/or symptoms due to abnormal excessive or synchronous neuronal activity in the brain" (Fischer et al, 2005). Epilepsy is "a disorder of the brain characterized by an enduring predisposition to generate epileptic seizures and by the neurobiologic, cognitive, psychological, and social consequences of this condition. The definition of epilepsy requires the occurrence of at least one epileptic seizure" (Fisher et al, 2005). Note that this epilepsy definition replaced the commonly used phrase "recurrent seizures", which translated to the occurrence of at least two seizures (Bromfield 2006, WHO 2012), with "enduring predisposition" (knowledge of family history, injury or structural abnormality) and at least one epileptic seizure.

Epidemiology

The estimated epilepsy prevalence in the United States in 2012 is 2.2 million people, which is about 0.7% of the population, with 150,000 new patients diagnosed each

year. 1 in 26 people in the United States will develop epilepsy during their lifetime (Institute Of Medicine 2012). World-wide, epilepsy prevalence is higher, about 0.9%, due to higher prevalence in developing countries. Not only is the incidence rate and prevalence higher in developing countries, the vast majority of the patients in those countries do not receive the appropriate treatments (WHO 2005).

Etiology

In general terms, epilepsy develops as a result of brain insults. The insult is followed by a long latent period in which the epileptogenic process takes place, followed by the appearance of spontaneous seizures. Idiopathic epilepsy, where the cause is not known, is assumed to be influenced by complex genetic and environmental interactions. Different epilepsy etiologies are associated with the development of the disorder at different ages and geographical locations. Congenital and developmental conditions are associated with epilepsy incidence in infancy to adolescence. Degenerative and cerebrovascular diseases are associated with epilepsy incidence in late middle to old age. Brain tumors, infections and traumatic brain injuries are risk factors for epilepsy at all ages.

Compared with developing countries, developed countries demonstrate trends of reduced epilepsy incidence in the young age and increased incidence in the more elderly groups. These trends are presumed to be due to better perinatal care and infection control in the young and longevity-related increased prevalence of degenerative and cerebrovascular diseases. Several infections, mostly parasitic, which are endemic to developing countries or are related to a lack of resources, can substantially increase the

prevalence of active epilepsy in under developed countries (Sander 2003, Ngugi et al 2013).

Epilepsy Types

Epilepsy is not a single disease, but is a spectrum of neurological disorders. The classification and terminology of epilepsies have been debated and modified for several decades. The high heterogeneity of epilepsy disorders makes the task of classifying them very challenging. Advances in technology and progression of scientific knowledge contribute to the need for dynamic re-classification. The International League Against Epilepsy (ILAE, http://community.ilae-epilepsy.org) has recently published a revised report (Berg et al 2010). In this thesis, we nevertheless chose to present the old classification, since most of the literature is based on the old classification and terminology and the revised ILAE classifications are still highly debated (Lüders et al 2012, Panayiotopoulos 2012).

The long term debate on classification of epilepsy and the multiple revisions demonstrate the extreme complexity of the disorder, with multiple etiologies and clinical manifestations, which also leads to inherent limitations in studying the disease. Epilepsy classification has typically been made using two orthogonal categories or axes. The first category describes the two modes of seizure onset. In partial or focal epilepsy (also known as petit mal), the seizure originates from a single hemisphere, while in generalized epilepsy (grand mal) the seizure originates in both hemispheres. A focal seizure can sometimes spread to become a generalized seizure. The second category describes if the etiology of the disease is known or not and is also divided to two general groups,

idiopathic and symptomatic. Idiopathic (or primary) means that the cause is unknown and this group includes the genetically determined epilepsies. Symptomatic epilepsy describes the conditions that arose from a known brain insults. Cryptogenic epilepsy is also included in the symptomatic group and describes conditions where there is a underling cause suspected, but no clear known insult. Examples of common epilepsy types, classified by the two orthogonal categories, are shown in table 1.

Epilepsy types	Partial Epilepsies	Generalized Epilepsies
Idiopathic	• rolandic epilepsy • childhood epilepsy with occipital paroxysms (CEOP)	• **benign neonatal (± familial) convulsions** • **myoclonic epilepsy** • **absence epilepsy**
Symptomatic	• **frontal lobe epilepsies** • **occipital lobe epilepsies** • **parietal lobe epilepsies** • **temporal lobe epilepsies** • **Rasmussen's encephalitis**	• **West syndrome** • **Lennox-Gastaut syndrome**

Table 1. Classification of Epilepsies. Classification of epilepsies and epileptic syndromes by mode of onset and by known / unknown etiology. Adapted from Bromfield et al 2006.

Treatment

Once epilepsy is diagnosed the decision to treat is not always straightforward. An individualized evaluation of the treatment benefits against possible adverse effects needs to be made. In some epilepsies, with good prognosis (benign neonatal or absence epilepsy) or rare seizures, the choice not to treat is sometimes preferred (Schmidt 2009).

Anti-epileptic Drugs (AED). Most patients are treated with AED, which are actually anticonvulsants, aimed at preventing the recurrence of seizures. In contrast, anti-epileptogenic drugs are aimed at preventing the development of epilepsy, after a known

brain insult, or stopping its progression after the first seizure occurs (Temkin 2009, Loeb 2011, Mani et al 2011, Löscher et al 2013). There is a large and growing number of approved AEDs. The drug of choice needs to be individualized to each patient with consideration of seizure type, epilepsy etiology, efficacy, adverse effects, pharmacokinetic profile, interaction with other medications and cost. The details of this individualization process are beyond the scope of this introduction. Briefly, if seizure freedom is not reached with the first drug, it can be substituted by a different drug or in multidrug 'add-on therapy', additional drugs with different mechanisms of action might be prescribed (Bromfield 2006, Schmidt 2009). The likelihood of seizure freedom was found to decline with successive drug regimens (Brodie 2013). Despite all the new AED that have been developed, seizures are often not controlled by AED and refractory or drug-resistant epilepsy is found in more than 30% of the patients (Schmidt 2009). According to the ILAE commission on therapeutic strategies (Kwan et al 2010) "drug resistant epilepsy may be defined as failure of adequate trials of two tolerated and appropriately chosen and used AED schedules (whether as monotherapies or in combination) to achieve sustained seizure freedom". In cases of drug resistant epilepsy (DRE) a surgical option needs to be considered.

Epilepsy Surgery. This treatment category commonly addresses resection surgery, although several non-resective surgical interventions are also used and will be briefly described later in this section. Generally, the indication for epilepsy surgery is DRE, with frequent disabling seizures.

Resection of the epileptogenic region, ranging from a portion of a lobe to a whole hemisphere, can be highly effective and potentially curative for focal epilepsies. The probability for post operation seizure freedom increases in lesional (involving a structural abnormality) epilepsy. These resection surgeries are most common for temporal lobe epilepsy (TLE). Extratemporal resection surgery has lower curative rate than temporal surgery, but may still be effective in reducing seizure symptoms (Téllez-Zenteno et al 2010). The criteria for resection surgery, besides DRE and significantly reduced life quality, also include the feasibility of removing the epileptic foci without resecting essential cortex. Therefore, surgery candidates go through an array of preoperative evaluations and risk assessments.

Several neuroimaging techniques help identify regions of malformation or lesions (MRI) or malfunctioning metabolism (fMRI /PET/SPECT). An important tool for identifying the epileptogenic region is the electroencephalograph (EEG) evaluation. Patients undergo long-term video-EEG monitoring to record several epileptiform (interictal - between seizures) and ictal discharges, to locate the region of seizure onset, as well as adjacent regions of abnormal interictal activity. When localization is not sufficient using scalp electrodes, the more sensitive subdural electrode grid can be positioned directly on the cortex surface, as phase one of the two phase surgical procedure. The resection of interictal epileptiforn regions is associated with improved surgical outcome. The combined findings from EEG evaluation and neuroimaging are used to define the epileptic foci and surrounding tissue to be removed in order not to

create new significant neurological deficit, as the result of the surgery (Bromfield 2006, Morace et al 2012, Noachtar & Borggraefe 2009 Wu et al 2010)

Non-resective surgical interventions, that do not involve tissue removal, are mostly palliative in nature, include corpus callosotomy which inhibits seizure spreading, multiple subpial transections and neurostimulation, which have been receiving growing attention. The basic idea of using neurostimulation to affect the EEG had been known for more than 70 years and with the technological improvement has recently developed into a practical option for treating epilepsy. Currently, vagus nerve stimulation (VNS) is the only FDA approved approach in this class of treatment, and the other methods to be described are in clinical trials. In general, neurostimulation can be done a) surgically through cranial nerves such as the vagus or non-surgically through trigeminal nerve stimulation (TNS) or by b) surgically through central nervous system stimulation such as deep brain stimulation (DBS) or the non-surgical transcranial magnetic stimulation. The mechanism of action of these neurostimulation approaches is not well understood, but is thought to work through modulation of neural network excitability. Neurostimulation can benefit patients with DRE who are not good candidates for resection surgery or can be used as adjunct therapy with AED. Neurostimulation is relatively safe, reversible and allows for fine tuning, although the overall efficacy is still lower then resection surgery (Lockman and Fisher 2009, Wu and Sharan 2012, Healy et al 2013).

Lifestyle Modifications. Several non-surgical, non-pharmaceutical techniques are known to help control seizures. a) Avoiding precipitating factors such as alcohol and stimulants, irregular sleeping patterns and flickering light stimulation. b) Practicing stress

reduction and relaxation techniques (Wolf 2002, Bromfield 2006, Díaz-Negrillo 2013).

c) Changing the regular diet to a ketogenic diet (KD) of restricted carbohydrates and increased fat, which increases the production of ketone bodies. The high efficacy of ketogenic diet had been established for almost a century, especially with children, however KD is very restrictive which leads to low tolerability. The KD has mostly minor adverse effects but there can be rare serious complications. Several less restrictive diet approaches, based on the same fundamental limitations has been tried with good success. The mechanism in which these diets affect seizures is not fully understood, although experimental evidence for several distinct mechanisms have been recently described (Duchowny 2005, Masino & Rho 2012, Danial 2013).

Summary of Clinical Epilepsy

Epilepsy is a relatively common and devastating neurological disease. It is treatable in most cases, though the adverse effects of treatment; whether pharmacological, surgical or behavioral, are many times still substantial enough to reduce the patient's quality of life and chances of prosperity. Excluding the option of resection surgery, the most common treatments are aimed at eliminating the symptoms by controlling seizures, rather than curing epilepsy. The surgical treatment can be curative with no need for AED or greatly reduced AEDs. The complexity of the disease, which is a derivative of the heterogeneity of the etiologies and clinical manifestations, and the multifactorial basis of epilepsy, combined with the natural limitations of studying the human brain; results in gaps in scientific knowledge and leads to suboptimal treatment. Better understanding of epileptogenesis, why do some brain regions change and what is

the difference between the epileptogenic and a healthy tissue, may allow the design of curative treatments or better medications. Improved medications, with higher efficacy and less adverse effects are needed for all epilepsy patients and specifically for those with DRE. Future more optimal pharmacological treatments may be able to prevent epilepsy in those with high risk of developing the disease or stop its progression once it is present.

Electrophysiology

Abnormal electrophysiology is the common clinical pathology of epilepsy. While in many patients the epileptogenic zone (EZ) is lesional, with MRI presenting some type of malformation or tumor, in other patients physical malformation cannot be detected and the localization of the epileptogenic foci is based entirely on EEG recording (Noachtar & Borggraefe 2009). The following overview will present the cellular basis for normal electrophysiology and pathophysiology in epilepsy.

Normal Neurophysiology

The normal neuronal network is composed of specialized cells which process and transfer electrical and chemical information. The intracellular signaling is by propagation of electrical action potentials along the neuronal axons. Intercellular signaling, or neurotransmission, can propagate in a dendrite-dendrite electrical synapse, or by neurotransmitters in the axon terminal - dendrite chemical synapse. Neurotransmission can have an excitatory or inhibitory nature, as a function of the participating neurons (Stufflebeam 2008). The neocortex contains 6 layers, the principal pyramidal neurons, which project information to distant areas, form excitatory synapses on the post synaptic

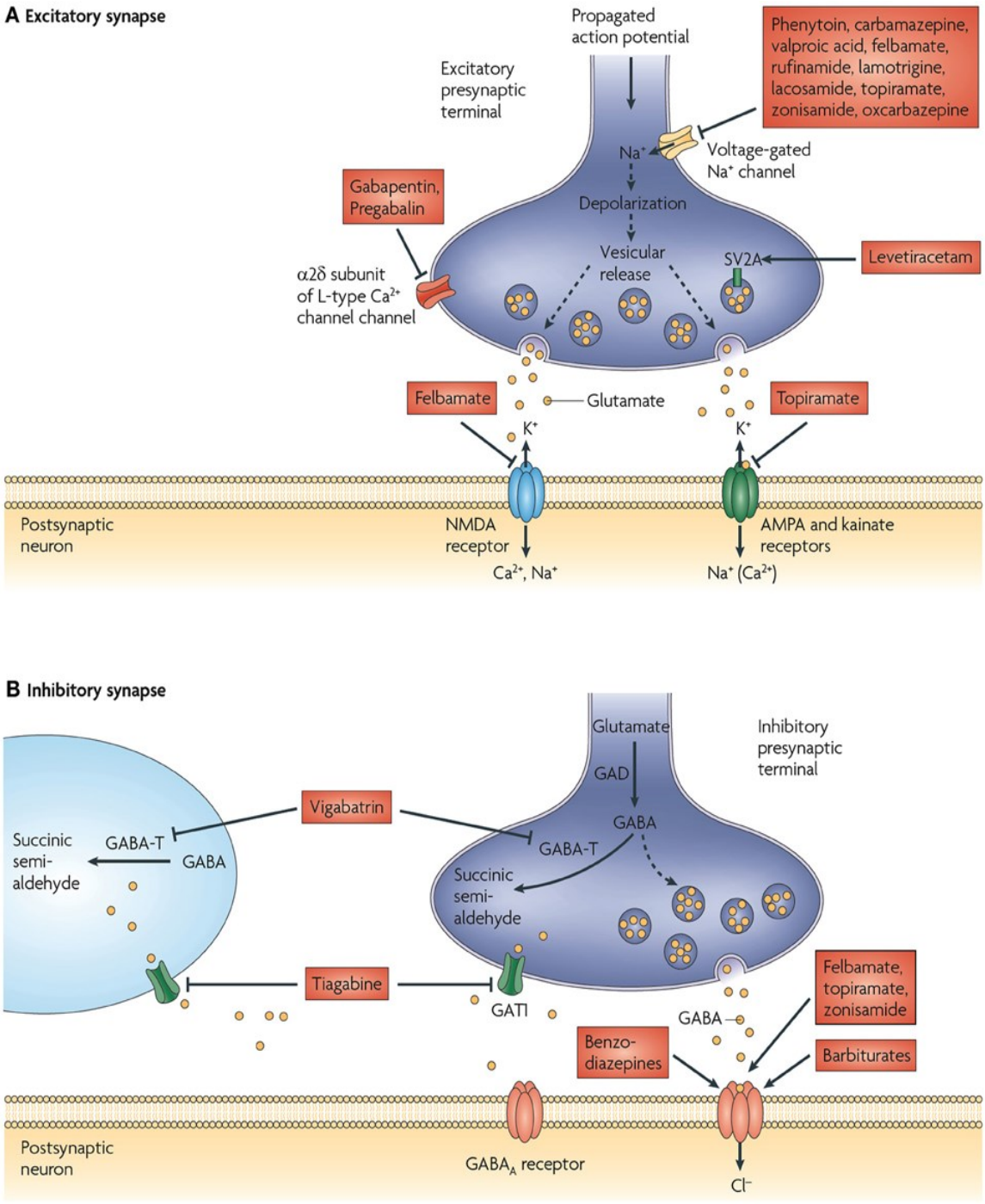

Figure 1. Proposed Mechanisms of Action of Currently Available AEDs at Excitatory and Inhibitory Synapses. Used with permission from Bialer & White (2010) *Nature Reviews Drug Discovery*. Jan;9(1):68-82.

neurons, while the more localized interneurons, mostly form inhibitory synapses. The players or components governing the normal neurophysiology are of interest in order to understand pathophysiology and as treatment intervention targets (Figure 1). At the intracellular level, localized changes in the transmembrane potential activate voltage gated ion channels and sodium-potassium pumps. When the propagated signal reaches an axon terminal, it triggers a calcium influx, which causes the exocytosis of the presynaptic vesicles, containing neurotransmitters, into the synaptic cleft.

Glutamate is the primary excitatory neurotransmitter at 80% of the human brain synapses and its two main classes of glutamate receptors are ionotropic and metabotropic. The three glutamate ionotropic receptors are, α-amino-2,3-dihydro-5-methyl-3-oxo-4-isoxazolepropanoic acid (AMPA), N-methyl-D-aspartate (NMDA) and the kainate receptor (Figure 1A). All three act as post synaptic ion channels. When activated by glutamate the receptors depolarize the membrane, by allowing influx of sodium and calcium ions into the postsynaptic neuron, with an outflow of potassium ions. This change in membrane conduction process is very fast and when excessive can lead to excitotoxicity (Bromfield 2006). Excess glutamate excitation leads to excessive calcium accumulation in the cell cytoplasm, which can trigger toxicity or even cell death. There are eight subtypes of glutamate metabotropic receptors (mGluRs). These are all G protein-coupled receptors (GPCRs), which upon glutamate activation start a cascade of signal transduction in the target cells. The mGluRs subtypes are grouped by their signaling nature, synaptic location (pre or postsynaptic) and potential agonists. The three groups are illustrated in Figure 2, with group I (1 or 5) (blue) considered to be excitatory

and groups II and III (2, 3, 4, 7 or 8) (black) being mostly inhibitory receptors (Benarroch 2008).

Gamma-amino-butyric-acid (GABA) is the major inhibitory neurotransmitter. It also interacts with two types of receptors. The postsynaptic ionotropic $GABA_A$ receptor, becomes permeable to chloride upon interaction with GABA, resulting in membrane hyperpolarization and inhibition of action potentials (Figure 1B). The metabotropic $GABA_B$ receptor, can be located pre- post- or extrasynaptically. Upon activation, presynaptic GPCRs can inhibit calcium channels to in turn inhibit the release of GABA or glutamate. Postsynaptic $GABA_B$ receptors can induce long-lasting hyperpolarization (inhibiting action potentials) by activation of inwardly rectifying potassium channels (Han et al 2012).

In addition to ionotropic and metabotropic receptors, both glutamate and GABA have specific transporters that effect the neurotransmitter concentration in the synaptic cleft by re-uptake into the neuron or astrocytes. Many more proteins and small molecules that effect neuronal excitability at the single neuron level, intrinsically or from its close environment, are present, but are not mentioned here. The next level governing the excitatory function is the network organization. The type of neurons interacting, their numbers and the nature of the circuit connectivity (feedback or feed-forward inhibitions), allow for the neuronal massages to be transmitted or stopped, as part of the normal neuronal function (Bromfield et al 2006, Stufflebeam 2008).

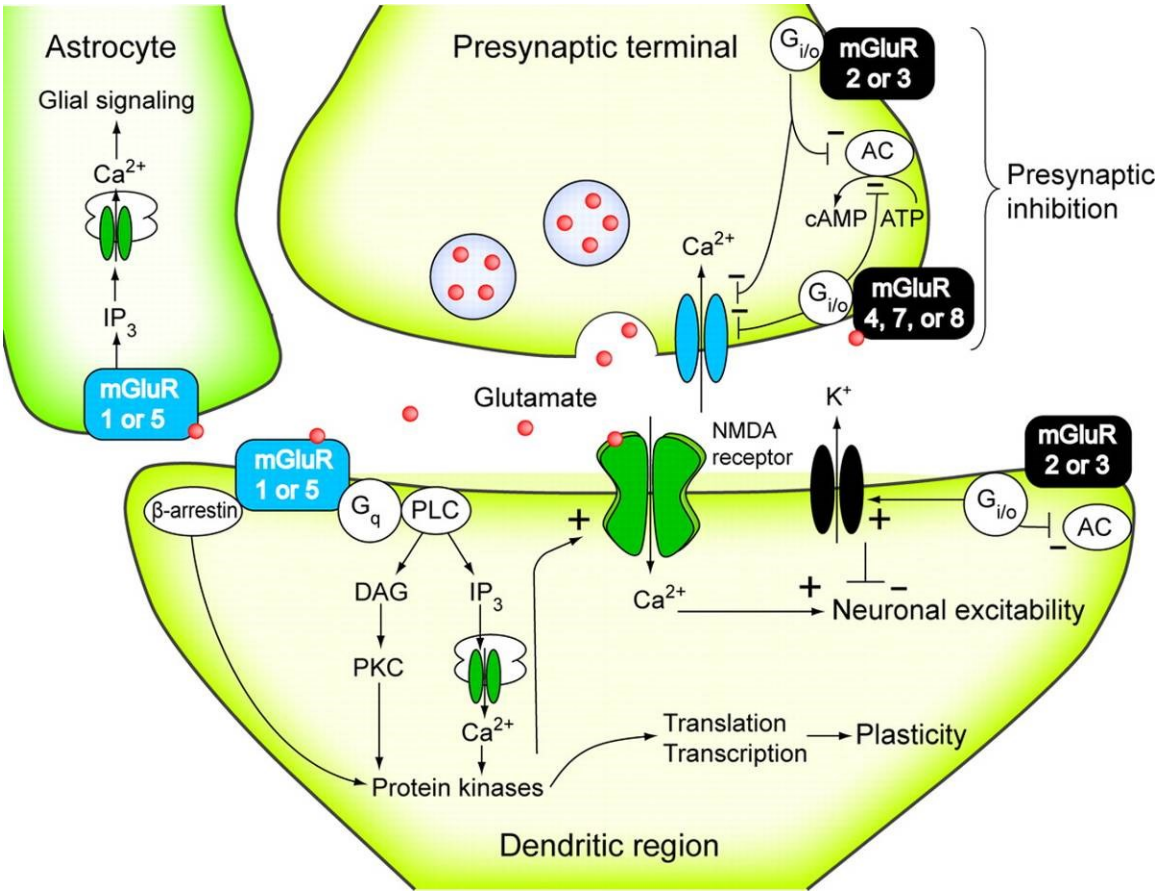

Figure 2. Distribution and Synaptic Modulatory Function of Metabotropic Glutamate Receptors (mGluRs) in Excitatory Synapses. The different numerical designations are described in the text. Used with permission from Benarroch E. (2008) *Neurology* 70 (12):964-968

Pathophysiology in Epilepsy

The complexity of the normal neurophysiology, which arises from the multiple components and effectors in single neurons, as well as the neuronal and astrocyte networks, is well established. The neuronal pathophysiology exemplified in epilepsy, defined as "abnormal excessive or synchronous electrical activity", can potentially occur due to several types of modulation, which result in a downstream effect of unbalanced higher excitatory or lower inhibitory neuronal function. The output at the neuronal level

is increased by inward flow of sodium or calcium ions or by decreases in the outward flow of potassium or inward chloride ions. At the neurotransmitter level, too much glutamate or aspartate or too little GABA, can induce seizures.

Such excessive changes in local concentrations of ions and neurotransmitters can result from intrinsic or extrinsic modulation processes. Changes to the local neuronal environment can be due to modulations of the proteins or metabolites in the extra cellular space (ECS), neighboring cells or due to astrocytic dysfunction. Network modulation can affect any of the components governing excitatory functions in the neuron and synapse levels. The modulation can affect channels, transporters or receptors at the gene transcription level, their numbers and cellular distribution, posttranslational modifications (PTMs), and their activation by secondary messengers and co-factors.

Increased excitability can also derive from changes in the neuronal networks. Axonal sprouting of excitatory pyramidal neurons, neuronal loss of inhibitory interneurons, or loss of interneuron inhibition, due to loss of its activating excitatory neuron, have all been suggested as ictogenic or epileptogenic network changes (Bromfield et al 2006).

EEG and Interictal Epileptiform Discharge (IED)

EEG studies have a central role in diagnosis and management of epilepsy. EEG provides a graphical display of the cortical electrical activity, is relatively inexpensive, and convenient. Clinically, rather than recording seizures, which are usually not frequent events, EEG is mostly used to detect interictal (between clinical attacks) epileptiform discharges, which are pathological activity patterns developed by epilepsy

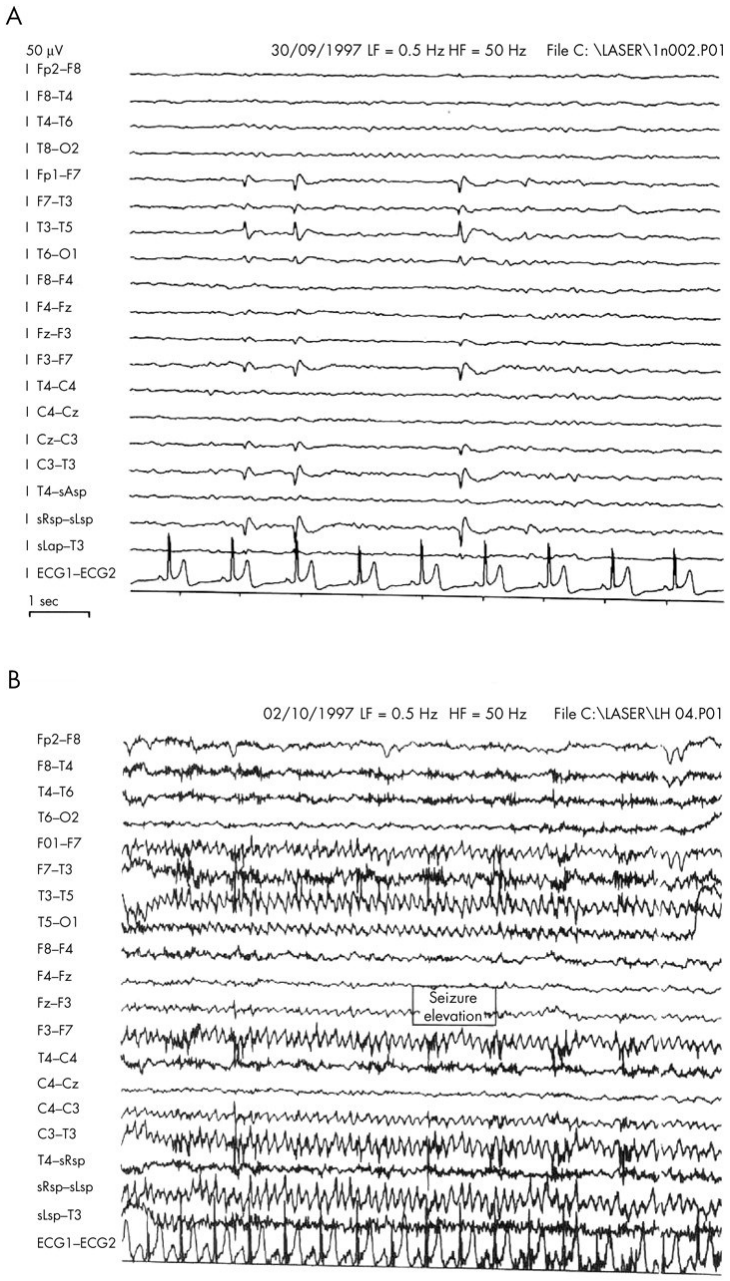

Figure 3. Correlation of Ictal and Interictal Discharges A) Interictal focal temporal discharges in left mesial TLE. B) Ictal rhythmic θ discharges of the same electrode. Used with permission from Smith SJM (2005) *Journal of Neurology Neurosurgery and Psychiatry* 76(2):2-7

patients. IED are distinctive sharp waves, spikes or complexes of electrical transients, which are distinguishable from the normal background activity registered by EEG. These

IED events are much more frequent than clinical seizures, about 50% of patients will display IED in a first recording and about 80% of epilepsy patients will present IED, if the study includes long term recording of wake and sleep patterns.

Typical IED and seizure patterns found in focal temporal lobe epilepsy are presented in Figure 3 A & B, respectively. Note the electrode T3 with most pronounced IED and seizure patterns indicates the epileptic foci. EEG is an important tool for making a differential diagnosis of epilepsy from other possible seizure causes; differentiating focal and generalized epilepsy, risk assessments for seizure recurring and localization of some epilepsy foci. Localization using scalp electrodes is limited due to incomplete spatial sampling, low sensitivity for cortical potentials and temporal propagation of electrical activity away from the foci. These limitations can be largely overcome by using long term subdural recording (Smith 2005, Bromfield et al 2006, de Curtis et al 2012).

Epilepsy Study Models

Multiple study models have been designed and tested during many decades of epilepsy research, in attempts to experimentally recreate the epileptogenic nature or epileptogenic process in systems ranging from cultured cells and rodents to primates. Naturally, the aims of the different studies affected the choice of experimental systems, whether the studies were designed to test the efficacy of new anticonvulsants or anti-epileptogenesis drugs in models demonstrating spontaneous seizures or high susceptibility to generating seizures. Variety in the study models arises from the need to experimentally mimic specific types of epilepsy, from the multiple etiologies (idiopathic

and symptomatic) and the multiple manifestations (generalized or focal, temporal or extra-temporal, with or without sclerosis, etc.). In other words, the complexity of the study models derives from the complexity of epilepsy types and classification, as discussed earlier. This overview will focus on the three major classes of animal models (Löscher 2011, White 2012, McNamara et al 2006).

Status Epilepticus (SE) Models

Status epilepticus (SE) is an unremitting seizure which is a medical emergency that requires medical intervention in humans in order to be stopped. A number of central nervous system (CNS) insults are associated with SE, such as stroke, drugs or alcohol abuse or withdrawal, sleep deprivation or a metabolic disturbance from a liver, kidney or gastrointestinal source. Post SE, patients are at elevated risk of developing epilepsy.

Models of post SE are typically using rats and inducing status epilepticus by applying electrical stimulation or chemical convulsants, such as the glutamate analog kainite or the cholinergic agonist pilocarpine, to a specific location (hippocampus) or broader areas in the brain. The resulted seizures are interrupted by researchers to prevent mortality after sufficient time had passed to ensure the development of spontaneous seizures, which will be delayed by a latent period of several weeks (Löscher 2002, White 2012).

Kindling Models

The term kindling commonly describes material that is easily ignited and is used in starting a fire. In rodent epilepsy models, kindling refers to a phenomenon where

repetitive seizure-inducing electrical or chemical (application of or withdrawal from) stimulation results in increasing seizures (easily igniting a bigger fire), both in duration and magnitude of response. The hypothesis underlying the progression of kindling is that each of the induced seizures recruits more neuronal circuits to the effected network. Although repetitive induced seizures are thought to lower the seizure threshold, spontaneous seizures are not typically achieved in kindling models and a trigger stimulus is still necessary (Bertram 2007, White 2012).

Post-traumatic Epilepsy (PTE) Models

Traumatic brain injury (TBI) holds the highest risk factor for epilepsy, and PTE accounts for a fifth of all symptomatic epilepsies. Consequently, experimental PTE has become a widely used tool for studying epileptogenesis. Different PTE models have been developed, seeking to more closely imitate the heterogenic nature of a variety of TBIs. Examples of several such PTE models, mostly with rodents, are described below (Pitkänen & McIntosh 2006, White 2012).

Cortical Injection of Ferrous Chloride. Injection of ferrous chloride solution into the rat cortex is thought to imitate TBI-related hemorrhages which breach the blood brain barrier, with hemoglobin extravasation and iron-mediated reactions, leading to generation of reactive oxygen species (ROS).

Cortical Undercut. This model imitates penetrating injury. A cut is executed through the cortex and into the underlying white matter, attempting to minimize damage to the dura and blood supply to differentiate it from the previous model.

Lateral Fluid Percussion Injury (FPI). Imitating closed head injuries with edema and increased intracranial pressure, by application of intracranial fluids with intact dura. This technique commonly generates mixed focal and diffused injury.

Summary of Epilepsy Animal Models

Many more animal epileptic models have been described in addition to those above. These include models that specifically address a certain etiology or manifestation, such as genetic idiopathic models, tetanus model for partial epilepsy, models that mimic febrile seizures or hypoxic-ischemic seizures.

The large number of animal models, which were specifically designed for AED discovery in the epilepsy spectrum, have been successful in terms of finding and developing numerous new drugs, over the last two decades, that suppress seizures by diverse mechanisms and expanding the therapeutic options. Nevertheless, it should be recognized that the percentage of patients with DRE has *not* decreased and not much was achieved so far in the category of anti-epileptogenic and disease modifying drugs, despite all the animal model work and drug development activities.

Many of the animal models described may be used in studying epileptogenic mechanisms, both before the appearance of spontaneous seizures and the progression of the disease after seizures appear. Indeed, many cellular changes have been found in these prior animal studies, which lead to several hypotheses for the epileptogenic process. The lack of an effective anti-epileptogenic drug, however, raises concerns and questions regarding the validity of the animal models that have been used in the search for human epilepsy cures (White 2012, Löscher 2011)

Systems Biology of Epilepsy Project (SBEP)

The need to understand cellular mechanisms of epileptogenesis, in order to find new drugs that will allow stopping the epileptic progression and even cure the disease, was previously discussed. During focal seizures abnormal electrophysiology spreads to neighboring areas or becomes generalized. Between seizures the epileptogenic brain regions still display abnormal electrophysiology. Thus, instead of targeting downstream cellular components which are assumed to be directly involved in the electrophysiology and seizures, the SBEP focuses on identifying the differences between brain areas with abnormal and normal interictal electrophysiology. A comprehensive epilepsy surgery program, in which epileptogenic areas of drug resistant epilepsy patients are localized and then removed, in addition to bringing most of the patients relief or cure from the disease, also provides electrically-characterized human brain samples to the SBEP. With considerations to not generate new neurological lesions, the surgical team typically resects, besides the electrophysiologically abnormal tissue, some nearby normal tissue, and therefore provides crucial control brain tissue from the same patient. The availability of this control tissue overcomes major study limitations in prior studies that derive inherently from using non-epileptic brain from a different person as a control sample.

In order to discover the molecular basis of epileptogenesis, the SBEP takes a broad approach to analyze these tissues by applying three nontargeted omics techniques to screen for epileptogenic changes at several molecular levels (Figure 4).

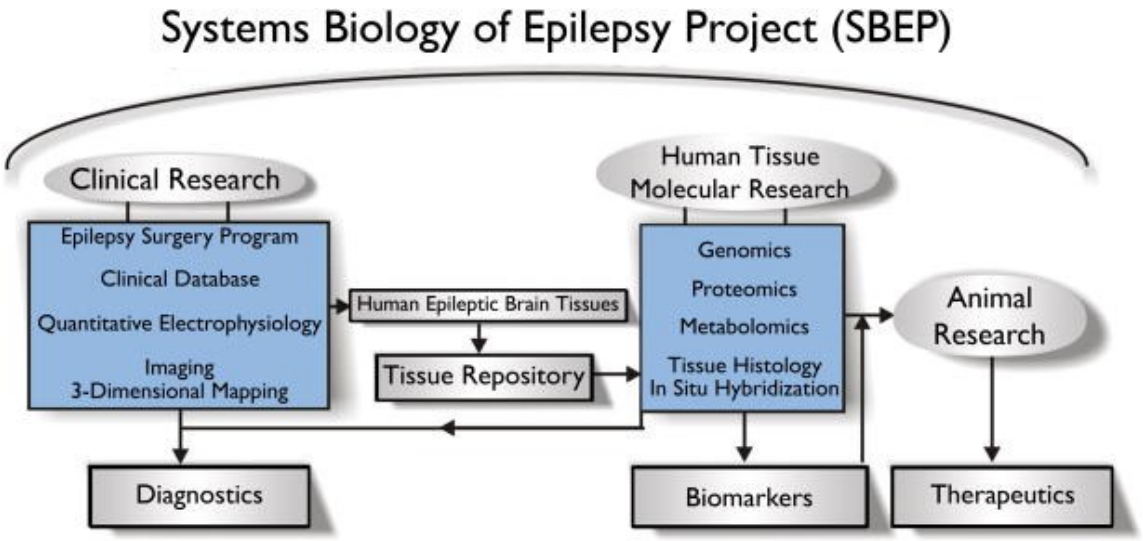

Figure 4. Overview of the Systems Biology of Epilepsy Project. Used with permission from Loeb JA (2010) *Epilepsia.* 51(3):171-7.

The integration of the findings from different omics studies with the clinical and histological findings is expected to generate new knowledge and increasingly detailed insight. In the next phase of the SBEP, new, knowledge-based epileptogenic hypotheses, candidate biomarkers or better drug targets can be tested in animal models (Loeb 2010, Loeb 2011).

Theories of Epileptogenesis

Considerations of the place of "epileptogenesis" in the chronology of epileptic disorders are important when assigning molecular and cellular events as potential intervention targets. A common view of epilepsy regards it as a progressive disorder, as illustrated in figure 5 (reviewed by Pitkänen & Sutula 2002, Pitkänen & McIntosh 2006, Pitkänen & Lukasiuk 2011, Engel et al 2013). Epileptogenesisis is the process of

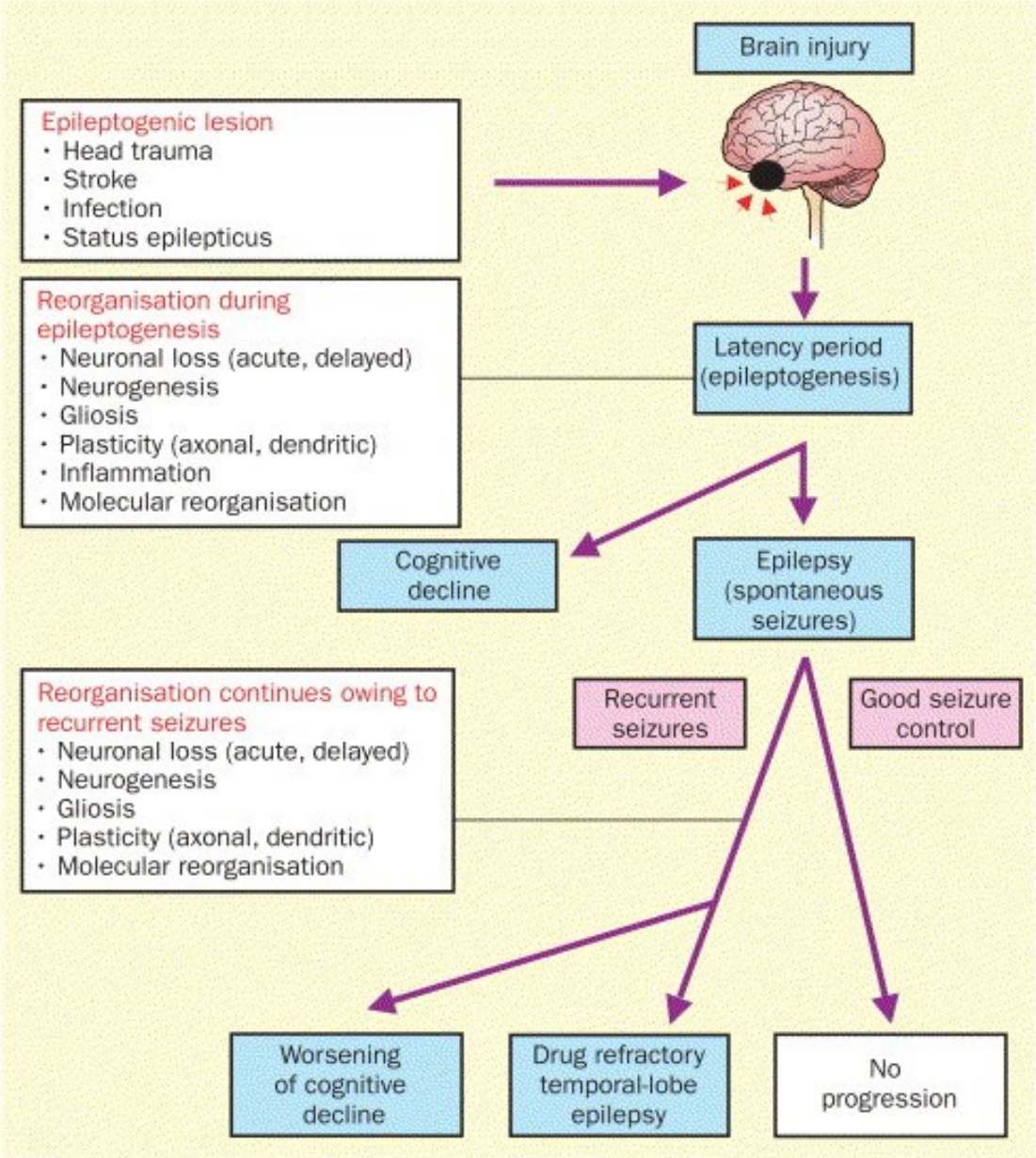

Figure 5. Epileptogenic Process in Symptomatic Temporal Lobe Epilepsy. Used with permission from Pitkänen & Sutula (2002) *Neurology* 1, 173-181.

neuronal tissue becoming abnormal, taking place both in the latent period before seizures appear and after seizures appear due to suboptimal seizure control, or possibly because of the AED itself. Phases of epileptogenesis, with activation of different molecular events,

have also been demonstrated by different models, within a latent period after insult (Figure 6). Although there is an overlap between molecular events that are taking place in the phases of epileptogenesis, it is not clear that the same pathways are involved in their generation in all phases. Note that many of the events, which are evident from multiple studies using different epileptic models, describe what seem to be opposite processes. Examples are neuronal death and neurogenesis, glial cell death and gliogenesis, vascular damage and angiogenesis (Pitkänen & McIntosh 2006). Due to the multiple models utilized in different studies, time points for all these events are unclear and the models are of questionable application for the progression or validity of these events in humans, it is no wonder a comprehensive epileptogenesis map, indicating the right target in the right time for intervention has not yet been established.

Another important consideration, when studying epileptogenesis, is the brain maturity of the target population. The developing brain, from infancy to adolescence, presents a different background of activated pathways and immature neuronal network systems, which gives it a naturally increased excitatory and decreased inhibitory nature. This is also probably the reason for the high occurrence of several epilepsies in childhood and commonly occurring resolution as the child "grows out" of the disease in several years (Rakhade and Jensen 2009). The scientific community is focusing increasing attention on the understanding of epileptogenesis in order to develop truly antiepileptogenic drugs, which is leading to new study designs with higher chronological resolution of the molecular events. Some of the antiepileptogenic treatments using animal

models have demonstrated efficacy as disease modifying drugs (reviewed by Pitkänen & Lukasiuk 2011).

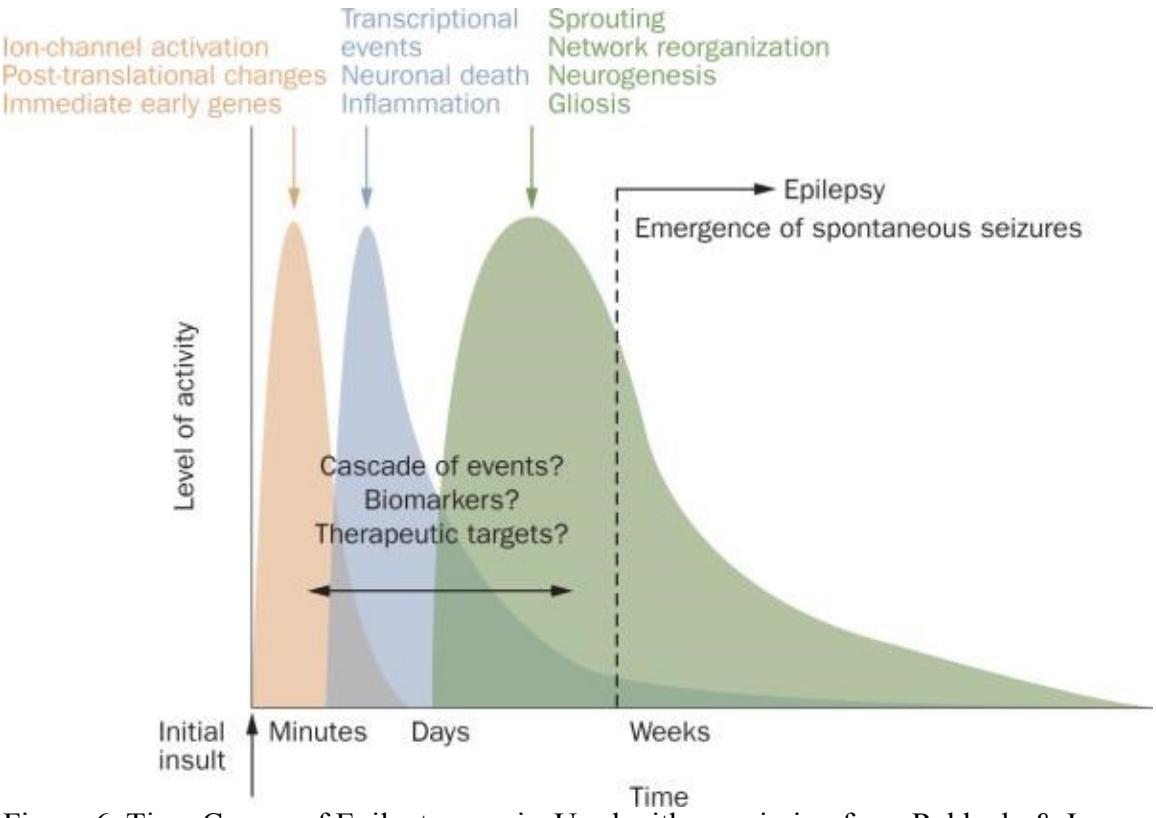

Figure 6. Time Course of Epileptogenesis. Used with permission from Rakhade & Jensen (2009) *Nature Reviews Neurology* **5**, 380-391

Several of the and most studied hypotheses of epileptogenesis revolve around a dysfunctional blood-brain barrier (BBB), dysfunctional astrocytes, increased angiogenesis and their interactions, as illustrated in Figure 7 (reviewed by Oby and Janigro 2006, Weissberg et al 2011, Liu et al 2012, Kovács et al 2012, Marchi et al 2012, Aronica et al 2012, Heinemann et al 2012, Seifert & Steinhäuser 2013, Morin-Brureau 2011). Interestingly, these hypotheses shift the perception from neurons being the primary epileptogenic "immediate suspects" to malfunctions of downstream players that

are at the root cause of generating seizures. Astrocytes are no longer looked at as mostly structural support or "glue" in the brain but as critical components in neurological regulation, as described below.

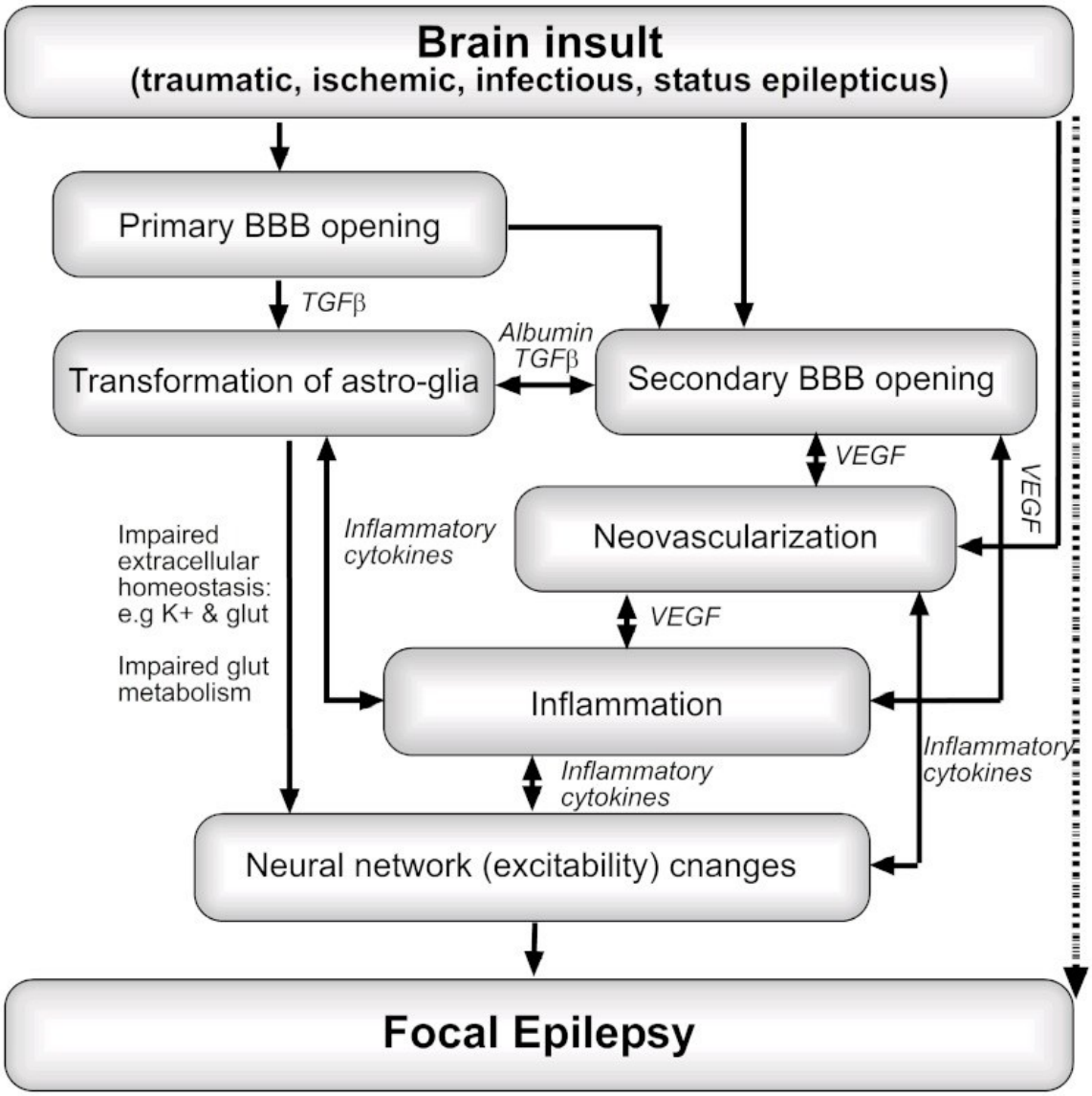

Figure 7. The Role of Blood-Brain Barrier Dysfunction in Epileptogenesis. Used with permission from Friedman & Heinemann (2012), In: Noebels et al, Jasper basic mechanisms of the epilepsies.

Astrocytes in Epilepsy

Astrocytes serve a set of complex functions in the normal brain. The astrocytic process is involved with pre and post synaptic neurons in the so-called tripartite synapse, governing neurotransmission. The astrocytic foot is a structural component of the BBB and astrocytes control vasomodulation. Astrocytes have major role in structural and metabolic support for neurons in the brain. They are involved in normal immune response and regulation of extracellular ionic concentration. Therefore, astrocytic dysfunction might be expected to affect epilepsy and epileptogenesis.

Astrocytes are presumed to maintain the extracellular potassium [K^+] regulation environment through their inwardly rectifying potassium (Kir) channels, gap junctions and AQP4 water channels. Impaired ion regulation due to impaired function or expression of these components, in cases of hippocampal sclerosis or activation of transforming growth factor beta (TGFβ), can result in hyperexcitability (Seifert et al 2010, Steinhäuser & Seifert 2012).

Astrocytes are notably the main regulators of the extracellular excitatory neurotransmitter glutamate. Excess synaptic glutamate is removed by the astrocytic excitatory amino acid transporters 1 and 2 (EAAT1 & 2). The glutamate removed is then inactivated / buffered by the astrocytic glutamine synthetase (GS). Several studies found these proteins to be down-regulated in epilepsy (Seifert et al 2010, Steinhäuser & Seifert 2012).

The glia-derived excitatory pathway, in which simultaneous excitation of neighboring neurons is triggered by astrocytic Ca^{2+} -induced glutamate release, favors

neuronal synchronization. Epilepsy related increases in astrocytic Ca^{2+} levels can therefore trigger seizures in the predisposed neighboring neurons (Seifert et al 2010).

Astrocytes also are involved in the CNS immune responses, being the source and target of many inflammatory molecules. Several studies have indicated that astrocyte-mediated inflammation is an epileptogenic mechanism (reviews Aronica et al 2012, Vezzani et al 2013).

In summary, an increasing body of evidence points at astrocytic function as a crucial component of normal electrophysiology. Dysfunction of any of the astrocytic roles, described above, or an upstream trigger for this dysfunction, should be studied further as possible targets for antiepileptogenic treatments.

PROTEOMIC ANALYSIS OF HUMAN EPILEPTIC NEOCORTEX PREDICTS VASCULAR AND GLIAL CHANGES IN REGIONS OF EPILEPTIC SPIKING

Introduction

Epilepsy is a neurological disorder that affects about 1% of the population worldwide. It is often called a spectrum disorder because of the large number of associated etiologies or 'brain insults'. Similarly, the symptomatic seizures can be clinically quite different depending on where they arise. While seizures can be treated symptomatically with anti-epileptic drugs (AEDs), about 30% of the patients have seizures that are refractory to medications and many of these can benefit from a surgical procedure that removes electrically defined brain regions, while preserving normal regions (Kwan & Brodie 2000, Yun et al 2006). These surgical procedures offer an opportunity to use proteomic and other high-throughput approaches on resected human brain tissues to probe the molecular basis of human epilepsy (Loeb 2010).

The heterogeneity in resected tissues generated from these surgeries has made it hard to study the pathogenesis of epilepsy, in part due to an absence of proper control samples. Previous studies have used specimens from non-epileptic, age and gender matched individuals as control samples (Yang et al 2005, Eun et al 2009), but this is far from optimal since natural biological variation could well mask epilepsy-specific changes. We have developed a Systems Biology of Epilepsy Project as a new approach to study human epilepsy. Rather than studying histologically pathological tissues, the System Biology of Epilepsy Project focuses on human neocortical tissues as a function of

the in vivo recorded electrical activities indicated by high spiking frequency between seizures (interictal). Comparisons are made internally within each patient between high- and low-spiking (or non-spiking) nearby tissue (Loeb 2011). In fact, high spike frequency in certain brain areas has been found to predict the ictal-onset locations, and resection of the interictal high spike tissue has been associated with good surgical outcomes (Asano et al 2003).

Patient #	Patient	Gender	Age	Spike frequency of sample		Patient histopathology
				High	Low	
1	ep122	F	15	6	0	Normal
2	ep132	F	10	116	1	Diffuse gliosis, inflammation
3	ep150	M	33	371	115	Normal
4	ep158	M	1	85	0	Gliosis
5	ep159	M	27	27	2	Mild gliosis
6	ep165	F	3	212	56	Mild gliosis

Table 2: Patient Clinical Information and Tissue Samples Used for this Study.
Note that the histopathology of each patient was determined on different tissue segment from each patient than those used for proteomic studies. The gliosis was most commonly subcortically in the white matter.

Using this experimental approach, we have previously found highly consistent changes in gene transcription between regions that produce seizures (Rakhade et al 2005, Beaumont et al 2012) and high levels of interictal spiking (Lipovich et al 2012), compared to nearby 'control' regions with little to no epileptic activities. Here, we have taken a proteomic

approach, using differential 2-dimensional gels (2D-DIGE), to study 6 pairs of high and low spiking human neocortical tissues to determine if there are common proteomic changes as function of abnormal epileptic activity across these patients. All of the tissues investigated here were also used to show common transcriptional changes (Lipovich et al 2012; Dachet et al 2013, under review). Our results show consistent changes in proteins that predict decreased glial cells and increased vascularity, as well as a hierarchy of ontological changes that could underlie the development of epilepsy.

Materials and Methods

Human Tissue Collection and Processing

Human neocortex samples were acquired from six patients with refractory epilepsy, following informed consent and institutional review board approval. Only tissue regions that were studied in vivo, using long-term subdural grid electrical recordings were used and were removed as part of the patients medical treatment in a two-stage surgical procedure at the Comprehensive Epilepsy Center at Wayne State University School of Medicine, as described earlier (Rakhade et al 2005, Beaumont et al 2012, Lipovich et al 2012). Briefly, recordings taken over several days were quantified for their intrinsic interictal spiking frequency. Regions showing high spike frequency were compared to nearby 'control' regions, defined as regions showing no or the least amount of epileptic activity. After excision, the brain samples were further dissected, as described by Loeb (2010) and Lipovich et al (2012) to provide adequate samples for a range of analyses within the Systems Biology of Epilepsy Project and to allow the future

integration of the data. Samples underwent subcellular fractionation to produce fractions, P1 – nuclear, P2 – membrane, and Supernatant – cytosol, as previously described by Beaumont et al (2012). The Bradford protein assay was used for protein quantification (Bradford 1976). The fractionated samples were frozen and sent to Montana State University on dry ice for proteomic analysis.

Protein Labeling and 2D-DIGE

Frozen samples were lyophilized at Montana State University and suspended in denaturing buffer (7M urea, 2M thiourea, 3% (w/v) CHAPS, 1% (w/v) amidosulfobetaine-14, 10mM Tris-HCl pH 8.4) to bring the protein concentration to 5mg/mL. Samples were reduced with 5mM tributylphosphine for 1 hr, followed by alkylation with 10mM 4-vinylpyridine for 2 hrs, all at 4ºC. The fluorescent dye labeling procedure was done as recommended by GE Healthcare with a few modifications. Briefly, all dyes, Cy2 (GE), Cy3 & Cy5 (synthesized by the Grieco group at MSU) were brought to 400pMole/µL in dry dimethylformamide, and reacted with the proteins at the ratio 8pMole dye/µg protein on ice in the dark for 30 min. The reactions were quenched with 1µL of 100mM lysine for 10 min. After labeling, reaction tubes were combined to contain 50µg of Cy3 labeled proteins from a High Spike sample, 50µg of Cy5 labeled proteins from a Low Spike sample from the same patient and 50µg of Cy2 labeled, pooled internal standard. The pooled internal standard of each subcellular fraction contained an equal amount of protein extract from High and Low Spike samples from all patients. A technical replicate was prepared with the same protein samples, using reciprocal dye labeling between High and Low Spike samples. The combined labeled

samples were brought to 450µL with re-hydration buffer (7M urea, 2M thiourea, 2% (w/v) CHAPS, trace of bromophenol blue, 0.5% (v/v) final concentration 3-11 non-linear ampholines (GE Healthcare)) and the solutions were loaded on 24 cm pH 3-11 non-linear IPG strips (GE Healthcare) for passive re-hydration over night at 4ºC in the dark. An Ettan IPGphor II was used for iso-electric focusing with the protocol recommended by the manufacturer. Focused IPGs were agitated for 30 min in equilibration buffer (6M urea, 375mM Tris-HCl pH 8.8, 20% (v/v) glycerol, 2% (w/v) SDS), loaded onto 11% SDS gels, and overlaid with agarose. The second dimension SDS-PAGE was carried out using Ettan DALT twelve System, and the protocol recommended by GE Healthcare.

Image Acquisition and Analysis

A Typhoon Trio (GE Healthcare) was used for fluorescence scanning. The scan resolution was 100µm/pixel and the manufacturer's recommended settings were used. The image analysis was carried out using Progenesis SameSpots software (Nonlinear Dynamics, version 3.1.3030.23662). The three subcellular fractions were analyzed as independent data sets, containing 12 gels and 36 analytical gel images in each set. Standard settings were used for spot detection, background subtraction and ratiometric normalization (equation 1). The initial statistical analysis utilized ANOVA test with p-value ≤ 0.05 and fold change (FC) ≥ 1.25 cutoffs to detect protein spot expression differences between High and Low Spike samples of each patient. Spots that were found to have expression differences in 3 or more patients were designated "noisy spots". Ratiometrically normalized spot volumes for each spot were exported for further analysis.

In order to quantify relative concentrations of GFAP, the intensities of all GFAP isoforms should be added together. Since different spots can not be related to each other when using ratiometric normalization, a second analysis united the data from all three sub cellular fractions and replaced ratiometric normalization with normalization by the total spot volume (equation 2) for each color image. The spot intensity values used for each spot were the average of the normalized volumes of its technical repetitions.

Eq. 1 – Ratiometric normalization for multiple stains per gel (with internal standard)

$$NV_n = \left[\frac{V_{n(exp)}}{V_{n(is)}}\right] \times \left[\frac{V_{t(is)}}{V_{t(exp)}}\right]$$

NV_n = ratiometric normalized volume of spot n
$V_{t(is)}$ = total spot volume of the internal standard image (Cy2)
$V_{t(exp)}$ = total spot volume of an experimental image (Cy3 or Cy5)
$V_{n(is)}$ = volume of spot n on the internal standard image
$V_{n(exp)}$ = volume of spot n on an experimental image

Eq. 2 – Total spot volume normalization for single stain gels (or semi-quantitative analysis)

$$NV_n = \left[\frac{V_n}{V_t}\right] \times S$$

NV_n = total spot volume method normalized volume of spot n
V_n = volume of spot n
V_t = total spot volume of all spots in that image ($V_1+V_2+...V_N$, where N = total number of spots)
S = scaling value (default 100)

Note: equations 1 & 2 follow the notation of Non-linear Dynamics.

Statistical Analysis

t-test - we used the lme function in the R package nlme (Pinheirom et al 2012) to independently test for significant natural log fold-change (high/low) difference from 0 for each protein spot. A p-value < 0.05 for the two-sided t-test and FC ≥ 1.25 was deemed significant. Since only 34 spots passed the t-test cutoffs (out of 4400 spots), we have not corrected for multiple testing, but many of these spots were authenticated. GFAP was validated by Western blots, and excluding the two spots with ambiguous MS identifications, all other statistically changing proteins had multiple isoforms, and each isoform passed the t-test cutoff or were close to it. Thus, the multiple independent identifications of the different isoforms strengthened the notion that these protein changes were not found by chance. By implementing the mixed model mechanism of lme, we accounted for the variance structure of technical repetitions that were nested within the values from the individual patients, which were imposed by the reciprocal dye-labeling design of the paired experiments.

SOIs Cluster analysis - we used Ward's Minimum Variance Method to perform hierarchical clustering in R (R Core Team 2012). Pairwise dissimilarities (distances) between observations were computed with Cluster Package (Maechler et al., 2012), using "Daisy" function and Gower's (1971) Metric.

Protein Identification by Mass Spectrometry

Preparative gels were run to resolve the proteins of each of the subcellular fractions for protein spot picking and mass spectral analysis. The preparative 2D gels contained a total of 500µg protein, including 450µg unlabeled fractionated epilepsy brain

tissue, plus 50µg of the Cy2 labeled internal standard, which was used for gel alignment with the analytical gels. After fluorescence imaging, preparative gels were stained with silver Coomassie (Candiano et al, 2004). Spots of interest were manually excised from the gels and in-gel digested with porcine trypsin (Promega) overnight at 37°C, as previously described by Shevchenko et al, 1996. Extracted peptides were analyzed, using one of the following two LC/MS/MS systems, previously described (Maaty et al 2012, Maaty et al 2013), with small modifications. One system was an Agilent 1100 LC trap (XCT-Ultra 6330), coupled with Agilent nano-chip LC (43mm 300A C18 separation column with 40nL trapping column). Peptides were eluted with a 5-95% acetonitrile gradient over 22 min. The second system was an Agilent 1100 HPLC coupled to a 6520 Accurate-Mass Quadrupole Time-of-Flight LC/MS (Q-TOF) and an in-line nano-chip LC, as described above (Agilent Technologies). Peptides were eluted with a 5-50% acetonitrile gradient over 16 min. MGF compound list files were generated using the default algorithms in the DataAnalysis 3.3 (Bruker Daltonics) and Qualitative Analysis B.04.00 (Agilent Technologies) for XCT and Q-TOF software, respectively. We used MASCOT in-house version 2.2 (Matrix science, London, UK) to query the MS/MS spectra, using the following parameters: database: SwissProt 2012 (534242 sequences; 189454791 residues), taxonomy: human (20317 sequences), enzyme: trypsin, allowing up to 1 missed cleavage, fixed modification: pyridylethyl (C), variable modifications: deamidated (NQ) and oxidation (M), peptide tolerance ± 1.2 Da and 30ppm, MS/MS tolerance ± 0.6 Da and 30 mmu for XCT and QTOF, respectively. Protein identification

was considered significant using the default threshold of $p < 0.05$. For MS results see supplementary material.

Pathway Analysis

Data were analyzed through the use of IPA (Ingenuity® Systems, www.ingenuity.com, version 14400082, release date 2012-11-01). The IPA core analysis was applied to the list of SOI with fold change values ≥ 1.3 FC cutoff and default parameters. The enrichment within the nervous system was tested using Fisher's exact test and predicted the involved pathways for each patient. A comparison analysis across the patient population was used to identify pathways for which involvement was frequently predicted (pathway –log(p-value) ≥ 1.3, in at least 3 patients).

Western Blots

5µg protein of the high and low spike samples from the Nuclear fraction of each patient, were each labeled with Cy3, as previously described, and resolved on mini 10% SDS-PAGE gels, following the standard Bio-Rad procedure. The proteins were then blotted on to Hybond-P membrane (GE Healthcare), using an XCell II apparatus (Invitrogen), following the manufacturer's recommended procedure. The membrane was blocked with 5% nonfat dry milk in TBST (20mM Tris pH 7.6, 140mM NaCl, 0.1% Tween 20) for 2 hrs, reacted with monoclonal mouse anti-GFAP (NeuroMab N206A/8) at 1:1000 dilution in TBST for 2 hrs, washed three times with TBST, reacted with Goat anti-mouse IgG Alexa 488 conjugated antibody (Invitrogen) at 1:2000 dilution in TBST for 2 hrs, and imaged with the Typhoon Trio (GE Healthcare). ImageJ (Rasband, et al

1997-2012) was used for quantification. Six high intensity Cy3-labeled nuclear fraction bands were used as loading controls.

Results

The Human Epileptic Neocortex Proteome

A surgical program provides the System Biology of Epilepsy Project and this proteomic study, with electrically characterized samples from patients with refractory epilepsy. The patients undergo a two stage procedure that begins with several days of subdural electroencephalography (EEG) recording, followed by excision of the epileptic foci and some electrically quieter "normal" surrounding tissue (as illustrated in the experimental flowchart in Figure 8).

2D SDS-PAGE was carried out with improved protein resolution, sensitivity and increased dynamic range, using subcellular fractionation and differential fluorescent labeling of High and Low Spiking sample pairs from each of 6 patients using the 2D DIGE method (Lilley & Friedman 2004). In total, more than 4400 protein spots were analyzed, in independent data sets from the three subcellular fractions. In a t-test ($p<0.05$, FC > 1.25), 34 spots were found to change between High and Low Spiking samples. 31 of these spots were identified by mass spectroscopy as 17 gene products, some of which existed in multiple isoforms. Eight gene products were up regulated and 9 were down regulated in high spiking regions (Table 3). Given the wide range of spike frequencies and potential variance in absolute protein expression between patients, we also hypothesized that spots that change within individual patients, but have a high variance

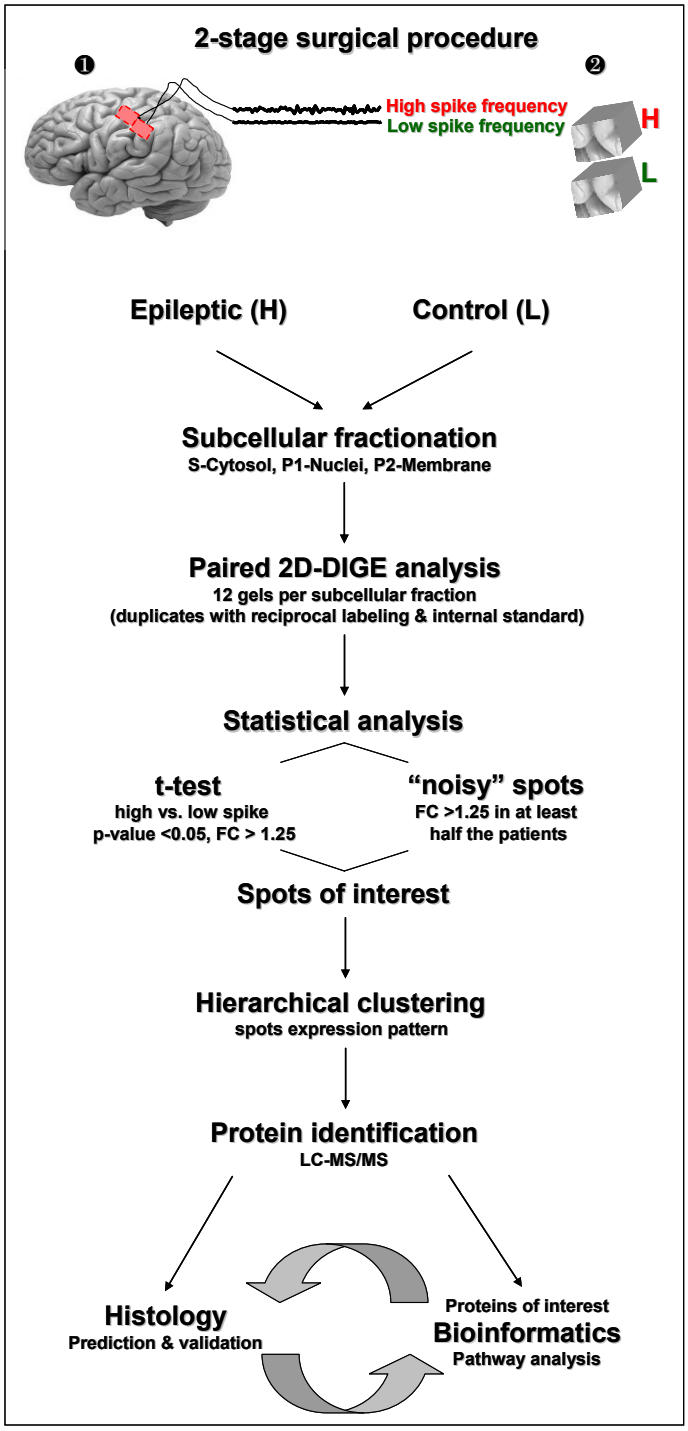

Figure 8: Experiment flowchart

between patients ("noisy" spots) are biologically significant and might indicate involvement in an active process or molecular pathway that is changing, but would not meet the criteria to pass a simple paired t-test. Therefore, we also selected these "noisy" spots (FC > 1.25, that were up or down regulated in the high spiking tissue in at least half the patients) of each sub-cellular fraction. A data set of 397 spots of interest (SOI) resulted, including statistically changing (t-test) and noisy spots from all three fractions and these SOI were further analyzed, using clustering methods. 2D maps of SOIs are shown in the supplementary material Figure S1.

In cases where a protein displayed a spot train of isoforms, in which each spot had a similar expression pattern, only selected isoform spots were picked for mass spectrometry-based protein identification, and the other isoforms in the regulated spot train were assumed to be the same protein. Some SOIs were very low in abundance, while some were not ubiquitously expressed, leading to their apparent absence in the preparative gels. In total, more than 90% of the 397 SOIs were identified as arising from 146 gene products, and we did not attempt to characterize the numerous isoform modifications present in the proteins at this stage in the project.

From Expression to Histological Changes through Hierarchical Clustering

In human studies, biological variation is typically conceived as an inherent limitation, which might mask disease or treatment affects. However, in this part of our study, when our focus was to find proteins which co-express (change in the same direction relative to the internal standard across all the samples, regardless of spike

frequency), rather than to find disease effects (proteins that change between High and Low spiking tissues), biological variation has actually been beneficial. The added variation created unique protein expression patterns and therefore enabled better separation of co-expressing protein groups (Figure 9). The use of a pooled internal standard facilitates the comparison of spot expression across the whole dataset. To provide more expression data points and higher pattern specificity, samples were treated independently, regardless of patient and spike frequency, and variation in expression between and within patients were weighted equally. All SOIs were clustered, according to their expression patterns, across the 12 samples (6 patients x 2 spike frequencies). Some spots cluster more tightly together, sharing short vertical branches on the dendrogram, shown in Figure 9A. These tight clustering observations were also validated by Leave One Out Cross Validation (data not shown).

The expression pattern similarities of a group of spots, within samples from the same patient, and more notably between patients, indicate that the changes of all protein spots in such a cluster should be treated as a collective, single finding, allowing for reduction in complexity of the dataset. For example, groups of non-differentially expressed isoforms, of a single protein, which is changing in expression across the samples, will have the same expression patterns (see Figure 9B-C). Another example is a protein complex that is expressed at different levels across the 12 samples, the subunits of the protein complex will have the same expression patterns (change in the same direction). It is likely that the tightness of the cluster will decrease with increasing numbers of gene products in the complex, due to multiple regulations and involvement of

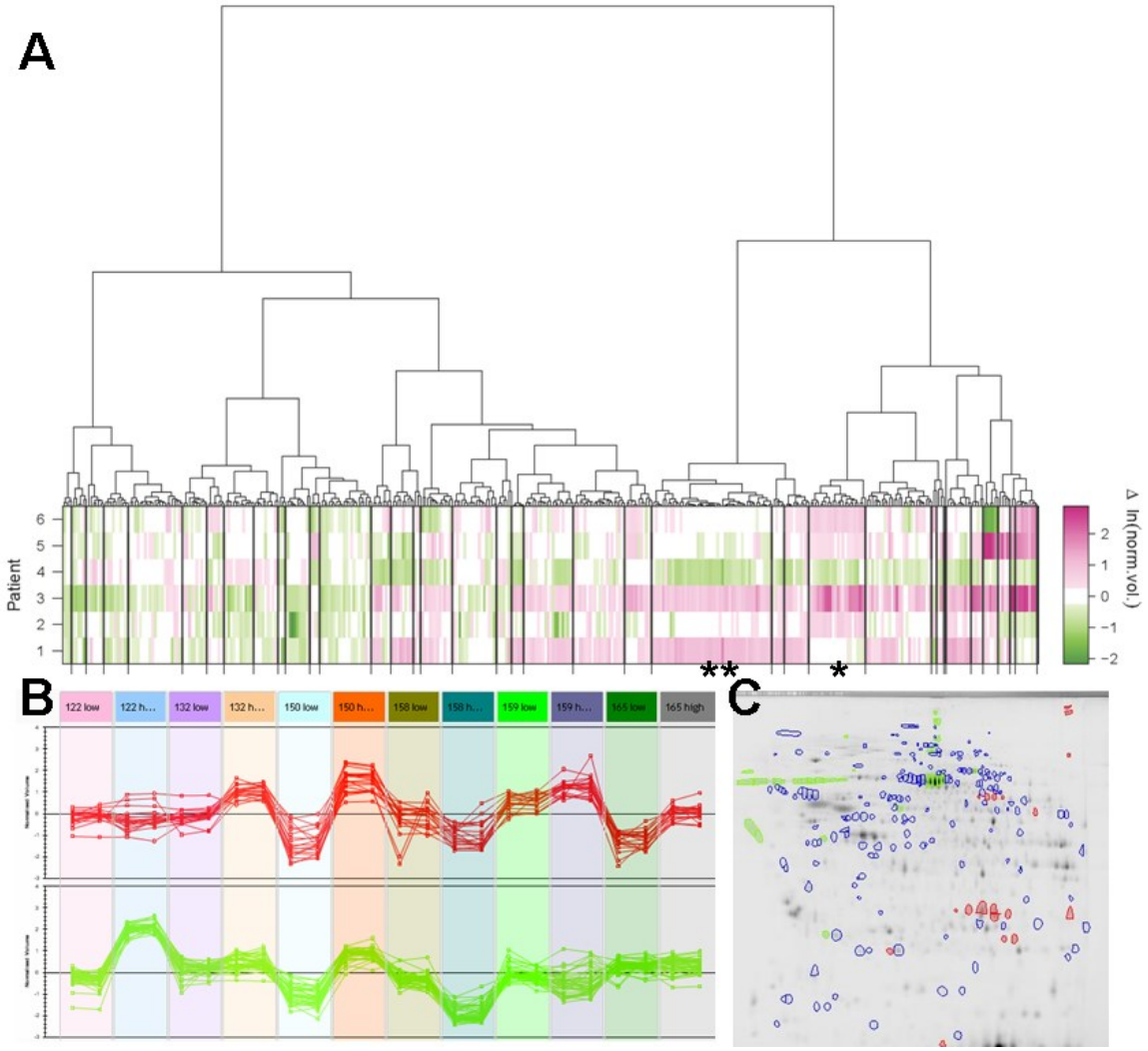

Figure 9: Hierarchical Clustering by Spot Expression Patterns. (A) Spots of interest from all three subcellular fractions clustered by expression patterns across all samples (dendrogram), aligned with the heat map of the fold changes in spots of interest (High /Low spiking) by patient. (B) Examples of two different expression patterns, which represent the colored spots in the 2D gel image to the right, grouped together into two distinct clusters. Each of the single lines connects a normalized spot volume of technical replicates of high and low spike frequency regions of all 6 patients (the high and low patient sample identifications are in the colored boxes above).(C) 2D gel location of soluble fraction erythrocyte protein spots (red) and extra cellular proteins (green) represented in clusters * and ** respectively. Note: horizontal spot trains are largely due to several isoforms of single proteins.

proteins which are ubiquitously expressed. However, due to the high biological variation and the resulting enhanced clustering power of this study, we applied the same logic in order to identify clusters that we hypothesize each represent changes in the number or phenotype of a given cell type with the complex neocortical tissue. A given cell type was predicted based on known cell-specific protein spots within a given group, identified using mass spectrometry. Detailed information on protein identification by fraction and spot is given in Table S4, on the SOIs cluster assignment in Table S3, and on MS analyses of SOIs by Mascot search output that is provided in table S5.

Several histological changes were predicted from the hierarchical clustering. Following the right most branch of the four main dendrogram branches in Fig 9A (see Figure S2 for enlarged dendrogram and cluster number designations), we found several indicators of blood, including platelets - indicated by a fibrinogen cluster (cluster 37), that includes multiple isoforms of two of the fibrinogen subunits (FGB, FGG). Evidence for fibroblasts, smooth muscle or possibly pericytes, was indicated in this branch by co-expression of TPM1, TPM2 and TAGLN (cluster 34). The presence of plasma in clusters 28 & 33 was indicated by proteins like albumin and components of high-density lipoprotein (APOA1, APOD). Finally, the presence of erythrocytes was indicated in cluster 27 primarily by hemoglobin, but also by a cluster of proteins, all of which are present in high abundance in red blood cells (RBCs) (HBA, HBB, catalase, CA1, BLVRB)(D'Amici 2012, Walpurgis et al 2012, Roux-Dalvai et al 2008). Since all tissue sample surfaces were rinsed to remove blood before homogenization, we attributed changes in blood levels to changes in vascularity in the tissues. Later analysis of the

Systems Biology of Epilepsy Project parallel transcriptomic study also predicted changes in vascularity, which were validated by histochemical staining as shown in Figure 11 (Dachet et al, 2013, under review).

The next dendrogram branch, second from the right in Figure 9a (cluster number 24 in Figure S2), contains mostly albumin isoforms, as well as other extra cellular proteins (ECP). The distinct protein expression patterns between the extra cellular and erythrocyte proteins (Figure 9B and cluster numbers 24 and 27 in Figure S2) indicated that the changes in albumin levels are not solely due to changes in vascularity (circulating serum albumin), and suggests the presence of albumin in the extra cellular matrix (ECM).

Many of the identified SOIs were related to cytoskeleton proteins, suggesting structural or migrational changes in affected cells. Dominating this group of proteins, with statistically significant down regulation in the high spike regions in all fractions of all patients was GFAP (~50kDa): a commonly used astrocytic marker. As one of major astrocytic intermediate filaments, the cytoskeletal GFAP mostly pellets in the nuclear fraction. The total nuclear fraction GFAP SOIs (the sum of 6 spots of ~50 kDa + 5 spots of 38-40 kDa) normalized spot volumes (figure 10A), confirmed the decrease of GFAP in the high spiking regions (paired t-test p-value 0.002, average FC 1.53, figure 10B). Western blot analysis validated the decrease of total nuclear GFAP in high spiking tissues (p-value 0.047, figure 10C). The spot group of lower molecular weight (LMW, 38-40 kDa) GFAP presented a different trend of expression across the patients. LMW GFAP spots were mostly up-regulated in high spiking regions and notably clustered with blood proteins as shown in cluster 32-33.

If the LMW GFAP were excluded from the analysis, the six 50kDa GFAP isoforms in the P1 (nuclear fraction) added together demonstrated a stronger down regulation in the high spiking regions (p-value 0.002, FC 1.79). Interestingly, the increase in total GFAP fold change (L/H spike) of the 50kDa isoforms was strongly correlated with increased spike frequency (frequency difference High-Low = Δspike) as shown in Figure 10D. The linear correlation coefficient was $r = 0.96$ with a p-value 0.002, using the Pearson product-moment correlation coefficient. Alternatively, since we had only six data points, we evaluated the non-parametric association and found Kendall tau coefficient of $r = 1$, p-value = 0.003 for the data plotted in Figure 10D.

The total GFAP changed only in the nuclear pellet fraction and did not significantly change between high and low spike regions in the P2 and Cytosol fractions. The total GFAP in the Cytosol fraction (Figure 10E), although still mostly higher in low spike within patients, demonstrated a very different expression pattern between the patients, when compared with the nuclear fraction (Figure 10B&E). The levels of cytosol GFAP were more in agreement with the level of gliosis, which was assigned to the patients by the pathological analysis (Table 2), and yet was not a good predictor for astrogliosis status. The GFAP soluble pool (in the cytosol fraction) is presumably related to the level of GFAP filaments (nuclear fraction) and might be affected by pathological conditions (Newcombe et al 1986). Therefore, we evaluated the ratio of total cytosol to total nuclear GFAP concentration, and found the ratio to be a good predictor for the patient's astrogliosis level, as can be seen by comparing the patient histopathology in Table 1 to the data in Figure 10F.

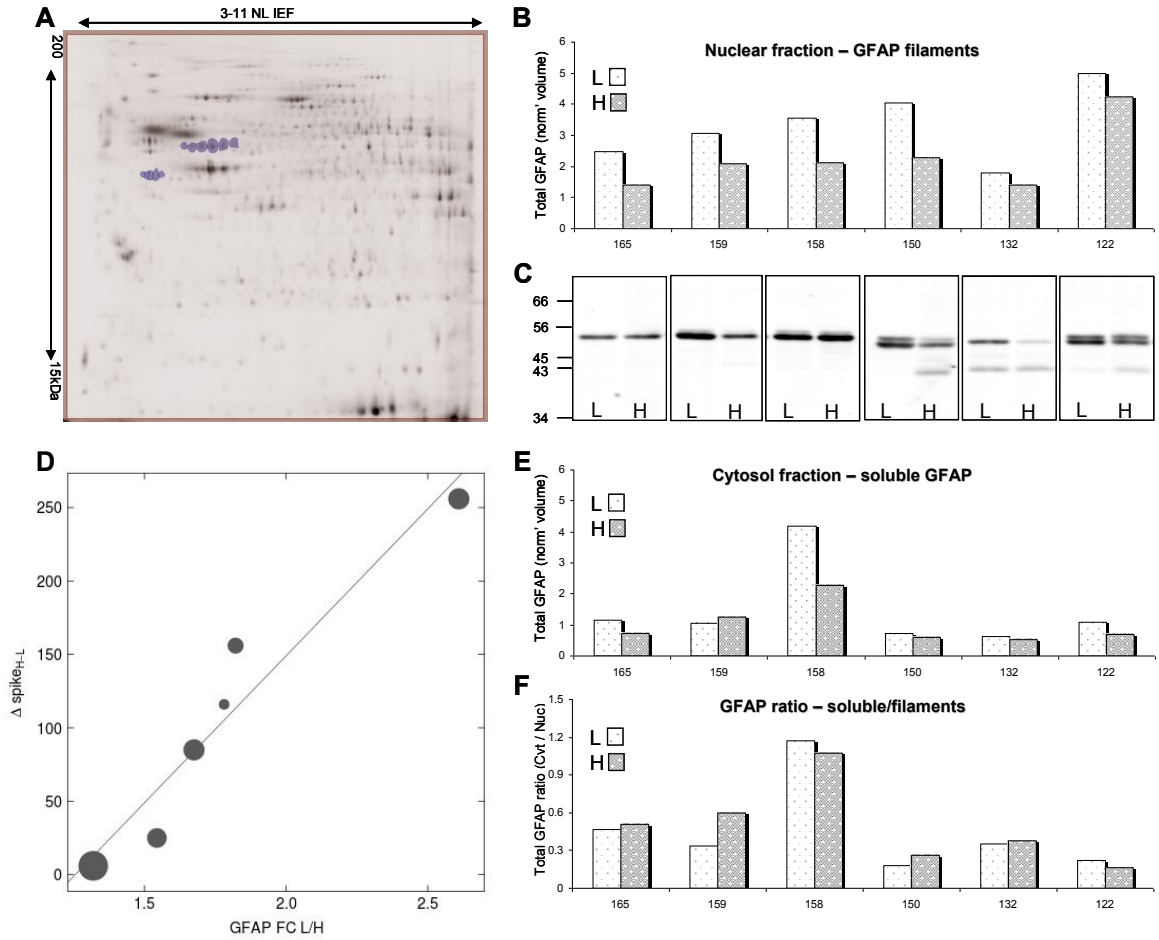

Figure 10: GFAP Quantification Studies. (A) 11 GFAP SOIs are the blue marked spots in 2D SDS-PAGE of the P1 fraction, which were used for quantification of total GFAP. (B) Total GFAP as the sum of total image intensity normalized volume (non-ratiometric) of nuclear GFAP spots shown by patient and spike frequency (L-low, H-High). GFAP is down regulated in high spike samples (paired t-test for all 11 spots or upper higher MW (~50kDa) 6 spots, p-value 0.002, average FC 1.53 or 1.79, respectively). (C) Western blot analysis for all nuclear fraction samples with monoclonal anti-GFAPα antibody, validating the down regulation of GFAP in high spike samples (p-value 0.047). (D) Correlation of fold change of nuclear fraction 50kDa GFAP (upper 6 spots) (L/H spike, circle sized by the weighted total intensity) with differences in spike frequency for individual patients (H-L). Y=200.29X–251, r = 0.96, p-value 0.002. (E) Sum normalized volume of cytosol GFAP spots by patient and spike frequency. (F) Cytosol to nuclear total GFAP ratio (11 spots).

Note - for GFAP quantification, the fluorescence spot intensities were normalized to the total signal in each gel image. Values are given as the sum of relevant spot normalized volumes in millions of volume units.

Bioinformatics Analysis of Proteins of Interest

The list of 397 SOIs, represent 146 gene product proteins of interest (POIs). Multiple representations of the same gene might arise from post transcriptional (alternative splicing and/or posttranslational) modifications, as well as a SOI occurring in more than one subcellular fraction. In this exploratory phase of the project, we did not investigate modifications of gene products, but the changes identified have singled out candidates for further study of modifications involved in the physiology. Additionally, it should be noted that the bioinformatics tools currently available do not take this level of protein isoform complexity into account.

Description of the 146 POIs are given in Table 3 and their FC by patient are shown by color codes. Since multiple isoforms were often summed to a single gene product, the protein fold change represents the average expression of each set of isoforms for each patient. Therefore, the absence of a significant, net fold change in at least three patients of a given protein with multiple SOIs, is likely to indicate approximate cancelation of FC by differential post-translational modifications. An exception was made with regard to analysis of GFAP, which had two distinct groups of multiple isoforms. The spot train having the expected MW and pI for full length GFAP, and several isoforms with lower than the predicted MW and different levels of acidic shift were analyzed separately as two gene products, GFAP ~50kDa and GFAP LMW (low molecular weight), respectively.

UniProtKB accession	Gene name	Note	Description	Patient spike ratio High/Low 1 2 3 4 5 6
P07741	APRT	1	Adenine phosphoribosyltransferase	
P69905	HBA	4	Hemoglobin, alpha	
P37840	SNCA	2†a	Synuclein, alpha (non A4 component of amyloid precursor)	
P16949	STMN1	2†a	Stathmin 1/oncoprotein 18	
P18206	VCL	3	Vinculin	
P04040	CAT	4	Catalase	
P30043	BLVRB	2	Biliverdin reductase B (flavin reductase (NADPH))	
P68871	HBB	1	Hemoglobin, beta	
Q16851	UGP2	1†a	UDP-glucose pyrophosphorylase 2	
P15924	DSP	1††a	Desmoplakin	
P30044	PRDX5	1	Peroxiredoxin 5	
P37802	TAGLN2	1	Transgelin 2	
P00915	CA1	11†a	Carbonic anhydrase I	
O00429	DNM1L	1	Dynamin 1-like	
Q15257	PPP2R4	1	Protein phosphatase 2A activator, regulatory subunit 4	
P11137	MAP2	1	Microtubule-associated protein 2	
Q01469	FABP5	2	Fatty acid binding protein 5 (psoriasis-associated)	
P31946	YWHAB	1‡	Tyrosine 3-monooxygenase/tryptophan 5-monooxygenase activation protein, beta polypeptide	
P63104	YWHAZ	1‡	Tyrosine 3-monooxygenase/tryptophan 5-monooxygenase activation protein, zeta polypeptide	
P00450	CP	1‡	Ceruloplasmin (ferroxidase)	
Q12860	CNTN1	1‡	Contactin 1	
P02675	FGB	5	Fibrinogen beta chain	
P32119	PRDX2	5†a	Peroxiredoxin 2	
P22314	UBA1	4	Ubiquitin-like modifier activating enzyme 1	
Q92777	SYN2	3†a	Synapsin II	
P25705	ATP5A1	3	ATP synthase, H+ transporting, mitochondrial F1 complex, alpha subunit 1, cardiac muscle	
Q9NZR1	TMOD2	2	Tropomodulin 2 (neuronal)	
P09493	TPM1	2	Tropomyosin 1 (alpha)	
P00918	CA2	4	Carbonic anhydrase II	
P45974	USP5	1	Ubiquitin specific peptidase 5 (isopeptidase T)	
P04217	A1BG	1	Alpha-1-B glycoprotein	
Q02252	ALDH6A1	2‡	Aldehyde dehydrogenase 6 family, member A1	

Table 3. Proteins of Interest (POIs). 146 POIs, representing 397 protein isoform SOIs.

Table 3. continued

UniProtKB accession	Gene name	Note	Description	Patient spike ratio High/Low 1 2 3 4 5 6
P05090	APOD	1	Apolipoprotein D	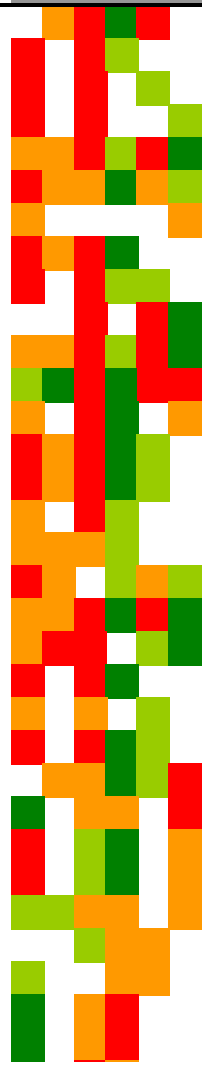
P61088	UBE2N	1	Ubiquitin-conjugating enzyme E2N	
O43301	HSPA12A	1‡	Heat shock 70kDa protein 12A	
P15311	EZR	1	Ezrin	
Q01995	TAGLN	2	Transgelin	
P14136	GFAP LMW	16	Glial fibrillary acidic protein	
Q16555	DPYSL2	14‡↑b	Dihydropyrimidinase-like 2	
P02763	ORM1	2	Orosomucoid 1	
P02774	GC	2	Group-specific component (vitamin D binding protein)	
Q9NQ66	PLCB1	2	Phospholipase C, beta 1 (phosphoinositide-specific)	
P07951	TPM2	2	Tropomyosin 2 (beta)	
P02679	FGG	8	Fibrinogen gamma chain	
P01857	IGHG1	3‡	Immunoglobulin heavy constant gamma 1 (G1m marker)	
P01009	SERPINA1	4	Serpin peptidase inhibitor, clade A (alpha-1 antiproteinase, antitrypsin), member 1	
P01011	SERPINA3	4	Serpin peptidase inhibitor, clade A (alpha-1 antiproteinase, antitrypsin), member 3	
Q9BUT1	BDH2	1	3-hydroxybutyrate dehydrogenase, type 2	
P62258	YWHAE	1	Tyrosine 3-monooxygenase/tryptophan 5-monooxygenase activation protein, epsilon polypeptide	
P22061	PCMT1	1	Protein-L-isoaspartate (D-aspartate) O-methyltransferase	
P60709	ACTB	6‡	Actin, beta	
P00441	SOD1	1	Superoxide dismutase 1, soluble (amyotrophic lateral sclerosis 1 (adult))	
P02768	ALB	50‡	Albumin	
P02787	TF	8	Transferrin	
P00738	HP	3	Haptoglobin	
Q6UWE0	LRSAM1	1	Leucine rich repeat and sterile alpha motif containing 1	
P63027	VAMP2	2†	Vesicle-associated membrane protein 2 (synaptobrevin 2)	
P11142	HSPA8	2‡	Heat shock 70kDa protein 8	
P38606	ATP6V1A	2‡	ATPase, H+ transporting, lysosomal 70kDa, V1 subunit A	
O14531	DPYSL4	2	Dihydropyrimidinase-like 4	
P63098	PPP3R1	1	Protein phosphatase 3 (formerly 2B), regulatory subunit B, alpha isoform	
Q14847	LASP1	2↓a	LIM and SH3 protein 1	
P09972	ALDOC	1‡	Aldolase C, fructose-bisphosphate	
Q96FC7	PHYHIPL	1‡	Phytanoyl-CoA 2-hydroxylase interacting protein-like	

Table 3. Continued

UniProtKB accession	Gene name	Note	Description	Patient spike ratio High/Low
P00505	GOT2	1	Glutamic-oxaloacetic transaminase 2, mitochondrial (aspartate aminotransferase 2)	
Q9ULD0	OGDHL	1	Oxoglutarate dehydrogenase-like	
P50213	IDH3A	1	Isocitrate dehydrogenase 3 (NAD+) alpha	
P50148	GNAQ	1	Guanine nucleotide binding protein (G protein), q polypeptide	
P26641	EEF1G	2‡	Eukaryotic translation elongation factor 1 gamma	
P12277	CKB	2	Creatine kinase, brain	
P13611	VCAN	1‡	Versican	
P54727	RAD23B	1‡	RAD23 homolog B (S. cerevisiae)	
P02647	APOA1	2	Apolipoprotein A-I	
Q05193	DNM1	7	Dynamin 1	
P60880	SNAP25	3	Synaptosomal-associated protein, 25kDa	
P46459	NSF	3‡	N-ethylmaleimide-sensitive factor	
P49368	CCT3	1‡	Chaperonin containing TCP1, subunit 3 (gamma)	
Q14194	CRMP1	4	Collapsin response mediator protein 1	
P21579	SYT1	1‡	Synaptotagmin I	
P27797	CALR	1‡	Calreticulin	
P07910	HNRNPC	1	Heterogeneous nuclear ribonucleoprotein C (C1/C2)	
Q9BPU6	DPYSL5	5	Dihydropyrimidinase-like 5	
P62333	PSMC6	1	Proteasome (prosome, macropain) 26S subunit, ATPase, 6	
Q92598	HSPH1	1	Heat shock 105kDa/110kDa protein 1	
P11216	PYGB	1‡	Phosphorylase, glycogen; brain	
P21399	ACO1	1‡	Aconitase 1, soluble	
P00352	ALDH1A1	1	Aldehyde dehydrogenase 1 family, member A1	
P08133	ANXA6	1‡	Annexin A6	
P54652	HSPA2	1‡	Heat shock 70kDa protein 2	
P52306	RAP1GDS1	2	RAP1, GTP-GDP dissociation stimulator 1	
P50995	ANXA11	1	Annexin A11	
P01023	A2M	5	Alpha-2-macroglobulin	
P09417	QDPR	2	Quinoid dihydropteridine reductase	
P06733	ENO1	2‡	Enolase 1, (alpha)	
P07355	ANXA2	2	Annexin A2	
P14618	PKM2	4‡	Pyruvate kinase, muscle	

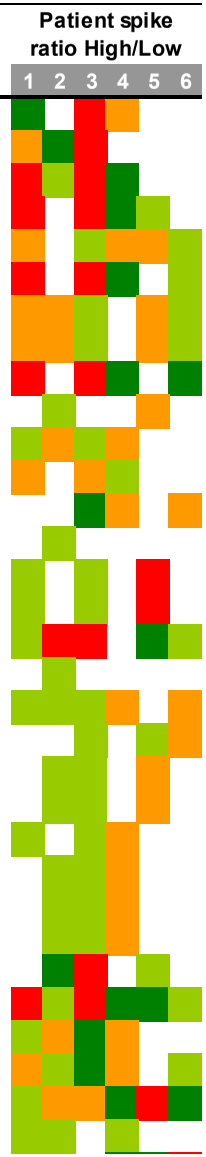

Table 3. Continued

UniProtKB accession	Gene name	Note	Description	Patient spike ratio High/Low 1 2 3 4 5 6
P40121	CAPG	1	Capping protein (actin filament), gelsolin-like	
O60641	SNAP91	1	Synaptosomal-associated protein, 91kDa homolog (mouse)	
Q00535	CDK5	1	Cyclin-dependent kinase 5	
P30038	ALDH4A1	1‡	Aldehyde dehydrogenase 4 family, member A1	
Q08209	PPP3CA	2	Protein phosphatase 3 (formerly 2B), catalytic subunit, alpha isoform	
P14625	HSP90B1	1	Heat shock protein 90kDa beta (Grp94), member 1	
P48147	PRER	1‡	Prolyl endopeptidase	
P26232	CTNNA2	1	Catenin (cadherin-associated protein), alpha 2	
P28161	GSTM2	1	Glutathione S-transferase M2 (muscle)	
P61204	ARF3	6‡	ADP-ribosylation factor 3	
P61158	ACTR3	2	ARP3 actin-related protein 3 homolog (yeast)	
O75891	ALDH1L1	2	Aldehyde dehydrogenase 1 family, member L1	
O60282	KIF5C	2	Kinesin family member 5C	
P61764	STXBP1	2‡	Syntaxin binding protein 1	
P50453	SERPINB9	1	Serpin peptidase inhibitor, clade B (ovalbumin), member 9	
Q16352	INA	1	Internexin neuronal intermediate filament protein, alpha	
P04083	ANXA1	1	Annexin A1	
P08758	ANXA5	1	Annexin A5	
P23528	CFL1	2	Cofilin 1 (non-muscle)	
P04406	GAPDH	2↓a	Glyceraldehyde-3-phosphate dehydrogenase	
Q9P1U1	ACTR3B	1	ARP3 actin-related protein 3 homolog B (yeast)	
P07196	NEFL	3	Neurofilament, light polypeptide 68kDa	
P31150	GDI1	4	GDP dissociation inhibitor 1	
Q9UPY8	MAPRE3	1	Microtubule-associated protein, RP/EB family, member 3	
Q9H115	NAPB	1	N-ethylmaleimide-sensitive factor attachment protein, beta	
Q00610	CLTC	1	Clathrin, heavy chain (Hc)	
P48643	CCT5	1	Chaperonin containing TCP1, subunit 5 (epsilon)	
P05091	ALDH2	2↓a	Aldehyde dehydrogenase 2 family (mitochondrial)	
P07197	NEFM	1	Neurofilament, medium polypeptide	
Q8IXJ6	SIRT2	1	Sirtuin 2	
O14979	HNRPDL	1‡↓a	Heterogeneous nuclear ribonucleoprotein D-like	
Q92561	PHYHIP	1‡↓a	Phytanoyl-CoA 2-hydroxylase interacting protein	

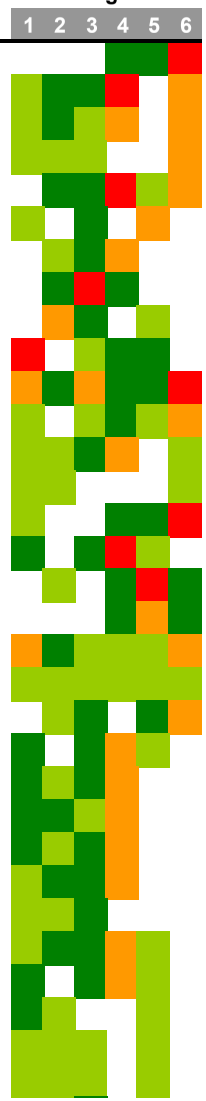

UniProtKB accession	Gene name	Note	Description	Patient spike ratio High/Low 1 2 3 4 5 6
P17600	SYN1	1	Synapsin I	
P34949	MPI	1‡	Mannose phosphate isomerase	
Q9Y570	PPME1	1‡	Protein phosphatase methylesterase 1	
O94811	TPPP	2	Tubulin polymerization promoting protein	
Q9UNZ2	NSFL1C	1	NSFL1 (p97) cofactor (p47)	
Q14894	CRYM	2	Crystallin, mu	
P09471	GNAO1	4↓a	Guanine nucleotide binding protein (G protein), alpha activating activity polypeptide O	
P68363	TUBA1B	1	Tubulin, alpha 1b	
P21796	VDAC1	1	Voltage-dependent anion channel 1	
Q71U36	TUBA1A	11‡	Tubulin, alpha 1a	
P19367	HK1	2	Hexokinase 1	
P02511	CRYAB	3↓b	Crystallin, alpha B	
P54920	NAPA	1	N-ethylmaleimide-sensitive factor attachment protein, alpha	
Q9BQE3	TUBA1C	1‡	Tubulin, alpha 1c	
O95741	CPNE6	1‡↓a	Copine VI (neuronal)	
P61978	HNRNPK	1‡↓a	Heterogeneous nuclear ribonucleoprotein K	
P45880	VDAC2	1	Voltage-dependent anion channel 2	
P14136	GFAP 50kDa	15↓ab	Glial fibrillary acidic protein	

Table 3 continued.

Notes: (xx) - indicates the number of isoforms (spots) of the identified protein, using bin-averages for fold change values. (‡) - indicates a spot with an ambiguous MS identification (see supplementary material for details and definitions). (†) - observed MW does not agree with expected MW. ↑ and ↓ indicate a spot with statistically significant up and down regulation, respectively. t-test p-value <0.05 (a) and < 0.005 (b).

Patient FC color: ■ ≤ (-1.5), ■ ≤ (-1.25), (-1.25) > □ < 1.25, ■ ≥ 1.25, ■ ≥ 1.5

Ingenuity Pathway Analysis (IPA) was used to predict involvement of Canonical Pathways for each patient. Many proteins are ubiquitously expressed in brain cells and might be involved in a number of Canonical Pathways. The differential expression and biological involvement of the erythrocyte proteins in relation to changes in vascularity, was already addressed. Therefore, erythrocyte proteins were removed (unless the proteins were also expressed outside the erythrocyte cluster) from the analyzed genes. After considering the differences in expression patterns of the blood components, as well as their size and likelihood of leaking out of the vessel under pathological conditions, the rest of the blood components were included in the analysis, since they might have interactions or cellular effects exterior to the blood vessels. Common involved pathways across the patient population were found using IPA comparison analysis. Pathways predicted to be involved in at least three patients were considered. The top 25 ranking canonical pathways involved in human neocortical epilepsy, and the relative contribution of each patient to the score are shown in Figure 12.

Discussion

Surgical resection of electrophysiologically characterized brain tissue from patients with refractory partial epilepsy can be highly beneficial (Spencer 2008, Ziemba et al 2011), and provides a unique opportunity to study the molecular and histological changes associated with abnormal electrophysiological properties of epileptic human neocortical brain regions. The System Biology of Epilepsy Project is taking advantage of this opportunity to generate a clinical and multi-omics database to further our knowledge

of the epileptogenic process and advance the search for better treatments (Loeb 2010, 2011). We used differential fluorescent labeling in 2D-DIGE to resolve and compare protein expression and modifications between high and low spiking frequency tissue sample pairs with no apparent histopathology. In the initial analysis we identified a subset of proteins of interest, suggesting that these proteins might be involved in the cellular changes that lead to epilepsy. Subsequent analysis focused on attempts to relate this subset of proteins to epilepsy-related biological changes. Using hierarchical clustering, we took advantage of the natural biological variation between patients as well as natural, or epilepsy induced variation within the samples of each patient, to allow the separation of groups of co-expressing protein spots that predicted histological changes.

High Interictal Spike Frequency is Associated with Vascular Modulation

Many of the changing proteins, when clustered by their expression patterns, suggest significant changes in blood vessels in high spiking neocortex. Although all but one (CA1) of the individual protein changes did not reach statistical significance alone, the group of proteins in the blood cluster suggested increased vascularity in high spike samples in four of the six patients. Patient 1 had no change and patient 4 showed an opposing trend, for this cluster, as well as most of the dataset. Since patient 4 is only one year old, his brain is in a different developmental stage, which might be expected to affect many of its “normal” and “epileptic” features.

The process of angiogenesis is associated with brain injury (Greenberg 2005, Xiong 2010) and was previously described in temporal lobe epilepsy (TLE)

(Papageorgiou et al 2011), with an association to increased BBB permeability (Rigau et al 2007, Morin-Brureau 2011). We predicted by both proteomic and transcriptomic studies, which were validated, using histochemical staining (see figure 11), that angiogenesis is also associated with interictal high spiking neocortical tissues.

This finding also demonstrates the power of protein expression clustering to interpret proteomic studies. Although carbonic anhydrase 1 (CA1) was statistically up-regulated in high spiking regions, its co-expression with hemoglobin, among other proteins highly abundant in erythrocytes, led us to interpret CA1 up-regulation as part of increased vascularity. You et al (2005) suggested four proteins (hemoglobin, catalase, peroxiredoxin and carbonic anhydrase I) as markers for blood contamination in proteomic analysis of cerebrospinal fluid (CSF). We suggest that the similar expression pattern of most of these proteins, with the addition of biliverdin reductase B (BLVRB), defines them as erythrocytes markers, in any tissue. This is especially true in gel-based proteomic studies, in which hemoglobin isoforms run close to the electrophoretic front and may frequently be excluded from the analysis. In a gel-free proteomic study, Visanji et al 2012 also found increased expression of catalase and CA1 in human epileptic brain, compared with controls, and localized both proteins to astrocytes. In addition to CA1 and catalase, they found seven hemoglobin isoforms, albumin, and alpha-2-macroglobolin to be up-regulated in epileptic brain. They suggested catalase and CA1 had epileptogenic roles in response to oxidative stress (catalase) and support to carbonic anhydrase 2 pro-apoptotic/epileptogenic role (CA1). Although these mechanisms cannot be ruled out, our proposed protein cluster marker provides an alternative explanation. We suggest that the

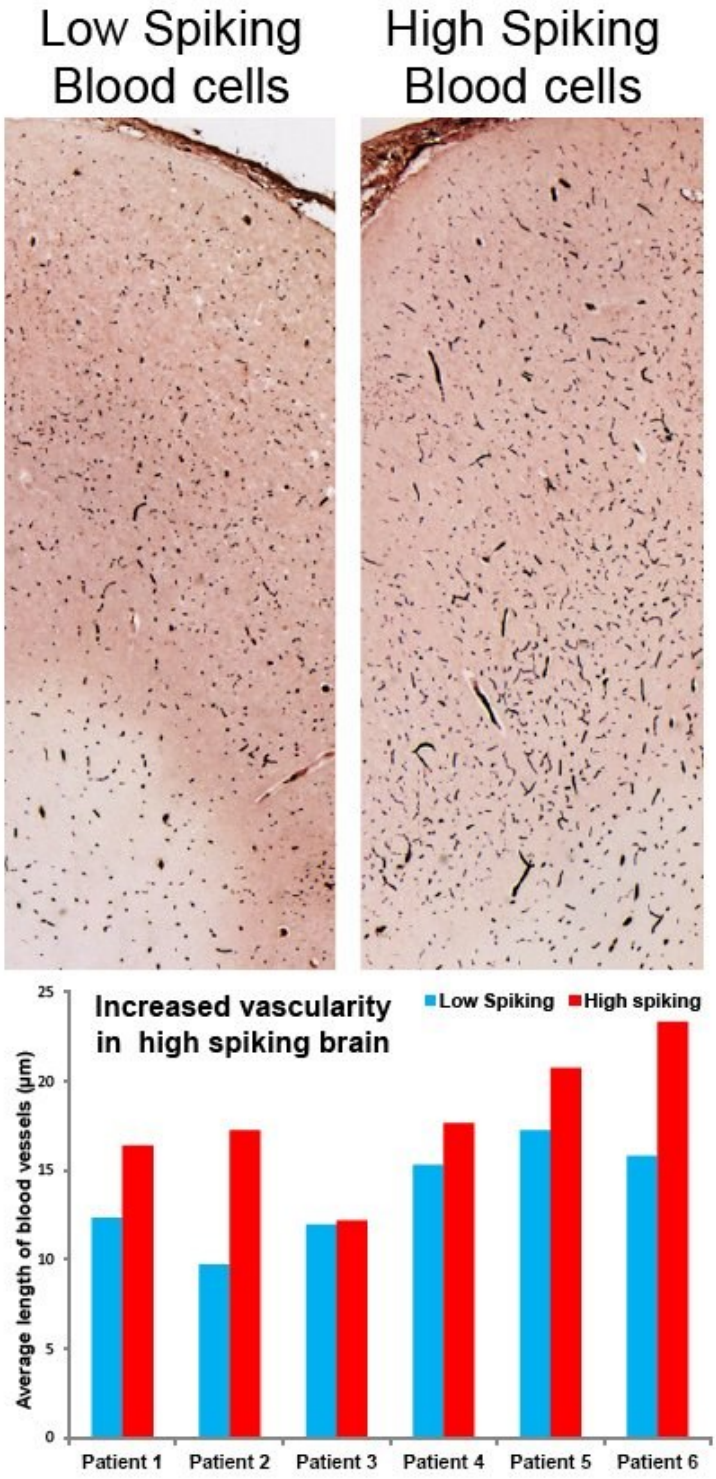

Figure 11. Angiogenesis is Associated with Interictal High Spiking Neocortical Tissues. Reprint from Dachet et al (2012), poster presented at Cold Harbor Spring Laboratory Systems Biology: Global Regulation of Gene Expression March 20 - 24, 2012

protein changes found by Visanji et al 2012 also indicate increased vascularity in the epileptic brain.

The astrocytic foot is a structural component of brain vasculature, which can explain the localization of catalase and CA1 to astrocytes. The hemoglobin isoforms, catalase and CA1 are the most abundant proteins in RBC (D'Amici 2012). Furthermore, CA1 expression is limited to RBC and the gastrointestinal tract (Boron, 2003). Additionally, alpha-2-macroglobolin and albumin are two major carriers of proteins in the serum (Kragh-Hansen et al 2002, Mantuano et al 2008). Taken together, our alternative explanation of increased vascularity in the epileptic tissues, accounts for changes in regulation of eleven of the twelve proteins found to change by Visanji et al.

Dysfunctional BBB in Epileptic Brain

A dysfunctional BBB is associated with large number of neurological disorders (Abbott 2006, Zlokovic 2008) and many studies address this phenomenon in epilepsy (reviewed by Oby and Janigro 2006, Weissberg et al 2011, Liu et al 2012, Kovács et al 2012, Marchi et al 2012). Our study provides further evidence for a leaky BBB in human epileptic neocortex, but without correlation to the level of interictal spiking. Increase in ECM Albumin is assumed to be the result of a leaky blood brain barrier (BBB) (Ivens et al 2007, Marchi et al 2012). Therefore, the ECP changes (clusters 24-26) are interpreted as due to a leaky BBB in the high spike area of patient number one, or due to decreased vascularity in high spike of patient four. For patients two, three, five and six, a possible explanation is an increased BBB leakiness in low spike tissue, counteracting the increase in albumin levels, due to increased vascularity in high spike tissue. Taken together, the

cluster analysis suggests epilepsy-related changes in BBB permeability or possibly a dysfunctional BBB. Further investigation using more detailed histochemical analysis is needed to clarify and further evaluate these suggestions.

The lack of association of BBB leakiness with high spike frequency in epileptic brain is not surprising. The interaction between seizures and dysfunctional BBB has been called “a puzzle of a chicken and egg” (Friedman 2011). Which one is the cause, which one is the effect and what is their temporal relationship? Seizures can affect BBB permeability (Janigro 1999) though it is not clear if such BBB alterations are restricted to the seizure focus. Experimental disruption of the BBB can induce an epileptic focus in the treated rat brain area (Seiffert et al 2004), or in the hemisphere contra-lateral to the BBB disruption in humans and large animals (Marchi et al 2007). The disruption is transient and largely reversible (Abbot et al 2010, Willis 2011) and the circumstantial evidence for BBB dysfunction, i.e. extravascular serum albumin, is temporary. In a process mediated by transforming growth factor beta receptor (TGF-βR), the serum-derived albumin is quickly taken up by astrocytes, followed by numerous changes in astrocytic protein expression, which are considered to be epileptogenic (Ivens et al 2007, Cacheaux et al 2009, David et al 2009). Given the dynamics of the BBB in epilepsy, it is therefore not surprising that although clearly involved, there was no significant correlation with spike frequency and BBB disruption.

High Interictal Spike Frequency is Associated with Decreased GFAPα

Reactive astrocytes over-expressing GFAP (=gliosis) is a hallmark of posttraumatic epileptic foci (Oberheim et al 2008). GFAP is the main intermediate filament in astrocytes. The expression of GFAP increases as a function of age and is affected by multiple pathological conditions (Middeldorp & Hol 2011). GFAP is normally found primarily in the water-insoluble pellet fraction (Eng 1985) as a polymer, with a small amount in the soluble protein fraction. However, astrogliosis increases the proportion of soluble GFAP (Newcombe et al 1986). We evaluated the relative GFAP concentration in both fractions and found that the increasing soluble to the insoluble GFAP concentration ratio correlated with levels of gliosis from the pathological assessment of the patients (Table 2), regardless of spiking frequency. This analysis predicted normal tissues to have a soluble GFAP concentration of between one-quarter to one-fifth of the concentration in the nuclear fraction. Diffuse and mild levels of gliosis were associated with increased shift to soluble GFAP, until the soluble and insoluble GFAP concentrations were about the same for the patient with the most pronounced gliosis.

While four out of the six patients were found to have some level of gliosis, 50kDa GFAP, as well as total nuclear GFAP, was down regulated in high spiking tissue of all the patients, when compared with a low spiking tissue. Furthermore, the fold change decrease in GFAP was related to the level of spiking, suggesting a causal relationship between the two phenomena. In addition to the unexpected decrease in GFAP, α-B-crystallin (CRYAB), another protein whose over-expression is a marker of epileptic foci

(Sarant & Flores-Sarnat 2009), was found in our study to be down regulated in the P2 fraction of high spiking tissue. CRYAB is small heat shock protein, known to be strongly induced in reactive astrocytes (Che et al 2001), has a role in the anti-inflammatory response, and an anti-apoptotic role in astrocytes (Ousman et al 2007). CRYAB is also known to regulate GFAP assembly and to co-aggregate with it in astrocytic inclusions (Hagemann et al 2009). It is unclear whether the changes in expression of the two proteins are related. It is possible that the co-reduction is due to a CRYAB & GFAP complex, to a reduction in reactive astrocytes, or to astrocytic apoptosis that may be mediated by the lack of protective CRYAB. The decrease in these two epilepsy foci markers in the high spike tissue, suggests that the cellular changes associated with abnormal electrophysiology are separate from the less localized cellular changes, such as astrogliosis, which are likely to be associated with general trauma or stress.

Several GFAP splice variants have been described in the literature (Middeldorp & Hol 2011), some of which have been found to be differentially expressed in epileptic lesions (Martinian et al 2009, Boer et al 2010). However, our MS analysis of 2D gel electrophoresis spots, in agreement with 1D western analysis, using a specific GFAPα monoclonal antibody, indicates that the canonical 50kDa GFAPα is the variant in the SOIs examined here. While the 50kDa GFAPα was down regulated in high spiking tissues, the insoluble 38-40 kDa GFAPα modified products had a mixed expression pattern and clustered with the blood proteins. Although the exact nature of this modification process was not studied here, this co-expression might indicate that insoluble 38-40 kDa GFAPα is an indicator for perivascular astrocytes or specific GFAP

modifications, associated with the astrocytic foot process, which is an integral component of the BBB (Abbott et al 2010).

An increasing body of evidence, identifying roles of astrocytic dysfunction in epilepsy, has been described (recent reviews Aronica et al 2012, Heinemann et al 2012, Seifert & Steinhäuser 2013). Witcher & Ellis (2012) addressed a paradox in TLE, of increased GFAP and decreased glutamate transporter EAAT2, which is predominantly expressed in astroglial cells and throughout the astrocytic membrane. They consolidated these co-occurring changes with the morphological interpretation of "…decrease in non-GFAP containing perisynaptic astrocytic processes…" Indeed, GFAP might not be an ideal marker for non-reactive astrocytes, since it is not expressed throughout the astrocyte cytoplasm and is not detectable in fine astrocytic processes (Sofroniew & Vinters 2010). In epilepsy models, expression studies of key astrocytic proteins such as aquaporin-4 and inwardly rectifying potassium channel Kir4.1, that are suspected to be epileptogenic, revealed reduction in their immunoreactivity, specifically in cortical (and not hippocampus) astrocytic processes (Kim et al 2010, Stewart et al 2010). Rakhade & Loeb (2008) found that the glutamate transporter EAAT2 was down-regulated in human neocortical epileptic foci in experimental settings, similar to our study. Thus, the decrease in GFAP in high spiking regions in our study supports a hypothesis that GFAP positive astrocytes are decreased. In addition, ALDH1L1, an alternative candidate for an astrocytic marker (Sofroniew & Vinters 2010), also exhibits a decrease in our dataset (FC 1.18, p-value 0.013). Additional studies are needed to more fully characterize the nature

of the changes in GFAP positive astrocytes, whether they are due to a reduction in the number of cells or to a change in their morphology.

Canonical Pathways Involved in Refractory Neocortical Epilepsy

In a global proteomics study, the significance of a single protein change in a biological pathway can be ambiguous. Even when it is known whether and how the changing protein is modified, the ambiguity can remain, since many proteins are involved in multiple pathways. Knowledge-based software, which predicts the involved pathways from lists of changing proteins, is a powerful tool in the complex field of neuroproteomics (Liu et al 2010). We queried Ingenuity Knowledge-Base Ingenuity Pathway Analysis (IPA) to predict the pathways involved for each of the patients and to identify the common, probable pathways that are associated with biological changes in the high spike frequency tissues.

Many of the identified common pathways partially overlap in the molecular level and share some of the same protein networks. For example, we have identified changes in several protein components of the adherens junction (AJ), which pointed to several of the proposed signaling pathways. “Remodeling of epithelial adherens junctions” and “Epithelial adherens junction signaling” highlighted by the IPA in Figure 12, can also indicate changes in AJs of endothelial cells (EC), and in our study appears to indicate changes involved in blood vessels or BBB. This notion is supported by other signaling pathways identified by Ingenuity analysis in our study, “germ cell–sertoli cell junctions signaling” and “sertoli cell–sertoli cell junction signaling”. Sertoli cells are obviously not

part of this neurological system, but the blood testis barrier and the BBB share some structural and protein component similarities, namely, components of tight junctions, AJs and gap junctions - which together generate the non-fenestrated barrier between compartments (Abbott et al 2006, Cheng & Mruk 2009). AJ changes in the BBB can affect its permeability (Willis 2011) and are also related to EC motility and angiogenesis (Guo et al 2007, Carmeliet et al 1999), re-enforcing our focus on vascularity and BBB dysfunction, as was also suggested by the hierarchical clustering.

An alternative interpretation to AJ changes in nervous system can be due to re-modeling of synaptic junctions, where the synapses are held together by AJ's (Yap et al 1997), as part of epilepsy related plasticity changes.

"Acute phase response signaling" was another pathway suggested by our study. Although this pathway might have relevance to epilepsy, our study, due to its experimental design, lacks the potential of finding systemic changes (in the blood) such as acute phase response. However, this pathway, which is represented by a group of modulated plasma proteins, might be mistakenly indicated in cases where there is increased vascularity or BBB dysfunction.

"Semaphorin signaling in neurons" and "axonal guidance signaling" found in our Ingenuity analysis, have a high degree component overlap. In a meta-analysis of refractory epilepsy transcription studies, Mirza et al 2011 found these pathways to be up-regulated. We have identified several proteins involved in these pathways, including multiple isoforms of the collapsin response mediator protein (CRMP) family. The CRMP family is homologous to dihydropyrimidinase, an enzyme responsible for uracil and

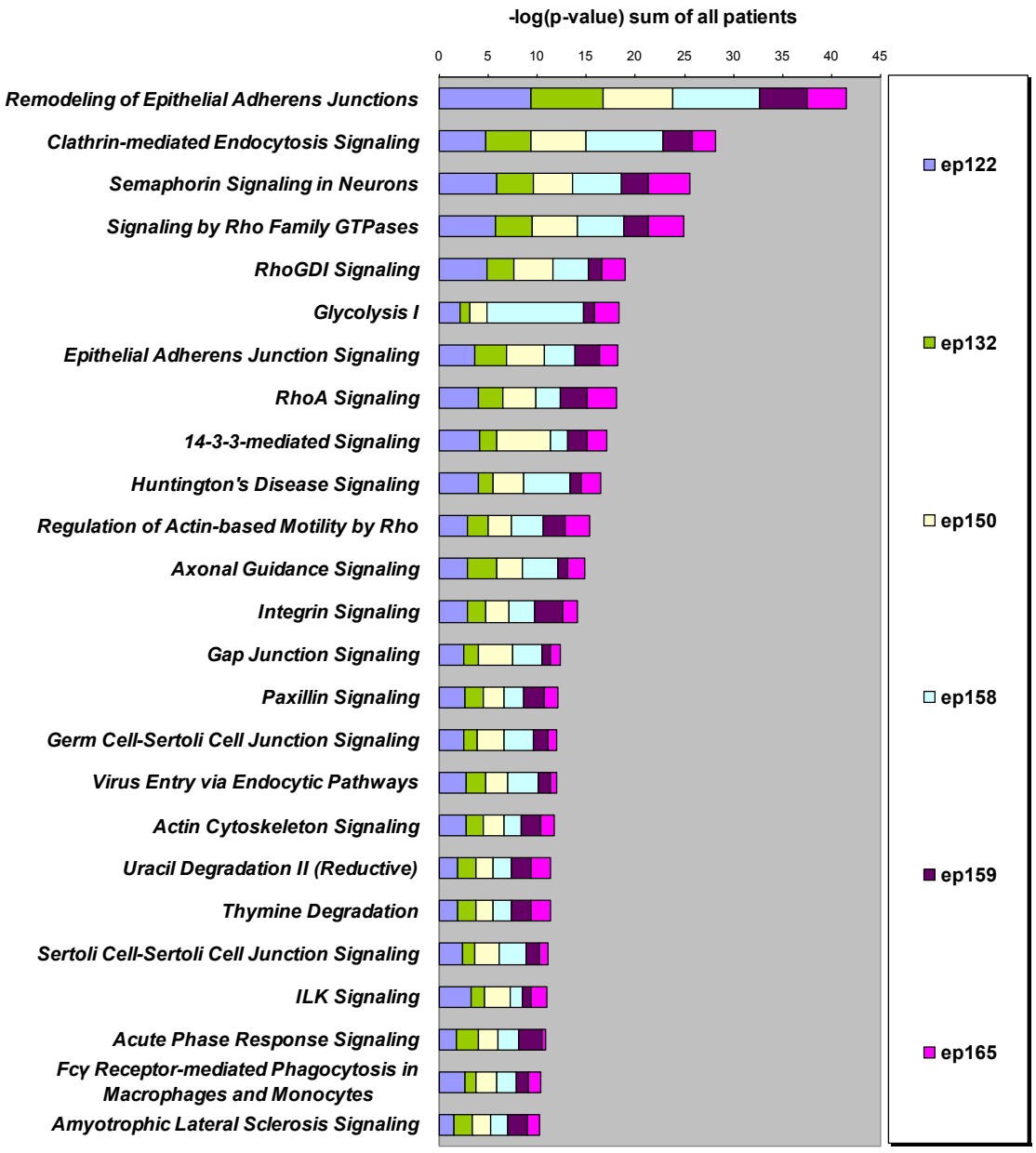

Figure 12: Canonical Pathways Involved in Refractory Epilepsy. Top 25 canonical pathways involved in refractory epilepsy, predicted with Ingenuity Pathway Analysis

thymine degradation, explaining the identification of these degradation pathways in our analysis. Of potentially great interest is CRMP2 (formally, dihydropyrimidinase-like protein-2 or DPYSL2), which we found to be up-regulated in high spiking tissues. CRMP2 is the most abundant and studied member of the CRMPs. It is known to have multiple neurological roles, and to be involved in several neuropathology conditions (Hensley et al 2011). The CRMP2 antagonist, Lacosamide, is specifically used to treat refractory partial epilepsy seizures, by mechanisms that might involve stabilization of neuronal firing through voltage-gated sodium channels regulation, or inhibition of abnormal axon sprouting (Kelemen & Halász 2010, Freitag et al 2007, Wilson et al 2012).

Biological Significance of Statistically Changing Proteins

As discussed earlier, understanding the biological significance of the change in a single protein in a proteomics study can be challenging. Therefore, we combined the statistically changing protein spots and the commonly changing spots ("noisy spots") for hierarchical clustering and pathway analyses. After the prediction of the histological modifications and cellular pathways involved in high spike frequency tissues, described above, we now return to some of the statistically changing proteins, not yet discussed, to re-assess our understanding of the origins of the changing processes. Guanine nucleotide-binding protein G(o) subunit alpha (GNAO1) and LIM And SH3 protein 1 (LASP1), are both involved in multiple cellular pathways. Our study did not elucidate a single pathway which clearly indicated the biological significance of the observed down regulation in

high spike tissue of GNAO1 and LASP1. However, we demonstrated that the expression patterns of GNAO1 in the P2 fraction and LASP1 in the P1 fraction are similar to those of the insoluble 50kDa GFAP and CRYAB isoforms (see clusters 1 & 13 respectively in table S3 in supplementary material). These GFAP and CRYAB changes were attributed to changes in GFAP positive astrocytes, earlier in the discussion, which also suggests that the changes in GNAO1 and LASP1 expressions may be of astrocytic origin.

Two neuronal phosphoproteins, alpha synuclein (SNCA) and synapsin II (SYN2), were up-regulated in high spike tissues. Both proteins might be involved in multiple pathways and processes. Neuritogenesis and synaptic transmission are of special interest, since both of these proteins localize in the presynaptic terminal and interact with cytoskeleton proteins in the nerve growth cone (Hashimoto et al 2002, Fornasiero et al 2010). SYN2 involvement in epilepsy is also suspected, since certain genetic variants of this protein contribute to the predisposition to epilepsy, as well as its differential effect on inhibitory and excitatory synapses (Fassio et al 2011). Another phosphoprotein stathmin1 (STMN1), which is involved in microtubule regulation, was found here to be up-regulated in high spiking tissues. Zhao et al (2012) found over-expression of STMN1 in the neocortex of patients with intractable temporal lobe epilepsy, when compared with neocortex of normal temporal lobes. They used immunoassays to localize the changes in STMN1 expression to neurons and suggested that STMN1 participates in neurite sprouting and synapse remodeling. Taken together, our results might indicate increased neurite sprouting and synapse remodeling in the high spike brain areas. In fact, our

recent study supports this interpretation, showing quantitative, layer-specific increases in presynaptic nerve terminals in epileptic brain regions (Beaumont 2012).

Further studies are needed to capture the nature of the posttranscriptional and posttranslational modifications of some of the protein spots and to validate and extend the suggested changes in cytoarchitecture of high frequency spiking brain areas.

Conclusions

This study compared the protein expression of low vs. high frequency interictal spiking in nearby human brain neocortex tissues from the same individuals, as part of the Systems Biology of Epilepsy Project. The focus on tissues with abnormal electrophysiology allows for differentiation of proteomic changes specifically associated with epileptic activity and not due to less localized secondary responses, such as inflammation or gliosis. We combined proteomic, statistical and bioinformatics tools to predict important histological changes and cellular pathways that associate with the abnormal electrophysiology. We found a decrease in astrocyte markers in the high spiking regions to be the only common histological change in all patients. Furthermore, the increase in spike frequency in different patients was strongly related to the level of decreased GFAP, astrocyte marker, suggesting causality between astrocytic reduction and abnormal electrophysiology.

Contrary to what is thought for forms of hippocampal epilepsy, where there is a diffuse increase in astrogliosis (astrocyte increases), our study suggests that the brain insults that trigger epilepsy in the neocortex are associated with an astrocytic reduction.

The reduction of reactive astrocytosis (GFAP) in regions of higher spiking suggests that these cells may actually protect the neocortex from epileptic discharges, rather than cause them. In contrast to a decrease in astrocytes, regions of high spiking neocortex showed an increase in vascularity. The lack of increased vascularity in patients who exhibit astrocytic reduction, might suggest that the angiogenesis observed is secondary to astrocytic changes.

This study is the first to correlate proteomic changes directly with in vivo recorded electrical brain activities that for the first time provides precise relationships between different regions of the neocortex which produce epileptic activities. This type of analysis has not been done for the hippocampus and may suggest that local regions of the hippocampus with extensive gliosis may not in fact be as epileptically active as nearby hippocampal areas with less gliosis.

The integration of the proteomic data with the clinical, histological and other high-throughput studies of Systems Biology of Epilepsy Project is leading to the discovery of a cellular interactome of epileptic neocortex. Such an interactome is expected to extend and deepen our understanding and derive new, knowledge based, hypotheses for epileptogenic mechanisms and therefore possibly new therapeutic opportunities.

TRENDS OF GLIAL FIBRILLARY ACIDIC PROTEIN ISOFORM EXPRESSION IN HUMAN EPILEPTIC NEOCORTEX

Introduction

Glial fibrillary acidic protein (GFAP) is the major intermediate filament of mature astrocytes and is frequently used as a biomarker for astrocytes and astrogliosis (Eng 1985). Its expression increases with age or can be stimulated by a wide range of insults and pathophysiological states, which also increase the proportion of the soluble GFAP (Fahrig 1994). Since this protein is involved in the astrocytic cytoskeleton, changes in expression of GFAP might affect the astrocyte function and structure.

Origin of Focus Interest in GFAP

Our interest in GFAP was generated from findings in our proteomic study (see chapter 2), which used 2D-DIGE to compare protein expression of high spiking neocortex to a nearby, more normal, brain sample from the same patient with refractory epilepsy, going through resective surgery. Changes in GFAP expression between high and low spiking tissue were found in all three subcellular fractions (P1, P2, Cytosolic), and each of the fractions resolved multiple GFAP isoforms, which we have divided into two groups by their molecular weight (~50kDa & lower molecular weight (LMW)). Expression GFAP in the P2 fraction was lower and mostly followed the same trends of the P1 fraction, therefore we focused on the P1 and cytosolic fractions for our further GFAP investigations. The summary of findings from our proteomic study is shown in table 4.

Cellular fraction / Isoform group	Nuclear	Soluble
~50kDa GFAP	↓in high spiking. * - all isoform spots. †	↓in high spiking. * - 4 more acidic spots
LMW GFAP	Mostly ↑in high spiking. Clustered (co-expressed) with vascularity	Mixed expression patterns
Total GFAP ‡	↓in high spiking. *†	↓in high spiking

Table 4. Summary of GFAP Findings from Our Proteomic Study. ↑, ↓ - up or down regulation respectively. * - change in regulation was statistically significant. †- exhibited negative correlation between the change in regulation (High/Low spiking) and the change in spiking frequency (High-Low spiking). ‡ - soluble to nuclear ratio predicted the histopathology level of white matter gliosis for each patient.

These findings may be very significant in the field of epilepsy research, primarily since the down regulation of GFAP in the epileptogenic zone (EZ) mostly contradicts the consensus association of epilepsy with gliosis (Oberheim et al 2008). We believe this contradiction arises from the lack of ability of the previous study models to separate secondary gliosis (due to inflammation) from the primary cause or cellular changes which cause the EZ. Furthermore, the reciprocal relationship between levels of GFAP and spiking frequency (see Figure 10D and table 4) suggesting causality and a possible protective role of GFAP (or astrocytes) in the EZ.

Many previous papers described LMW GFAP bands on one dimensional (Eng 1985, Newcombe et al 1986, Malloch et al 1987) or two dimensional (Muntané et al 2006, Korolainen et al 2005) western blots. Although these are generally regarded as proteolytic products of GFAP, their occurrence between 36kDa and 50kDa probably has

a biological reason and suggests that these LMW isoforms have possible biological function. In our proteomic study, one of the observations from hierarchical clustering of all spots by their expression patterns was that the P1 (i.e. cytoskeletal and non-soluble) LMW GFAP isoforms clustered with the protein group that indicated and was validated as indicating increased vascularity. Astrocytic foot processes are part of the blood brain barrier. Thus finding GFAP in the group that represents changes in vascularity is not surprising, but this co-expression was only true for the LMW isoforms and not for the canonical 50kDa GFAP, which might suggest a structural difference between GFAP in the astrocyte soma and the GFAP in the perivascular astrocytic foot.

Study Approach and Aims

Taken together, the different expression patterns of the multiple GFAP isoforms, in different subcellular fractions, under different levels of astrogliosis, made it clear that GFAP is a complicated protein. Our approach was to first further characterize the GFAP expression, which we hoped will lead to a better targeted experimental design in future studies, aimed at answering questions that arose from our proteomic study.

A highly detailed histochemical study is needed to answer questions regarding the spatial distribution of astrocytic changes that was indicated in our proteomic study and to specifically define the GFAP and astrocyte (by different biomarkers) distributions, size and numbers in the epileptogenic neocortex, comparing High and Low spiking tissue. This part of the study will be carried out in the future. Further proteomic characterization can provide molecular background to help explain histological findings and the observed expression patterns.

Aim One – Mapping the GFAP Isoforms: since our previous study focused on differentially expressed proteins in the epileptogenic neocortex, our first purpose here was to follow all the GFAP isoforms expressed in both nuclear and soluble fractions of normal and reactive (astrogliosis) human brain tissues.

Aim Two – Expression Pattern Study: to identify common expression patterns between the expressed isoforms and try to relate those to amino acids modifications in the proteins.

Materials and Methods

Quantitative Analyses of GFAP Isoforms

The quantitative analyses in this chapter were an extension of the work done to quantitatively address the changes in GFAP in chapter two. See the previous chapter for description of sample sources and preparations, 2D-DIGE and analysis using total spot volume normalization.

Qualitative Analysis of GFAP Isoform Distribution

Human Brain Samples and Processing. Four human neocortical brain samples, which were surgically removed from refractory epilepsy patients, were provided by the SBEP tissue depository. Note that samples were from different individuals than in the previous proteomic studies and therefore the electrophysiology was not considered. Instead, samples were selected for different levels of astrogliosis, which was assessed by

immunohistochemistry. Subcellular fractionation procedures and protein extraction and quantitation were described earlier in chapter 2.

2D Gels and Western Blots. Protein visualization with 2D gels and western blots was done as described in chapter 2 with a few modifications. Internal standards (IS), containing equal amounts of all samples were made for each (P1 and Cyt) fraction and labeled with Cy2 fluorescent dye. Each one of the samples (4 brain samples x 2 fractions, P1 and Cyt) was labeled with Cy3 and co-resolved with the internal standard on a medium range 4-7 IPG on a large format (24cm x 18cm x 1.5mm) 11% Gels, as previously described.

After imaging, the resolved proteins were blotted on 20x20cm Hybond-P membranes (GE Healthcare), using a Trans blot Plus cell (Biorad), following the recommended procedure by the manufacturer (Biorad). The rest of the procedure was done as described in chapter 2 with some modifications. We used rabbit polyclonal anti GFAP antibody, which was diluted to 1:10,000 (Dako) and goat anti rabbit IgG Dylight (Thermo scientific) at 1:20,000. The membranes were imaged as described in chapter 2. Progenesis SameSpots and PG-240 software (nonlinear dynamics) were used for image processing and alignment.

Mass Spectrometry Study of GFAP

The most intense spot of 50kDa GFAP was manually picked from preparative gels, as earlier described. We used three proteases in parallel attempts to sequence the full protein. Tryptic digestion was performed as described earlier. In addition, the

endoproteinases Glu-C (V8) and ASP-N (Sigma) were, used as recommended by the vendor technical bulletin. Peptide extracts from all three proteolytic procedures were analysied by LC-MS/MS (Chip LC C-18 reverse-phase column), as described earlier. In addition, some tryptic and V8 samples were sent to Agilent for analysis using a Q-TOF with Chip LC HILIC column, seeking to investigate the most polar peptides and modified peptides.

Results

GFAP Isoform Distribution

Labeling the samples with fluorescence dyes, allows for perfect alignment of the western blot signals to the 2D-DIGE analysis (see Figure 13), and due to the amplification of the western blot signal with fluorescence secondary antibody, we were able to show that the GFAP isoforms, which generated our interest in the protein (50kDa and LMW GFAP), represent the two main GFAP isoform trains in the human neocortex samples. The two major trains, also denoted as “Heavy” and “light” GFAP by their respective molecular weights, and isoform trains of several intermediate proteolytic products with lower intensity were consistently found in all samples, regardless of subcellular fraction or astrogliosis levels (Figure 14).

This specific experimental design, which includes a fluorescently labeled internal standard, to improve the alignment accuracy, slightly compromised the quantitation using western blots, since the proteins from both the target sample and the internal standard were blotted and therefore contributed to the GFAP western signals. For that reason, we

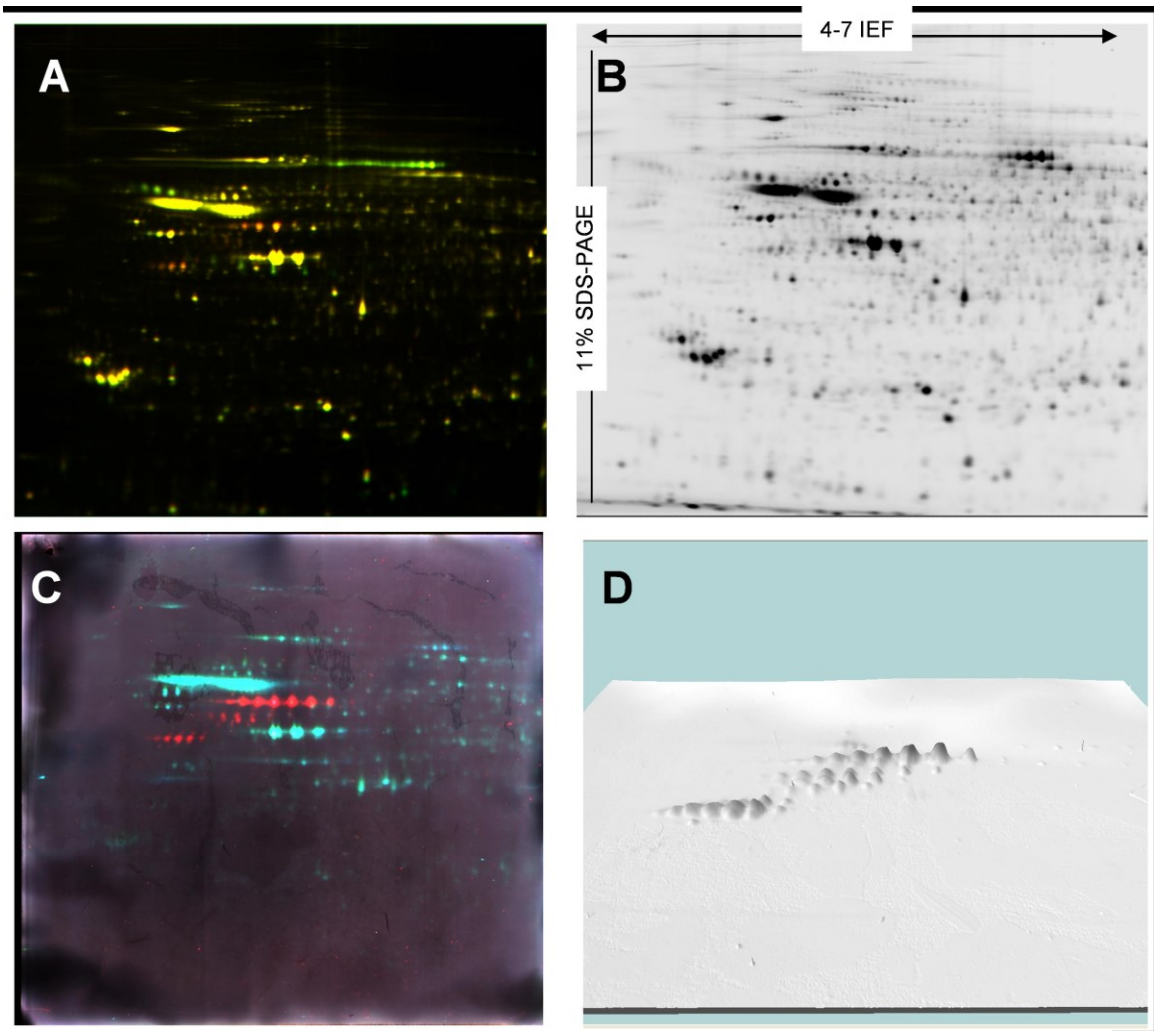

Figure 13. GFAP Isoform Distributions. A and B are representative 2D- Gel images of the nuclear fraction from human epileptic neocortex with astrogliosis, showing fluorescence images overlays of nuclear samples overexpressing GFAP (in red) with IS (green) (A) or IS alone (B). C and D are representative images of the 2D-western blot. Three fluorescence images overlay: IS in blue, nuclear sample with astrogliosis in green and secondary fluorescent antibody to the primary anti-GFAP in red (C) and 3D western blot image (D).

also validated the specific isoform distribution, using the more quantitative fluorescence overlays of each sample with its IS (for example see Figure 13A).

Due to the western blot signals being nonlinear and slightly compromised by our experimental design, leading to lowered quantitation power, and in addition to the low

intensity of intermediate GFAP isoforms trains in the analytical gels, further analysis was therefore returned to the Heavy and Light GFAP from the much larger proteomic dataset described in chapter 2.

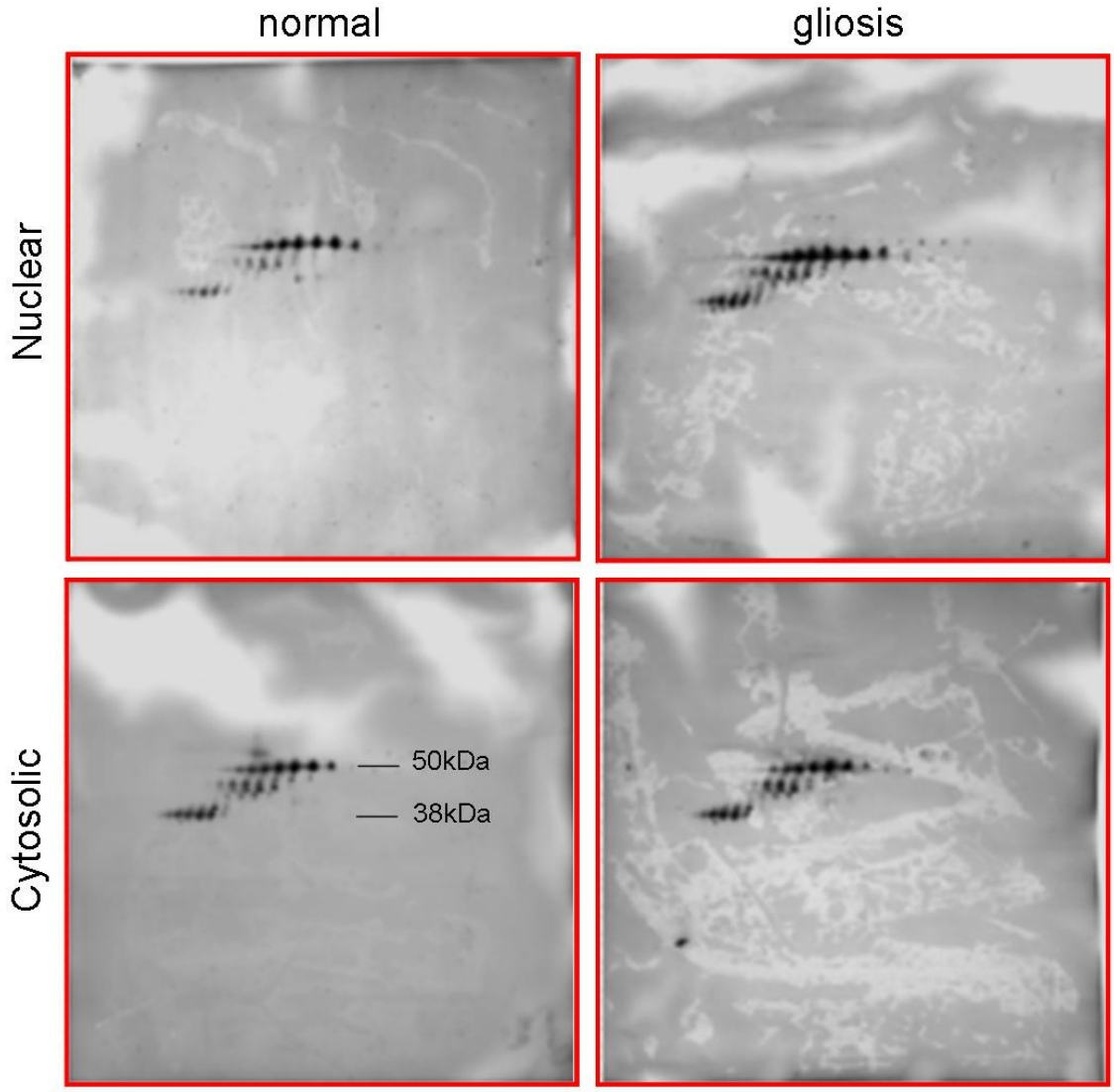

Figure 14. Qualitative Comparison of GFAP Isoform Distribution under Different Conditions.

GFAP Isoform Expression Patterns and Relationships

Some of the GFAP expression patterns that were related to spiking and gliosis levels, were already discussed in chapter 2 and are summarized in table 4 above. In the next step we investigated the relationship of Heavy and Light GFAP isoform spot trains. Figure 15A shows the total GFAP in our 24 samples (6 patients, 2 spiking levels, 2 subcellular fractions). As expected from the involvement of GFAP in the cytoskeleton, we observed higher GFAP concentration in the nuclear (P1) fraction in all but one patient, who had marked gliosis. The ratio of Light to Heavy GFAP isoforms trains was generally higher in the cytosolic fraction, when compared with the nuclear fraction of the same patient. The exceptions to this observation were generally samples that had low GFAP expression and therefore their ratios were presumably more highly affected by background noise.

Investigations of isoform patterns within each train (Heavy and Light) have not yielded any conclusions, though we did find a correlation of the acidic shift in the Heavy train with the increase in the ratio of the Light and Heavy GFAP isoforms trains (Figure 16). This correlation was limited to the cytosolic fraction.

GFAP Mass Spectrometry Study

After recognizing the correlation of the acidic shift of the cytosolic Heavy GFAP train increased in proportion to the Light GFAP train, the next step was to use MS to investigate the proteolytic process leading to the Light train and the amino acid (AA) modifications leading to the acidic shift. For that purpose we used MS files from our

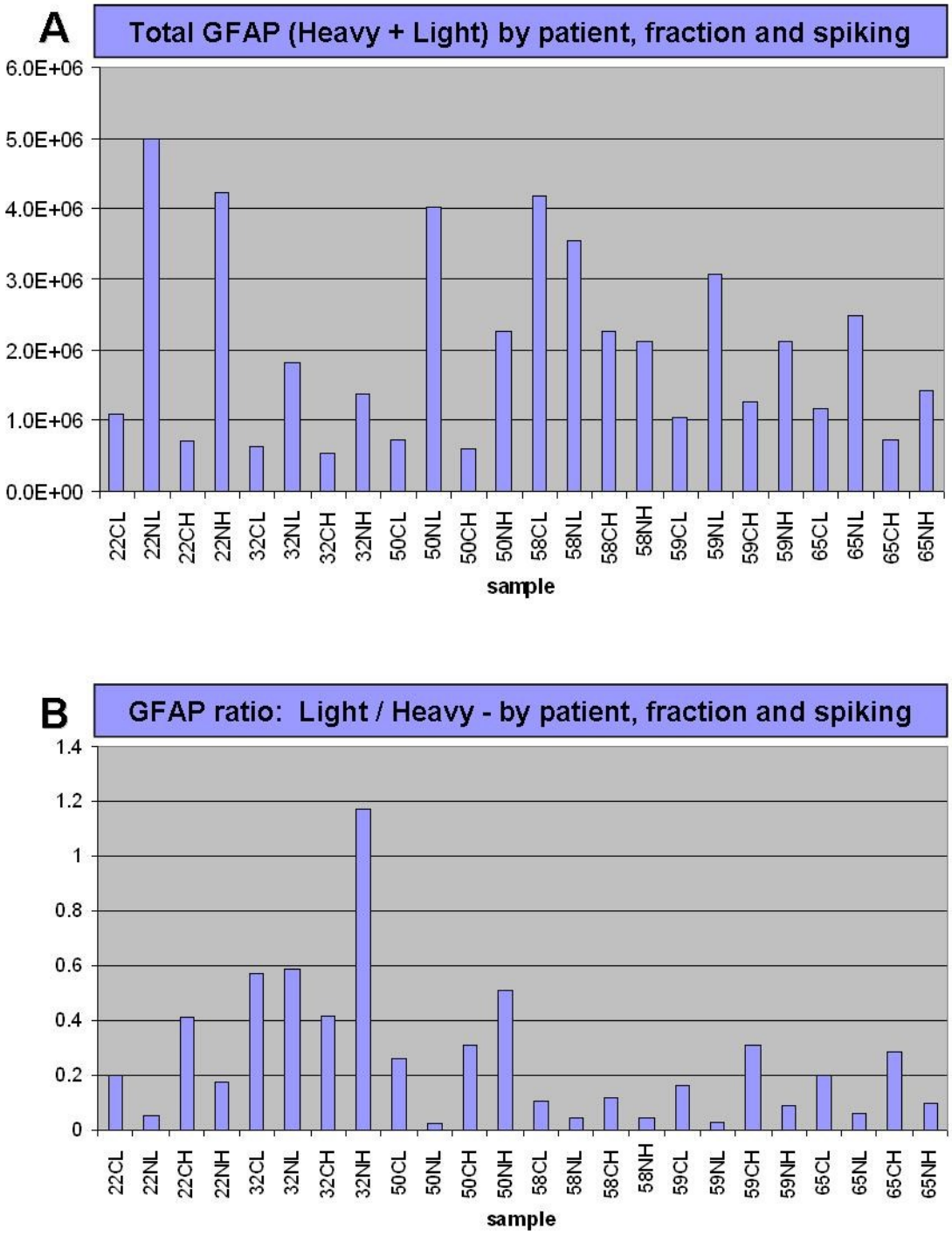

Figure 15. Quantitative GFAP – Trains and Trends. Total GFAP (A) and ratio of light to heavy GFAP (B) by patient #(22, 32,50,58,59,65), fraction (C- cyt, N- nuclear) and spiking level (L- low, H- high).

previous study (chapter 2), as well as several new MS analyses, using preparative human neocortex samples described in this chapter.

By comparing the matching identified peptides of Heavy and Light trains, we predicted the proteolytic process observed is cleaving peptides mostly from the N-terminal region of the protein, which is the "head" domain of the filament monomer. Our sequence coverage was from AA 13-405, and 76-390 (432 AA in native protein) for Heavy and Light GFAP spots, respectively (Image 17). Three proteases, Trypsin, AspN and GluC were used individually as well as reverse phase and hydrophilic interaction liquid chromatography (HILIC) in attempts to obtain the maximum coverage of the most intense Heavy train spot, which lead to the coverage of 77% of the sequence, though neither of the N terminal or the C terminal ends were found, as shown in Figure 17.

Discussion

Comparison of Our Findings with the Literature

Glial fibrillary acidic protein is an important protein for normal astrocytic function. The regulation and modification of GFAP occurs at several levels, which highly increases the complexity of the protein expression. Mutations in the GFAP gene can lead to Alexander disease (Brenner et al 2001), there are multiple human GFAP splice isoforms (Middeldrop & Hol 2011), and an array of known GFAP PTMs including highly studied multiple phosphorylations (Takemura et al 2002, Inagaki et al 1994, Korolainen et al 2005), glycosylation (Korolainen et al 2005), citrullination (Nicholas et al 2004), and more.

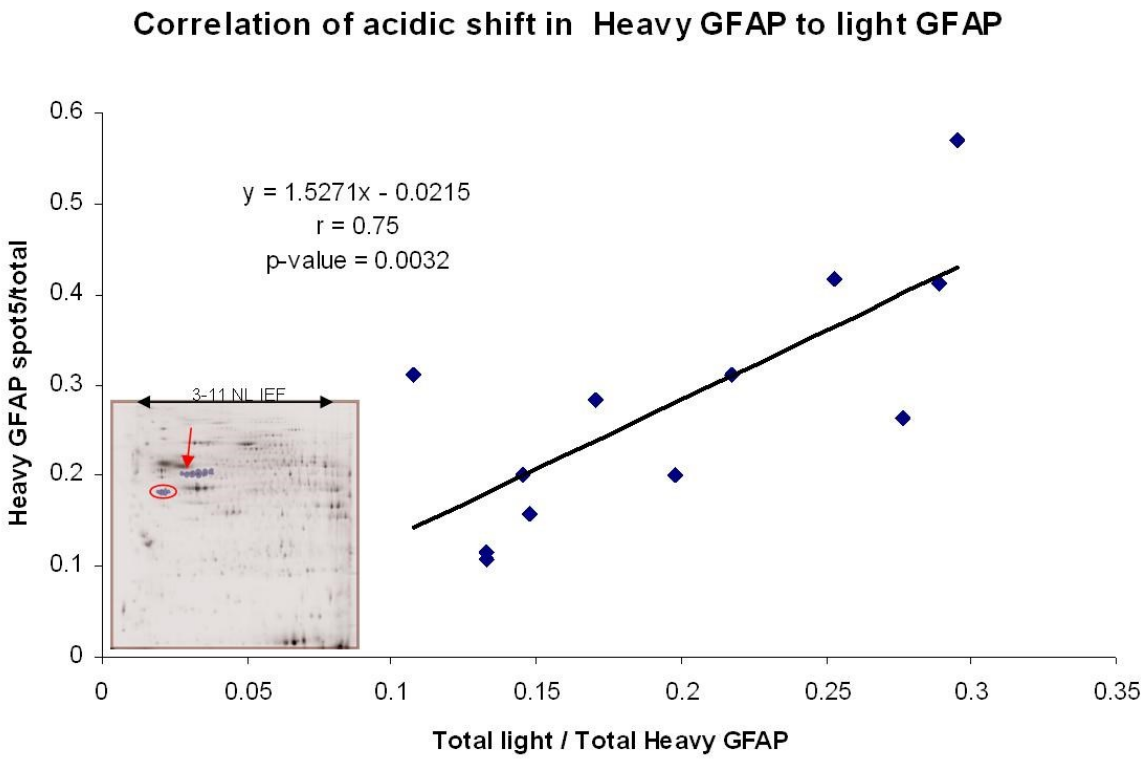

Figure 16. Correlation of Acidic Shift in Heavy GFAP Train to the Ratio of Light (red circle) to Heavy GFAP isoforms trains. The acidic shift is expressed as the proportion of the acidic spot 5 (pointed by the red arrow) relative to the total Heavy train volume.

Our GFAP isoform distribution turned out to be highly comparable with human cortex GFAP isoform distributions found by others (Muntané et al 2006, Korolainen et al 2005). The qualitative analysis suggests that the GFAP isoform distribution (number of isoforms and the spatial location on the 2-D map) is not changing between the cytosol and nuclear subcellular fractions, nor is it affected by gliosis. These findings were in limited number of observations and were compromised by internal standards in the western blots, as discussed earlier and therefore, a more refined experiment, design for visualization of detailed GFAP distributions, based on our experience, but with even better resolution, should be considered.

GFAP assembly and disassembly are controlled by phosphorylation and de-phosphorylation at multiple sites and by multiple enzymes (Inagaki et al 1994, Tsujimura et al 1994). Phosphorylation inhibits the assembly of GFAP monomers and controls the disassembly of the polymeric filaments. Each phosphorylation shifts the isoelectic point and is resolved on the 2D gels and it is therefore not surprising that the nuclear, non-soluble polymeric GFAP expresses so many isoforms. Beside the different combinatorial options with other PTMs that affect the protein pI, multiple phosphorylations are plausible in tissues that contain active astrocytes with active cytoskeletons.

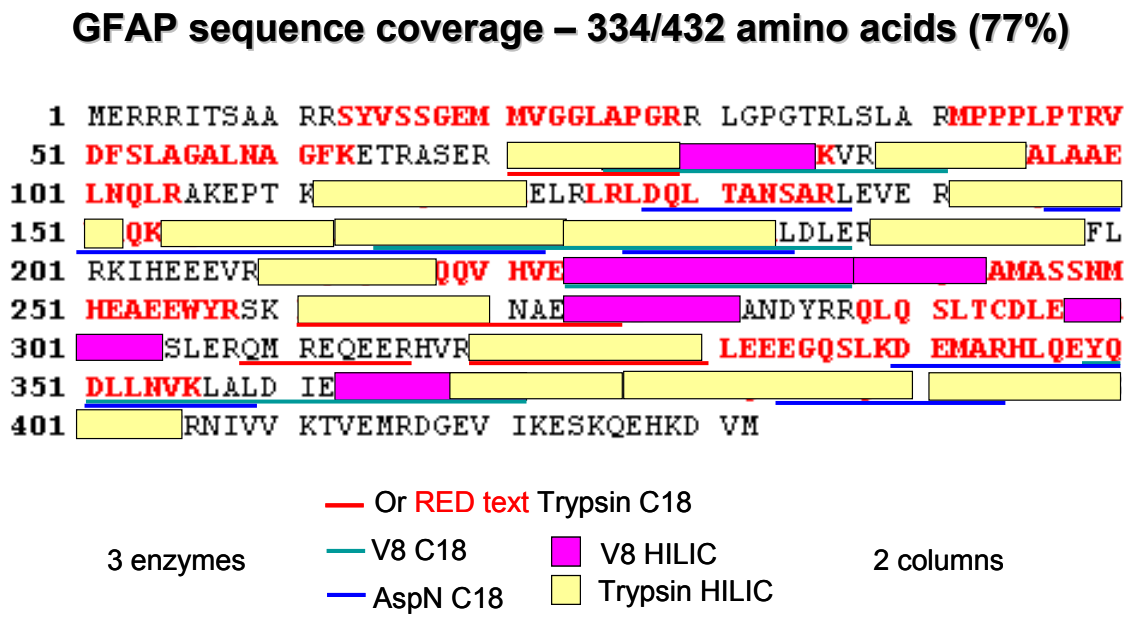

Figure 17. Sequence Coverage of the most Intense Spots in Heavy GFAP Spot Train.

Our findings that shift from nuclear polymeric to soluble isoforms and shift to more acidic modified isoforms appear to be correlated with increased degradation, are in agreement with the findings of Porchet et al (2003) who studied GFAP in aging and Alzheimer diseased human cortex. A possible molecular explanation for these findings is

given by Takemura et al (2002), who describes the protective role of GFAP phosphorylation in reducing the protein turnover rate. If our observed acidic shift is due to phosphorylation, than it is possible that the less phosphorylated (more basic) isoforms are more easily targeted for proteolytic processing, which results in increased relative proportion of the acidic isoforms in the Heavy train, as well as the increased ratio of Light to Heavy spot trains we observed.

Prospective Approach and Experiments Plans

We have not, so far, gained any explicit knowledge to help explain our previous observations regarding the decrease in nuclear Heavy train GFAP and the clustering of Light train GFAP with increased vascularity in the epileptogenic zone.

It might be expected that the decrease in nuclear 50kDa GFAP is governed by posttranslational modification of the protein rather than at the transcription level, based on the lack of differential GFAP findings in the SBEP transcriptomic study (Loeb JA, unpublished data) and based on the multiple modifications that are known to control the filament assembly. One specific GFAP modification we suspect in our sample and were not yet able to detect is citrullination. This is a specific arginine modification that causes an acidic shift in the isoelectric point by elimination of the positive charge. The GFAP filament monomer head is highly crowded with arginines and their citrullination might interfere with assembly / disassembly processes by affecting the accessibility of the phosphoenzymes or by other mechanisms. Intermediate filaments are common targets for citrullination and in human cortex GFAP citrullination was detected in Alzheimer disease and Multiple sclerosis (Nicholas et al 2004, Ishigami et al 2005). The mechanism

Nicholas and Ishigami proposed for pathological effects of GFAP citrullination were by promoting filament disassembly and by enhancing to immune response.

We suspect citrullination to occur in the N terminal region of GFAP since citrullin is present in the non-truncated 50kDa GFAP (Nicholas et al 2004). We were not able to detect the N-terminal peptides so far by mass-spectrometry and we might be able to validate this modification using an anti-citrullin antibody. We could not find a reliable commercially available citrullin antibody and are now in the process of establishing a collaboration to secure the appropriate reagents. Another promising avenue for future investigations will be additional MS studies, using optimization for detection of citrullinated peptides, phosphorylation state, and other modifications, such as electron transfer dissociation.

Conclusion

Some characterization of GFAP isoforms and the correlation of the isoforms with eleptogenesis were gained in this work. This knowledge might contribute to better understanding of GFAP in epilepsy and in other neurological diseases. This study assists in re-focusing and re-directing future experiments. The combination of proteomic and mass spectrometry with immunochemistry and histoimmunology are more promising directions for full characterization of GFAP isoforms in the human brain epileptic neocortex.

CONCLUSIONS AND PERSPECTIVES

This project is the first proteomic analysis of electrically mapped human brain tissue associated with epileptic seizures, compared to nearby much less electrically active brain tissue from the same individuals. This strategy was made possible as part of the multidisciplinary Systems Biology of Epilepsy Project. Other research groups in the project are characterizing histology, messenger RNA expression, long non-coding RNA expression and metabolomic abnormalities in the patient samples. As this data is assembled, the next step will be to integrate the data into systems biology models that can stimulate validation experiments and perhaps new approaches to prevention of the development of epilepsy after brain insults or to discover more effective pharmaceutical treatments.

We identified numerous human brain proteins and protein isoforms in nuclear, membrane and cytosolic fractions. Many of the isoforms identified did not have the molecular weight or isoelectric point that is predicted from the full transcript of the parent gene, pointing to the importance of proteolytic modification or other substantial posttranslational modification of these protein species. The identification of this body of proteins and the clusters of proteins that vary together may be useful to other investigators who are striving to understand the mechanisms of epilepsy and eliptogenesis as well as other neurological diseases.

This project illustrates advantages of proteomics using differential 2D gel analysis to reveal changes in patterns of intact protein expression levels and posttranslationally modified protein isoforms, between different tissues. For example, a major finding is the

changes in isoforms of the protein GFAP that are correlated with electrical spiking frequency in the brain regions that are associated with epileptic seizures. Such patterns of modified protein isoforms would tend to be missed by the widely used shotgun proteomics methods, which digest all the proteins to peptides and uncouple many of the combinations of posttranslational modifications, before separation and analysis. Clustering of the protein isoforms by their expression patterns appears to provide more informative findings than changes in single proteins. Another major finding, which was revealed from clustering, is the prediction of increased vascularity in the high-spiking tissues, which was previously unrecognized, but was subsequently confirmed by histology.

The realization that GFAP is implicated in epileptogenesis and elevated electrical spike activity focuses attention on the possible role of brain astrocytes in epileptogenesis. GFAP is a marker for astrocytes and the role of astrocytes in maintaining the blood brain barrier, providing nutrients to neurons, and controlling neuron excitability is being increasingly appreciated in the field. This work also tends to draw attention on the need to characterize the multiple isoforms of the proteins that change in association with epilepsy. It may be that advances in top-down proteomics will facilitate the characterization of the detailed protein modifications that are observed to change in these studies. The next steps in future work are to develop systems biology models of epileptogenesis, drawing on the wide range of –omic data that is being developed by the multidisciplinary research teams in the Systems Biology of Epilepsy Project.

REFERENCES CITED

Abbott NJ, Patabendige AA, Dolman DE, Yusof SR, Begley DJ: Structure and function of the blood-brain barrier. *Neurobiol Dis* 2010, 37(1):13-25.

Abbott NJ, Ronnback L, Hansson E: Astrocyte-endothelial interactions at the blood-brain barrier. *Nat Rev Neurosci* 2006, 7(1):41-53.

Aronica E, Ravizza T, Zurolo E, Vezzani A: Astrocyte immune responses in epilepsy. *Glia* 2012, 60(8):1258-1268.

Asano E, Muzik O, Shah A, Juhasz C, Chugani DC, Sood S, Janisse J, Ergun EL, Ahn-Ewing J, Shen C *et al*: Quantitative interictal subdural EEG analyses in children with neocortical epilepsy. *Epilepsia* 2003, 44(3):425-434.

Beaumont TL, Yao B, Shah A, Kapatos G, Loeb JA: Layer-specific CREB target gene induction in human neocortical epilepsy. *J Neurosci* 2012, 32(41):14389-14401.

Becker AJ, Chen J, Zien A, Sochivko D, Normann S, Schramm J, Elger CE, Wiestler OD, Blumcke I: Correlated stage- and subfield-associated hippocampal gene expression patterns in experimental and human temporal lobe epilepsy. *Eur J Neurosci* 2003, 18(10):2792-2802.

Benarroch EE: Metabotropic glutamate receptors: synaptic modulators and therapeutic targets for neurologic disease. *Neurology* 2008, 70(12):964-968.

Berg AT, Berkovic SF, Brodie MJ, Buchhalter J, Cross JH, van Emde Boas W, Engel J, French J, Glauser TA, Mathern GW *et al*: Revised terminology and concepts for organization of seizures and epilepsies: report of the ILAE Commission on Classification and Terminology, 2005-2009. *Epilepsia* 2010, 51(4):676-685.

Bertram E: The relevance of kindling for human epilepsy. *Epilepsia* 2007, 48 Suppl 2:65-74.

Beyreuther BK, Freitag J, Heers C, Krebsfanger N, Scharfenecker U, Stohr T: Lacosamide: a review of preclinical properties. *CNS Drug Rev* 2007, 13(1):21-42.

Bialer M, White HS: Key factors in the discovery and development of new antiepileptic drugs. *Nat Rev Drug Discov* 2010, 9(1):68-82.

Blume WT, Luders HO, Mizrahi E, Tassinari C, van Emde Boas W, Engel J, Jr.: Glossary of descriptive terminology for ictal semiology: report of the ILAE task force on classification and terminology. *Epilepsia* 2001, 42(9):1212-1218.

Boer K, Middeldorp J, Spliet WG, Razavi F, van Rijen PC, Baayen JC, Hol EM, Aronica E: Immunohistochemical characterization of the out-of frame splice variants GFAP Delta164/Deltaexon 6 in focal lesions associated with chronic epilepsy. *Epilepsy Res* 2010, 90(1-2):99-109.

Bradford MM: A rapid and sensitive method for the quantitation of microgram quantities of protein utilizing the principle of protein-dye binding. *Anal Biochem* 1976, 72:248-254.

Brenner M, Johnson AB, Boespflug-Tanguy O, Rodriguez D, Goldman JE, Messing A: Mutations in GFAP, encoding glial fibrillary acidic protein, are associated with Alexander disease. *Nat Genet* 2001, 27(1):117-120.

Brodie MJ: Road to refractory epilepsy: the Glasgow story. *Epilepsia* 2013, 54 Suppl 2:5-8.

Cacheaux LP, Ivens S, David Y, Lakhter AJ, Bar-Klein G, Shapira M, Heinemann U, Friedman A, Kaufer D: Transcriptome profiling reveals TGF-beta signaling involvement in epileptogenesis. *J Neurosci* 2009, 29(28):8927-8935.

Candiano G, Bruschi M, Musante L, Santucci L, Ghiggeri GM, Carnemolla B, Orecchia P, Zardi L, Righetti PG: Blue silver: a very sensitive colloidal Coomassie G-250 staining for proteome analysis. *Electrophoresis* 2004, 25(9):1327-1333.

Carmeliet P, Lampugnani MG, Moons L, Breviario F, Compernolle V, Bono F, Balconi G, Spagnuolo R, Oosthuyse B, Dewerchin M *et al*: Targeted deficiency or cytosolic truncation of the VE-cadherin gene in mice impairs VEGF-mediated endothelial survival and angiogenesis. *Cell* 1999, 98(2):147-157.

Che Y, Piao CS, Han PL, Lee JK: Delayed induction of alpha B-crystallin in activated glia cells of hippocampus in kainic acid-treated mouse brain. *J Neurosci Res* 2001, 65(5):425-431.

Cheng CY, Mruk DD: An intracellular trafficking pathway in the seminiferous epithelium regulating spermatogenesis: a biochemical and molecular perspective. *Crit Rev Biochem Mol Biol* 2009, 44(5):245-263.

Cray C, Zaias J, Altman NH: Acute phase response in animals: a review. *Comp Med* 2009, 59(6):517-526.

D'Amici GM, Rinalducci S, Zolla L: Depletion of hemoglobin and carbonic anhydrase from erythrocyte cytosolic samples by preparative clear native electrophoresis. *Nat Protoc* 2011, 7(1):36-44.

Danial NN, Hartman AL, Stafstrom CE, Thio LL: How does the ketogenic diet work? Four potential mechanisms. *J Child Neurol* 2013, 28(8):1027-1033.

David Y, Cacheaux LP, Ivens S, Lapilover E, Heinemann U, Kaufer D, Friedman A: Astrocytic dysfunction in epileptogenesis: consequence of altered potassium and glutamate homeostasis? *J Neurosci* 2009, 29(34):10588-10599.

de Curtis M, Jefferys JGR, Avoli M: Interictal Epileptiform Discharges in Partial Epilepsy: Complex Neurobiological Mechanisms Based on Experimental and Clinical Evidence. In: Noebels JL, Avoli M, Rogawski MA, Olsen RW, Delgado-Escueta AV, editors. Jasper's Basic Mechanisms of the Epilepsies [Internet]. 4th edition. Bethesda (MD): National Center for Biotechnology Information (US); 2012.

Diaz-Negrillo A: Influence of sleep and sleep deprivation on ictal and interictal epileptiform activity. *Epilepsy Res Treat* 2013,:492524.

Duchowny MS: Food for thought: the ketogenic diet and adverse effects in children. *Epilepsy Curr* 2005, 5(4):152-154.

Eng LF: Glial fibrillary acidic protein (GFAP): the major protein of glial intermediate filaments in differentiated astrocytes. *J Neuroimmunol* 1985, 8(4-6):203-214.

Engel J, Jr., Pitkanen A, Loeb JA, Dudek FE, Bertram EH, 3rd, Cole AJ, Moshe SL, Wiebe S, Jensen FE, Mody I *et al*: Epilepsy biomarkers. *Epilepsia* 2013, 54 Suppl 4:61-69.

Eun JP, Choi HY, Kwak YG: Proteomic analysis of human cerebral cortex in epileptic patients. *Exp Mol Med* 2004, 36(2):185-191.

Fahrig T: Changes in the solubility of glial fibrillary acidic protein after ischemic brain damage in the mouse. *J Neurochem* 1994, 63(5):1796-1801.

Fassio A, Raimondi A, Lignani G, Benfenati F, Baldelli P: Synapsins: from synapse to network hyperexcitability and epilepsy. *Semin Cell Dev Biol* 2011, 22(4):408-415.

Fisher RS, van Emde Boas W, Blume W, Elger C, Genton P, Lee P, Engel J, Jr.: Epileptic seizures and epilepsy: definitions proposed by the International League Against Epilepsy (ILAE) and the International Bureau for Epilepsy (IBE). *Epilepsia* 2005, 46(4):470-472.

Fornasiero EF, Bonanomi D, Benfenati F, Valtorta F: The role of synapsins in neuronal development. *Cell Mol Life Sci* 2010, 67(9):1383-1396.

Friedman A, Heinemann U: Role of Blood-Brain Barrier Dysfunction in Epileptogenesis. In: Noebels JL, Avoli M, Rogawski MA, Olsen RW, Delgado-Escueta AV, editors. Jasper's Basic Mechanisms of the Epilepsies [Internet]. 4th edition. Bethesda (MD): National Center for Biotechnology Information (US); 2012.

Friedman A, Kaufer D, Heinemann U: Blood-brain barrier breakdown-inducing astrocytic transformation: novel targets for the prevention of epilepsy. *Epilepsy Res* 2009, 85(2-3):142-149.

Friedman A: Blood-brain barrier dysfunction, status epilepticus, seizures, and epilepsy: a puzzle of a chicken and egg? *Epilepsia* 2011, 52 Suppl 8:19-20.

Greenberg DA, Jin K: From angiogenesis to neuropathology. *Nature* 2005, 438(7070):954-959.

Guo R, Sakamoto H, Sugiura S, Ogawa M: Endothelial cell motility is compatible with junctional integrity. *J Cell Physiol* 2007, 211(2):327-335.

Hagemann TL, Boelens WC, Wawrousek EF, Messing A: Suppression of GFAP toxicity by alphaB-crystallin in mouse models of Alexander disease. *Hum Mol Genet* 2009, 18(7):1190-1199.

Hamby ME, Coppola G, Ao Y, Geschwind DH, Khakh BS, Sofroniew MV: Inflammatory mediators alter the astrocyte transcriptome and calcium signaling elicited by multiple G-protein-coupled receptors. *J Neurosci* 2012, 32(42):14489-14510.

Han HA, Cortez MA, Snead OC: GABAB Receptor and Absence Epilepsy. In: Noebels JL, Avoli M, Rogawski MA, Olsen RW, Delgado-Escueta AV, editors. Jasper's Basic Mechanisms of the Epilepsies [Internet]. 4th edition. Bethesda (MD): National Center for Biotechnology Information (US); 2012.

Hashimoto M, Hsu LJ, Rockenstein E, Takenouchi T, Mallory M, Masliah E: alpha-Synuclein protects against oxidative stress via inactivation of the c-Jun N-terminal kinase stress-signaling pathway in neuronal cells. *J Biol Chem* 2002, 277(13):11465-11472.

Healy S, Lang J, Te Water Naude J, Gibbon F, Leach P: Vagal nerve stimulation in children under 12 years old with medically intractable epilepsy. *Childs Nerv Syst* 2013, 29(11):2095-2099.

Heinemann U, Kaufer D, Friedman A: Blood-brain barrier dysfunction, TGFbeta signaling, and astrocyte dysfunction in epilepsy. *Glia* 2012, 60(8):1251-1257.

Hensley K, Venkova K, Christov A, Gunning W, Park J: Collapsin response mediator protein-2: an emerging pathologic feature and therapeutic target for neurodisease indications. *Mol Neurobiol* 2011, 43(3):180-191.

Hertz L, Peng L, Dienel GA: Energy metabolism in astrocytes: high rate of oxidative metabolism and spatiotemporal dependence on glycolysis/glycogenolysis. *J Cereb Blood Flow Metab* 2007, 27(2):219-249.

Inagaki M, Nakamura Y, Takeda M, Nishimura T, Inagaki N: Glial fibrillary acidic protein: dynamic property and regulation by phosphorylation. *Brain Pathol* 1994, 4(3):239-243.

Institute of Medicine (US) Committee on the Public Health Dimensions of the Epilepsies; England MJ, Liverman CT, Schultz AM, Strawbridge LM, editors. Epilepsy Across the Spectrum: Promoting Health and Understanding. Washington (DC): National Academies Press (US); 2012.

Ishigami A, Ohsawa T, Hiratsuka M, Taguchi H, Kobayashi S, Saito Y, Murayama S, Asaga H, Toda T, Kimura N *et al*: Abnormal accumulation of citrullinated proteins catalyzed by peptidylarginine deiminase in hippocampal extracts from patients with Alzheimer's disease. *J Neurosci Res* 2005, 80(1):120-128.

Ivens S, Kaufer D, Flores LP, Bechmann I, Zumsteg D, Tomkins O, Seiffert E, Heinemann U, Friedman A: TGF-beta receptor-mediated albumin uptake into astrocytes is involved in neocortical epileptogenesis. *Brain* 2007, 130(Pt 2):535-547.

Janigro D: Blood-brain barrier, ion homeostatis and epilepsy: possible implications towards the understanding of ketogenic diet mechanisms. *Epilepsy Res* 1999, 37(3):223-232.

Kelemen A, Halasz P: Lacosamide for the prevention of partial onset seizures in epileptic adults. *Neuropsychiatr Dis Treat* 2010, 6:465-471.

Kim JE, Yeo SI, Ryu HJ, Kim MJ, Kim DS, Jo SM, Kang TC: Astroglial loss and edema formation in the rat piriform cortex and hippocampus following pilocarpine-induced status epilepticus. *J Comp Neurol* 2010, 518(22):4612-4628.

Korolainen MA, Auriola S, Nyman TA, Alafuzoff I, Pirttila T: Proteomic analysis of glial fibrillary acidic protein in Alzheimer's disease and aging brain. *Neurobiol Dis* 2005, 20(3):858-870.

Kovacs R, Heinemann U, Steinhauser C: Mechanisms underlying blood-brain barrier dysfunction in brain pathology and epileptogenesis: role of astroglia. *Epilepsia*

2012, 53 Suppl 6:53-59.

Kragh-Hansen U, Chuang VT, Otagiri M: Practical aspects of the ligand-binding and enzymatic properties of human serum albumin. *Biol Pharm Bull* 2002, 25(6):695-704.

Kwan P, Arzimanoglou A, Berg AT, Brodie MJ, Allen Hauser W, Mathern G, Moshe SL, Perucca E, Wiebe S, French J: Definition of drug resistant epilepsy: consensus proposal by the ad hoc Task Force of the ILAE Commission on Therapeutic Strategies. *Epilepsia* 2010, 51(6):1069-1077.

Kwan P, Brodie MJ: Early identification of refractory epilepsy. *N Engl J Med* 2000, 342(5):314-319.

Lilley KS, Friedman DB: All about DIGE: quantification technology for differential-display 2D-gel proteomics. *Expert Rev Proteomics* 2004, 1(4):401-409.

Lipovich L, Dachet F, Cai J, Bagla S, Balan K, Jia H, Loeb JA: Activity-dependent human brain coding/noncoding gene regulatory networks. *Genetics* 2012, 192(3):1133-1148.

Liu JY, Thom M, Catarino CB, Martinian L, Figarella-Branger D, Bartolomei F, Koepp M, Sisodiya SM: Neuropathology of the blood-brain barrier and pharmaco-resistance in human epilepsy. *Brain* 2012, 135(Pt 10):3115-3133.

Liu X, Wen F, Yang J, Chen L, Wei YQ: A review of current applications of mass spectrometry for neuroproteomics in epilepsy. *Mass Spectrom Rev* 2010, 29(2):197-246.

Lockman J, Fisher RS: Therapeutic brain stimulation for epilepsy. *Neurol Clin* 2009, 27(4):1031-1040.

Loeb JA: A human systems biology approach to discover new drug targets in epilepsy. *Epilepsia* 2010, 51 Suppl 3:171-177.

Loeb JA: Identifying targets for preventing epilepsy using systems biology. *Neurosci Lett* 2011, 497(3):205-212.

Loscher W, Klitgaard H, Twyman RE, Schmidt D: New avenues for anti-epileptic drug discovery and development. *Nat Rev Drug Discov* 2013, 12(10):757-776.

Loscher W: Animal models of epilepsy for the development of antiepileptogenic and disease-modifying drugs. A comparison of the pharmacology of kindling and post-status epilepticus models of temporal lobe epilepsy. *Epilepsy Res* 2002, 50(1-

2):105-123.

Loscher W: Critical review of current animal models of seizures and epilepsy used in the discovery and development of new antiepileptic drugs. *Seizure* 2011, 20(5):359-368.

Luders HO, Amina S, Baumgartner C, Benbadis S, Bermeo-Ovalle A, Devereaux M, Diehl B, Edwards J, Baca-Vaca GF, Hamer H *et al*: Modern technology calls for a modern approach to classification of epileptic seizures and the epilepsies. *Epilepsia* 2012, 53(3):405-411.

Maaty WS, Lord CI, Gripentrog JM, Riesselman M, Keren-Aviram G, Liu T, Dratz EA, Bothner B, Jesaitis AJ: Identification of C-terminal phosphorylation sites of N-formyl peptide receptor-1 (FPR1) in human blood neutrophils. *J Biol Chem* 2013, 288(38):27042-27058.

Maaty WS, Steffens JD, Heinemann J, Ortmann AC, Reeves BD, Biswas SK, Dratz EA, Grieco PA, Young MJ, Bothner B: Global analysis of viral infection in an archaeal model system. *Front Microbiol* 2012, 3:411.

Malloch GD, Clark JB, Burnet FR: Glial fibrillary acidic protein in the cytoskeletal and soluble protein fractions of the developing rat brain. *J Neurochem* 1987, 48(1):299-306.

Mani R, Pollard J, Dichter MA: Human clinical trials in antiepileptogenesis. *Neurosci Lett* 2011, 497(3):251-256.

Mantuano E, Mukandala G, Li X, Campana WM, Gonias SL: Molecular dissection of the human alpha2-macroglobulin subunit reveals domains with antagonistic activities in cell signaling. *J Biol Chem* 2008, 283(29):19904-19911.

Marchi N, Angelov L, Masaryk T, Fazio V, Granata T, Hernandez N, Hallene K, Diglaw T, Franic L, Najm I *et al*: Seizure-promoting effect of blood-brain barrier disruption. *Epilepsia* 2007, 48(4):732-742.

Marchi N, Granata T, Ghosh C, Janigro D: Blood-brain barrier dysfunction and epilepsy: pathophysiologic role and therapeutic approaches. *Epilepsia* 2012, 53(11):1877-1886.

Martinian L, Boer K, Middeldorp J, Hol EM, Sisodiya SM, Squier W, Aronica E, Thom M: Expression patterns of glial fibrillary acidic protein (GFAP)-delta in epilepsy-associated lesional pathologies. *Neuropathol Appl Neurobiol* 2009, 35(4):394-405.

Masino SA, Rho JM: Mechanisms of Ketogenic Diet Action. In: Noebels JL, Avoli M, Rogawski MA, Olsen RW, Delgado-Escueta AV, editors. Jasper's Basic Mechanisms of the Epilepsies [Internet]. 4th edition. Bethesda (MD): National Center for Biotechnology Information (US); 2012.

McNamara JO, Huang YZ, Leonard AS: Molecular signaling mechanisms underlying epileptogenesis. *Sci STKE* 2006, 2006(356):re12.

Middeldorp J, Hol EM: GFAP in health and disease. *Prog Neurobiol* 2011, 93(3):421-443.

Mirza N, Vasieva O, Marson AG, Pirmohamed M: Exploring the genomic basis of pharmacoresistance in epilepsy: an integrative analysis of large-scale gene expression profiling studies on brain tissue from epilepsy surgery. *Hum Mol Genet* 2011, 20(22):4381-4394.

Morace R, Di Gennaro G, Picardi A, Quarato PP, Sparano A, Mascia A, Meldolesi GN, Grammaldo LG, De Risi M, Esposito V: Surgery after intracranial investigation with subdural electrodes in patients with drug-resistant focal epilepsy: outcome and complications. *Neurosurg Rev* 2012, 35(4):519-526; discussion 526.

Morin-Brureau M, Lebrun A, Rousset MC, Fagni L, Bockaert J, de Bock F, Lerner-Natoli M: Epileptiform activity induces vascular remodeling and zonula occludens 1 downregulation in organotypic hippocampal cultures: role of VEGF signaling pathways. *J Neurosci* 2011, 31(29):10677-10688.

Muntane G, Dalfo E, Martinez A, Rey MJ, Avila J, Perez M, Portero M, Pamplona R, Ayala V, Ferrer I: Glial fibrillary acidic protein is a major target of glycoxidative and lipoxidative damage in Pick's disease. *J Neurochem* 2006, 99(1):177-185.

Newcombe J, Woodroofe MN, Cuzner ML: Distribution of glial fibrillary acidic protein in gliosed human white matter. *J Neurochem* 1986, 47(6):1713-1719.

Ngugi AK, Bottomley C, Kleinschmidt I, Wagner RG, Kakooza-Mwesige A, Ae-Ngibise K, Owusu-Agyei S, Masanja H, Kamuyu G, Odhiambo R *et al*: Prevalence of active convulsive epilepsy in sub-Saharan Africa and associated risk factors: cross-sectional and case-control studies. *Lancet Neurol* 2013, 12(3):253-263.

Nicholas AP, Sambandam T, Echols JD, Tourtellotte WW: Increased citrullinated glial fibrillary acidic protein in secondary progressive multiple sclerosis. *J Comp Neurol* 2004, 473(1):128-136.

Noachtar S, Borggraefe I: Epilepsy surgery: a critical review. *Epilepsy Behav* 2009, 15(1):66-72.

Oberheim NA, Tian GF, Han X, Peng W, Takano T, Ransom B, Nedergaard M: Loss of astrocytic domain organization in the epileptic brain. *J Neurosci* 2008, 28(13):3264-3276.

Ousman SS, Tomooka BH, van Noort JM, Wawrousek EF, O'Connor KC, Hafler DA, Sobel RA, Robinson WH, Steinman L: Protective and therapeutic role for alphaB-crystallin in autoimmune demyelination. *Nature* 2007, 448(7152):474-479.

Panayiotopoulos CP: The new ILAE report on terminology and concepts for the organization of epilepsies: critical review and contribution. *Epilepsia* 2012, 53(3):399-404.

Papageorgiou IE, Gabriel S, Fetani AF, Kann O, Heinemann U: Redistribution of astrocytic glutamine synthetase in the hippocampus of chronic epileptic rats. *Glia* 2011, 59(11):1706-1718.

Pitkanen A, Lukasiuk K: Mechanisms of epileptogenesis and potential treatment targets. *Lancet Neurol* 2011, 10(2):173-186.

Pitkanen A, McIntosh TK: Animal models of post-traumatic epilepsy. *J Neurotrauma* 2006, 23(2):241-261.

Pitkanen A, Sutula TP: Is epilepsy a progressive disorder? Prospects for new therapeutic approaches in temporal-lobe epilepsy. *Lancet Neurol* 2002, 1(3):173-181.

Porchet R, Probst A, Bouras C, Draberova E, Draber P, Riederer BM: Analysis of glial acidic fibrillary protein in the human entorhinal cortex during aging and in Alzheimer's disease. *Proteomics* 2003, 3(8):1476-1485.

Rakhade SN, Jensen FE: Epileptogenesis in the immature brain: emerging mechanisms. *Nat Rev Neurol* 2009, 5(7):380-391.

Rakhade SN, Loeb JA: Focal reduction of neuronal glutamate transporters in human neocortical epilepsy. *Epilepsia* 2008, 49(2):226-236.

Rakhade SN, Yao B, Ahmed S, Asano E, Beaumont TL, Shah AK, Draghici S, Krauss R, Chugani HT, Sood S *et al*: A common pattern of persistent gene activation in human neocortical epileptic foci. *Ann Neurol* 2005, 58(5):736-747.

Rigau V, Morin M, Rousset MC, de Bock F, Lebrun A, Coubes P, Picot MC, Baldy-Moulinier M, Bockaert J, Crespel A *et al*: Angiogenesis is associated with blood-brain barrier permeability in temporal lobe epilepsy. *Brain* 2007, 130(Pt 7):1942-1956.

Roux-Dalvai F, Gonzalez de Peredo A, Simo C, Guerrier L, Bouyssie D, Zanella A, Citterio A, Burlet-Schiltz O, Boschetti E, Righetti PG *et al*: Extensive analysis of the cytoplasmic proteome of human erythrocytes using the peptide ligand library technology and advanced mass spectrometry. *Mol Cell Proteomics* 2008, 7(11):2254-2269.

Sander JW: The epidemiology of epilepsy revisited. *Curr Opin Neurol* 2003, 16(2):165-170.

Sarkisian MR: Overview of the Current Animal Models for Human Seizure and Epileptic Disorders. *Epilepsy Behav* 2001, 2(3):201-216.

Sarnat HB, Flores-Sarnat L: Alpha-B-crystallin as a tissue marker of epileptic foci in paediatric resections. *Can J Neurol Sci* 2009, 36(5):566-574.

Schmidt D: Drug treatment of epilepsy: options and limitations. *Epilepsy Behav* 2009, 15(1):56-65.

Seifert G, Carmignoto G, Steinhauser C: Astrocyte dysfunction in epilepsy. *Brain Res Rev* 2010, 63(1-2):212-221.

Seifert G, Steinhauser C: Neuron-astrocyte signaling and epilepsy. *Exp Neurol* 2013, 244:4-10.

Seiffert E, Dreier JP, Ivens S, Bechmann I, Tomkins O, Heinemann U, Friedman A: Lasting blood-brain barrier disruption induces epileptic focus in the rat somatosensory cortex. *J Neurosci* 2004, 24(36):7829-7836.

Smith SJ: EEG in the diagnosis, classification, and management of patients with epilepsy. *J Neurol Neurosurg Psychiatry* 2005, 76 Suppl 2:ii2-7.

Sofroniew MV, Vinters HV: Astrocytes: biology and pathology. *Acta Neuropathol* 2010, 119(1):7-35.

Spencer S, Huh L: Outcomes of epilepsy surgery in adults and children. *Lancet Neurol* 2008, 7(6):525-537.

Steinhauser C, Seifert G: Astrocyte dysfunction in epilepsy. In: Noebels JL, Avoli M, Rogawski MA, Olsen RW, Delgado-Escueta AV, editors. Jasper's Basic Mechanisms of the Epilepsies [Internet]. 4th edition. Bethesda (MD): National Center for Biotechnology Information (US); 2012.

Stewart TH, Eastman CL, Groblewski PA, Fender JS, Verley DR, Cook DG, D'Ambrosio R: Chronic dysfunction of astrocytic inwardly rectifying K+ channels specific to

the neocortical epileptic focus after fluid percussion injury in the rat. *J Neurophysiol* 2010, 104(6):3345-3360.

Takemura M, Gomi H, Colucci-Guyon E, Itohara S: Protective role of phosphorylation in turnover of glial fibrillary acidic protein in mice. *J Neurosci* 2002, 22(16):6972-6979.

Tellez-Zenteno JF, Hernandez Ronquillo L, Moien-Afshari F, Wiebe S: Surgical outcomes in lesional and non-lesional epilepsy: a systematic review and meta-analysis. *Epilepsy Res* 2010, 89(2-3):310-318.

Temkin NR: Preventing and treating posttraumatic seizures: the human experience. *Epilepsia* 2009, 50 Suppl 2:10-13.

Tsujimura K, Tanaka J, Ando S, Matsuoka Y, Kusubata M, Sugiura H, Yamauchi T, Inagaki M: Identification of phosphorylation sites on glial fibrillary acidic protein for cdc2 kinase and Ca(2+)-calmodulin-dependent protein kinase II. *J Biochem* 1994, 116(2):426-434.

Vezzani A, Friedman A, Dingledine RJ: The role of inflammation in epileptogenesis. *Neuropharmacology* 2013, 69:16-24.

Visanji NP, Wong JC, Wang SX, Cappel B, Kleinschmidt-Demasters BK, Handler MH, Ochi A, Otsubo H, Rutka JT, Go C *et al*: A proteomic analysis of pediatric seizure cases associated with astrocytic inclusions. *Epilepsia* 2012, 53(3):e50-54.

Walpurgis K, Kohler M, Thomas A, Wenzel F, Geyer H, Schanzer W, Thevis M: Validated hemoglobin-depletion approach for red blood cell lysate proteome analysis by means of 2D PAGE and Orbitrap MS. *Electrophoresis* 2012, 33(16):2537-2545.

Weissberg I, Reichert A, Heinemann U, Friedman A: Blood-brain barrier dysfunction in epileptogenesis of the temporal lobe. *Epilepsy Res Treat*, 2011:143908.

White HS: Animal Models for Evaluating Antiepileptogenesis. In: Noebels JL, Avoli M, Rogawski MA, Olsen RW, Delgado-Escueta AV, editors. Jasper's Basic Mechanisms of the Epilepsies [Internet]. 4th edition. Bethesda (MD): National Center for Biotechnology Information (US); 2012.

Williams LM, Fu Z, Dulloor P, Yen T, Barron-Casella E, Savage W, Van Eyk JE, Casella JF, Everett A: Hemoglobin depletion from plasma: considerations for proteomic discovery in sickle cell disease and other hemolytic processes. *Proteomics Clin Appl* 2010, 4(12):926-930.

Willis CL: Glia-induced reversible disruption of blood-brain barrier integrity and neuropathological response of the neurovascular unit. *Toxicol Pathol* 2011, 39(1):172-185.

Wilson SM, Xiong W, Wang Y, Ping X, Head JD, Brittain JM, Gagare PD, Ramachandran PV, Jin X, Khanna R: Prevention of posttraumatic axon sprouting by blocking collapsin response mediator protein 2-mediated neurite outgrowth and tubulin polymerization. *Neuroscience* 2012, 210:451-466.

Witcher MR, Ellis TL: Astroglial networks and implications for therapeutic neuromodulation of epilepsy. *Front Comput Neurosci* 2012, 6:61.

Wolf P: The role of nonpharmaceutic conservative interventions in the treatment and secondary prevention of epilepsy. *Epilepsia* 2002, 43 Suppl 9:2-5.

WHO: Epilepsy fact sheet Oct 2012. http://www.who.int/mediacentre/factsheets/fs999/en/

WHO: Atlas: epilepsy care in the world, 2005. http://www.who.int/mental_health/publications/atlas_epilepsy_care_2005/en/

Wu C, Sharan AD: Neurostimulation for the treatment of epilepsy: a review of current surgical interventions. *Neuromodulation* 2013, 16(1):10-24; discussion 24.

Wu JY, Sankar R, Lerner JT, Matsumoto JH, Vinters HV, Mathern GW: Removing interictal fast ripples on electrocorticography linked with seizure freedom in children. *Neurology* 2010, 75(19):1686-1694.

Xiong Y, Mahmood A, Chopp M: Angiogenesis, neurogenesis and brain recovery of function following injury. *Curr Opin Investig Drugs*2010, 11(3):298-308.

Yang JW, Czech T, Gelpi E, Lubec G: Extravasation of plasma proteins can confound interpretation of proteomic studies of brain: a lesson from apo A-I in mesial temporal lobe epilepsy. *Brain Res Mol Brain Res* 2005, 139(2):348-356.

Yap AS, Brieher WM, Gumbiner BM: Molecular and functional analysis of cadherin-based adherens junctions. *Annu Rev Cell Dev Biol* 1997, 13:119-146.

You JS, Gelfanova V, Knierman MD, Witzmann FA, Wang M, Hale JE: The impact of blood contamination on the proteome of cerebrospinal fluid. *Proteomics* 2005, 5(1):290-296.

Yun CH, Lee SK, Lee SY, Kim KK, Jeong SW, Chung CK: Prognostic factors in neocortical epilepsy surgery: multivariate analysis. *Epilepsia* 2006, 47(3):574-

579.

Zhao F, Hu Y, Zhang Y, Zhu Q, Zhang X, Luo J, Xu Y, Wang X: Abnormal expression of stathmin 1 in brain tissue of patients with intractable temporal lobe epilepsy and a rat model. *Synapse* 2012, 66(9):781-791.

Ziemba KS, Wellik KE, Hoffman-Snyder C, Noe KH, Demaerschalk BM, Wingerchuk DM: Timing of antiepileptic drug withdrawal in adult epilepsy patients after neocortical surgical resection: a critically appraised topic. *Neurologist* 2011, 17(3):176-178.

Zlokovic BV: The blood-brain barrier in health and chronic neurodegenerative disorders. *Neuron* 2008, 57(2):178-201.

APPENDIX A

SUPPLEMENTARY MATERIAL FOR CHAPTER 2

SUPPLEMENTARY MATERIAL – DEFINITIONS AND CONTENT

ID Level

Tables S3-5 contain a column which indicate the level of certainty for each protein identification. The four ID levels are: $ - identification, * - assumption, / - ambiguous and X – unidentified. The assignment of an ID level to a spot was decided as follow.

$ - Identification

Assigned in cases of MS ID of a single protein with multiple peptides or Western blot validation.

* - Attribution

Assigned when the protein ID was inferred from the MS information and/or 2D-PAGE information. For example a) MS ID of a protein by a single peptide (OHW), b) in case of a spot in which multiple proteins were found by MS analysis or when there is no MS analysis, comparing the spot's expression pattern with those of identified, neighboring or partially overlapping spots, can assist in excluding or assigning protein identification. c) Mascot emPAI quantitation tool can be beneficial in selecting or excluding proteins when multiple proteins are indicated by MS to the same spot. Since all SOIs were chosen based on experimental changes (ratio of spike frequencies), the emPAI indication of one of the proteins found in the spot as much more abundant than the others, suggests this protein is more likely to be causing the spot's intensity change.

/ - Ambiguous

Assigned when the MS analysis of the spot (or of neighboring spot with similar expression pattern, in cases of no MS analysis) found more than one protein that could not be excluded (as described above).

X – Unidentified

Assigned for spots in which no protein identification was found in MS analysis and could not be inferred from other neighboring spots.

Supplementary Figures and Tables Navigation

Figure S1 – 2D Maps of all Spots of Interest (SOIs)

Each image represents 2D-PAGE of proteins from one subcellular fractions using pH range of 3-11 (non-linear) and MW range 200-15kDa. SOIs are marked by blue perimeter and spot number. Note - the SOIs numbers in the cytosolic fraction are split across two images (CytA & CytB) in order to allow their visualization.

Figure S2 – Spots of Interest (SOIs) Dendrogram

Visualization of hierarchical clustering of 397 SOIs by their expression patterns. The dendrogram was divided into two main branches (A & B) and an enlarge image of each branch is shown. An arbitrary distance cutoff was used to separate the dataset to 37 groups of spots.

Table S3 – Spots of Interest by Cluster

SOIs ordered by their dendrogram position. Include the protein assignment and the spot expression ratios (H/L) for each patient.

Table S4 – Spots of Interest by Fraction and Spot Number

Spots ordered by fractions and spot number, includes protein assignment and description.

Table S5 – Spots of Interest Mascot Search Information

Provides Mascot search information of identified proteins.

Table S6 - Proteins that were Identified from a Single Peptide (one hit wonders, OHW)

This file contains the spectra and masses of the fragmented peptide. Notes: a) all the proteins had supportive information for identification (see table S6), b) all OHW received a decreased ID level (* instead of $).

Figure S1 – 2D maps of all Spots of Interest in the three subcellular fractions. The spots identified are listed in Table S4. P1 is the nuclear fraction and P2 is the membrane fraction. CytA and CytB are identical images of the cytosolic fraction used to accommodate different SOI numbers.

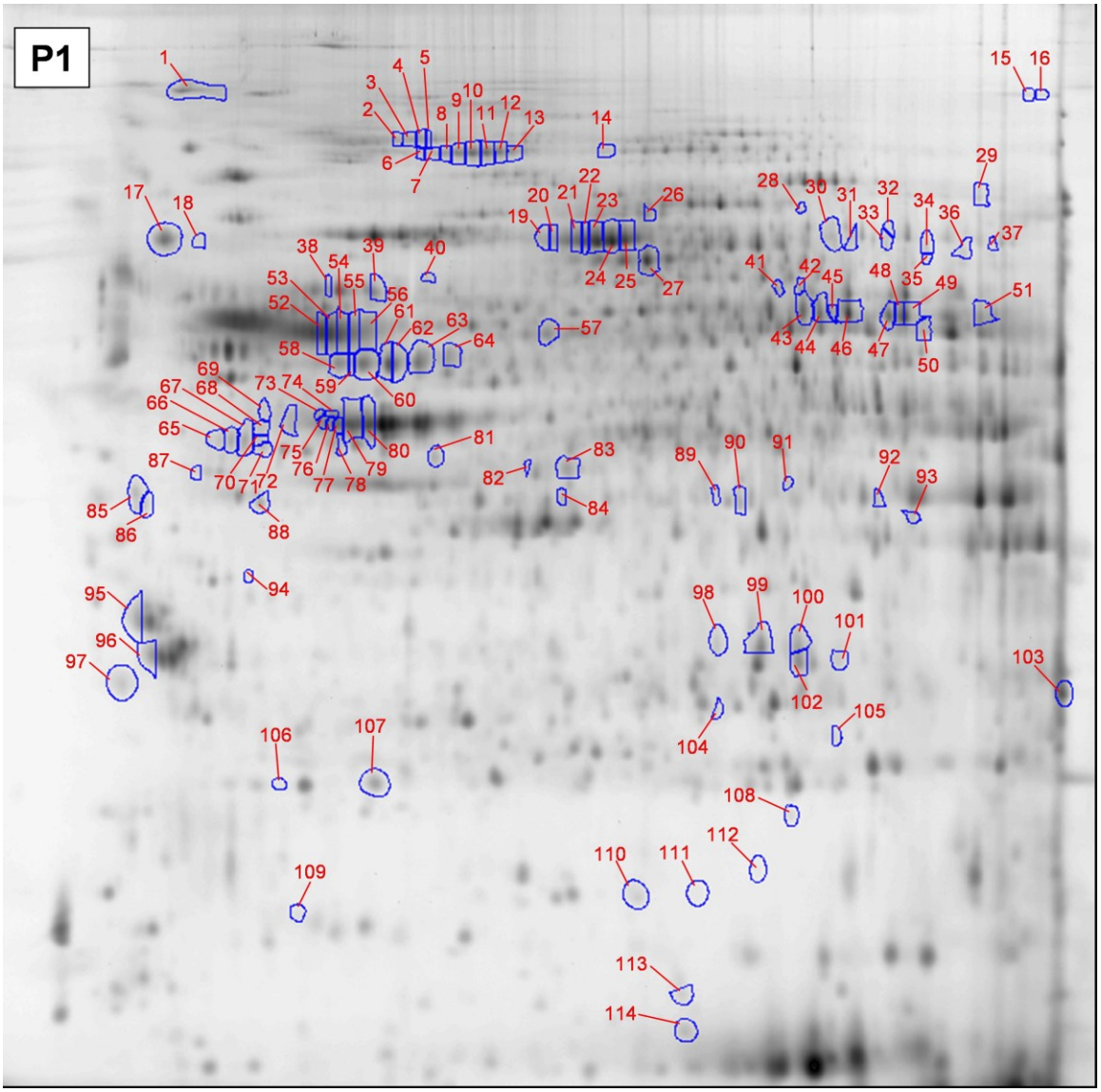

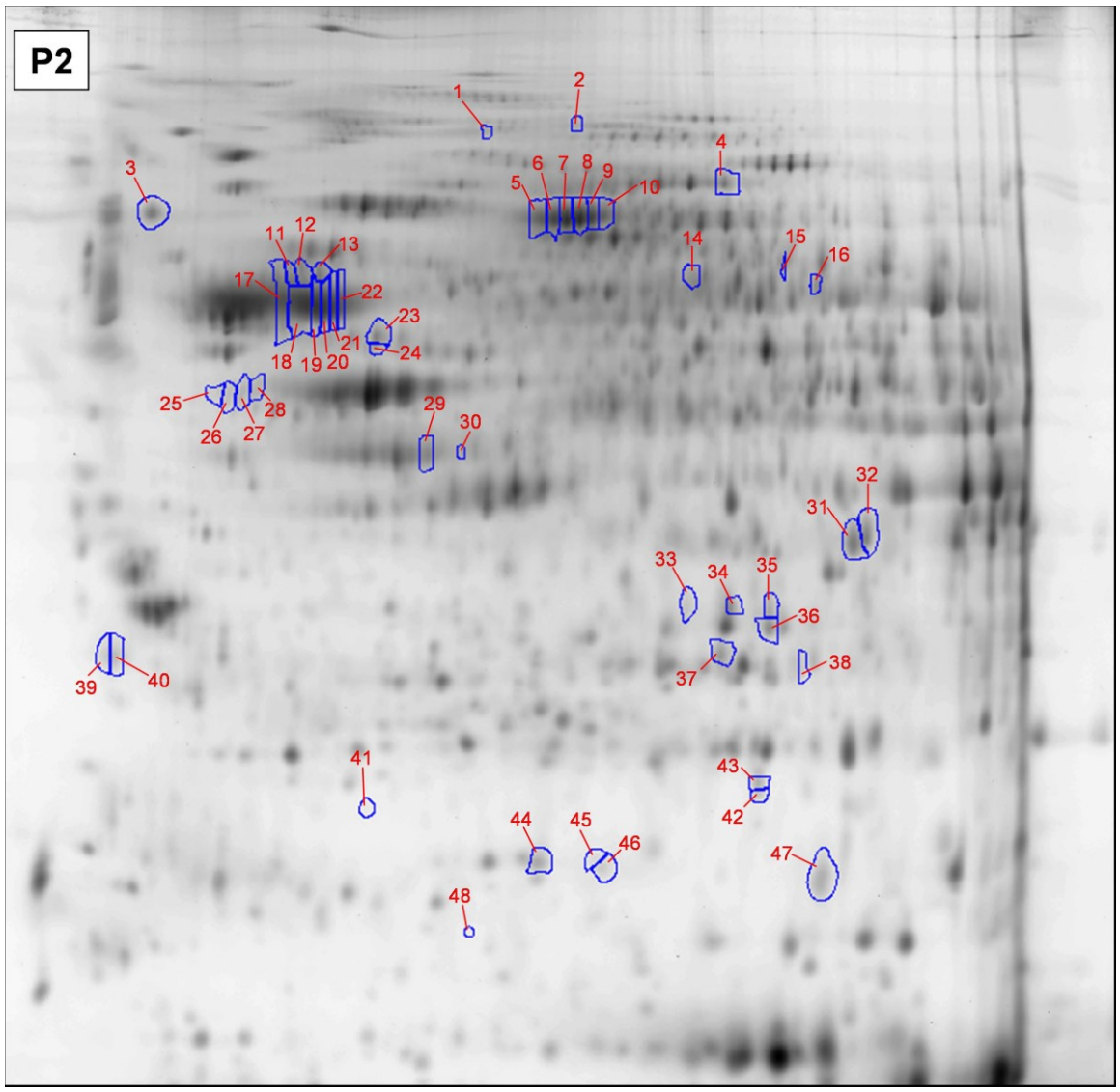
P2
1
2
3
4
5
6
7
8
9
10
11
12
13
14
15
16
17
18
19
20
21
22
23
24
25
26
27
28
29
30
31
32
33
34
35
36
37
38
39
40
41
42
43
44
45
46
47
48

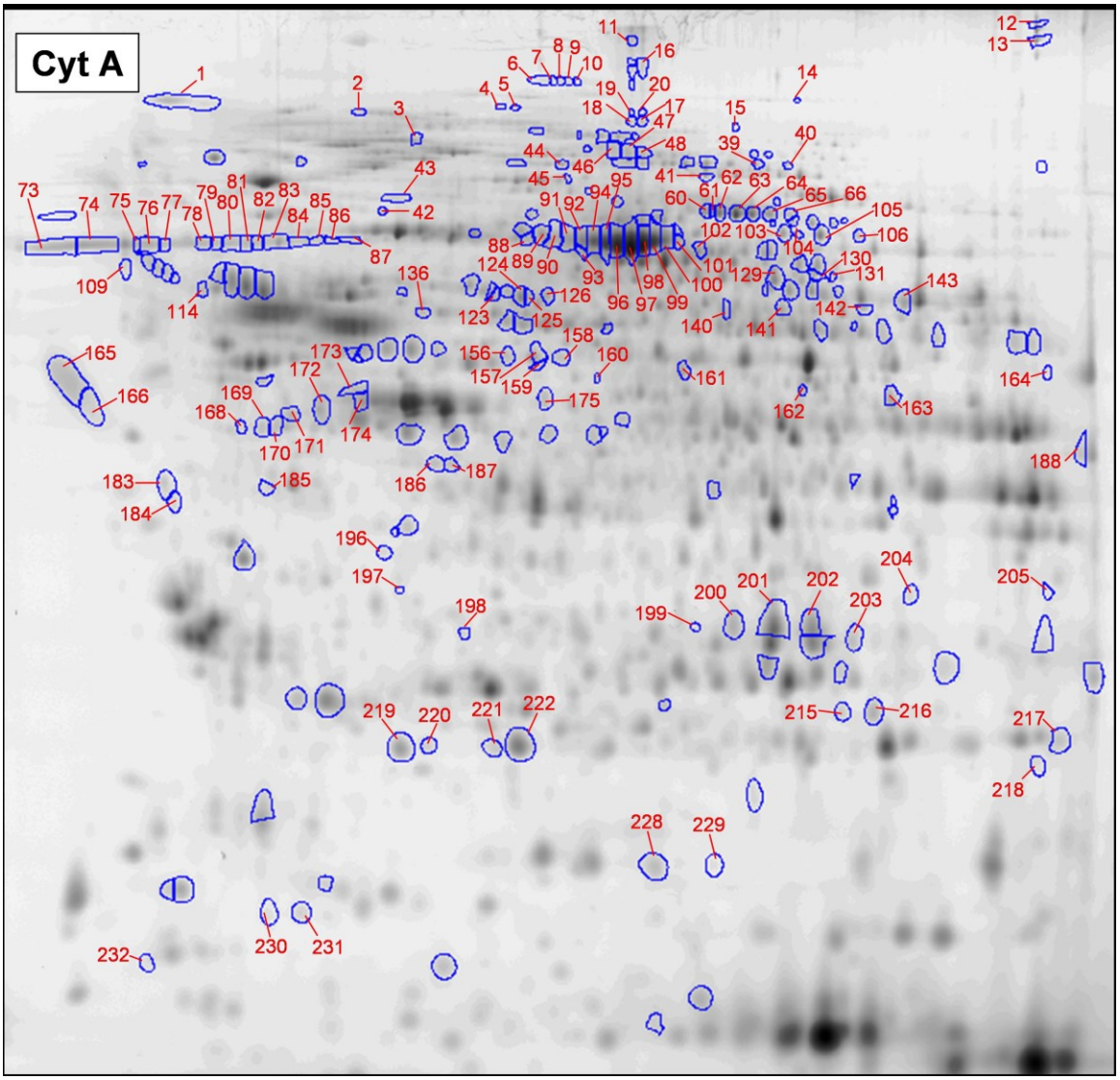
Cyt A

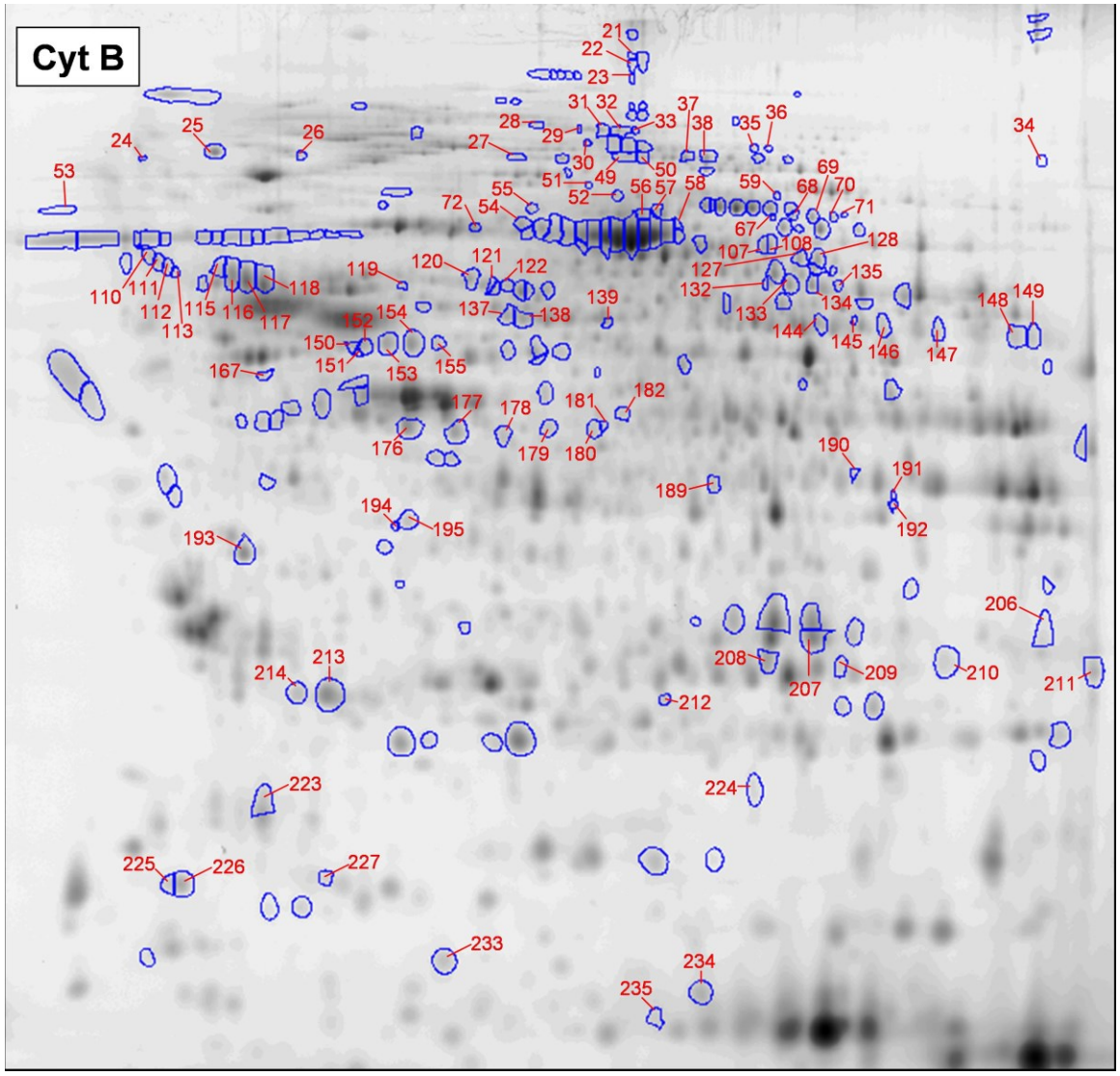
Cyt B
21
22
23
31
32
37
33
38
35
36
34
25
26
28
29
27
24
30
53
51
49
50
56
57
58
59
69
68
70
71
55
52
72
54
67
107
108
128
127
135
120
121
122
119
132
134
139
137
138
133
144
145
146
147
148
149
110
111
112
113
115
116
117
118
152
154
150
151
153
155
167
177
178
181
182
176
179
180
190
191
189
192
194
195
193
206
208
207
209
210
211
213
214
212
223
224
225
226
227
233
234
235

Figure S2 – Spots of Interest (SOIs) Expanded Dendrogram

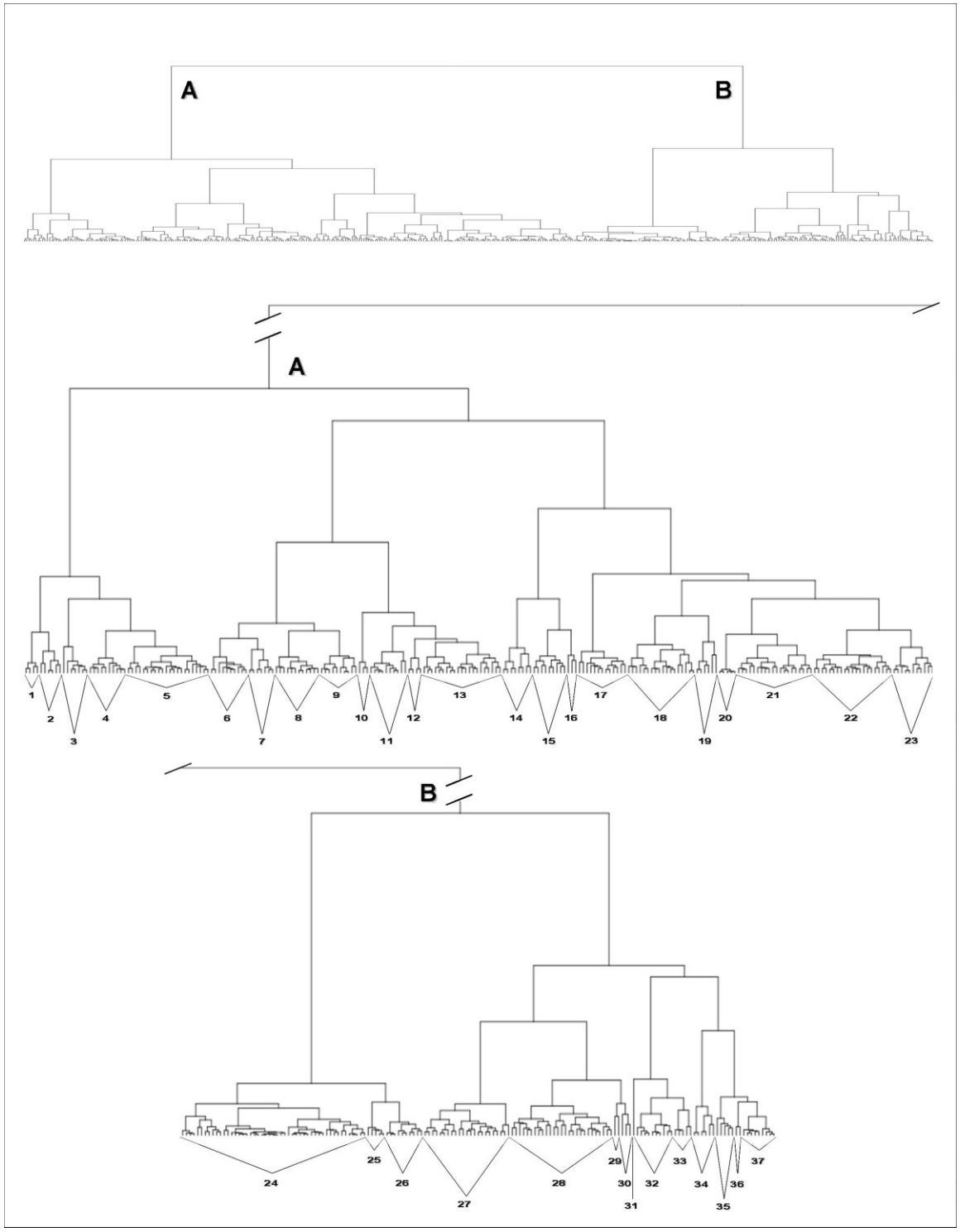

Table S3 – Spots of Interest by Cluster

Cluster #	ID level	Gene name	Accesion #	MS file	2D map	spot #	t-test p-value/FC	Expression ration High/Low spike ep122	ep132	ep150	ep158	ep159	ep165
1	$	GFAP	P14136	QTOF_152	P1	62	0.001/1.7	0.74	0.62	0.45	0.67	0.66	0.44
	$	GNAO1	P09471	QTOF_130	P2	30	0.016/1.4	0.67	0.53	0.57	0.93	0.79	0.94
	*	TUBA1A	Q71U36		P1	55		0.55	0.53	0.52	1.12	0.99	0.88
	*	TUBA1A	Q71U36	QTOF_138	P1	56	0.05/1.3	0.60	0.73	0.49	0.99	1.00	0.86
2	$	GFAP	P14136	QTOF_106	P1	63	0.004/1.7	0.70	0.77	0.34	0.57	0.69	0.55
	$	GFAP	P14136	QTOF_154	P1	64		0.67	0.99	0.31	0.73	0.87	0.76
	$	CRYAB	P02511	QTOF_122	P2	42	0.038/1.5	0.93	0.49	0.34	0.86	0.74	0.76
	$	CRYAB	P02511	XCT_078	P2	43	0.035/1.4	0.89	0.56	0.34	0.86	0.72	0.81
	$	NEFL	P07196	QTOF_107	P1	17		0.30	0.81	0.34	2.52	0.60	1.31
	X	no ID			P2	41		0.44	1.02	0.41	1.03	0.85	0.75
3	$	GSTM2	P28161	QTOF_012	CytB	212		1.05	1.28	0.64	1.02	0.78	0.88
	$	ENO1	P06733	QTOF_006	CytA	162		2.24	1.17	0.47	1.38	1.06	0.49
	*	TF	P02787		CytB	70		0.96	0.96	0.43	2.35	0.60	0.72
	$	TF	P02787	QTOF_049	CytB	69		1.09	1.05	0.34	2.09	0.68	0.80
	$	NSFL1C	Q9UNZ2	XCT_056	CytB	167		0.91	1.24	0.74	1.03	0.58	0.74
	*	QDPR	P09417	QTOF_011	CytB	208		1.01	0.76	0.40	1.30	0.81	0.98
	*	TF	P02787		CytB	68		1.48	1.06	0.46	1.37	0.68	0.90
4	$	TPPP	O94811	QTOF_074	P1	103		0.59	1.07	0.38	1.08	0.67	0.80
	$	NEFM	P07197	QTOF_001	P1	1		0.43	0.96	0.49	1.49	0.69	1.15
	$	NEFL	P07196	QTOF_113	P2	3		0.49	0.69	0.38	1.59	0.77	1.21
	*	CRYAB	P02511		P1	108	0.04/1.3	0.77	0.75	0.42	1.11	0.77	0.68
	*	QDPR	P09417	QTOF_125	P2	37		0.75	1.70	0.63	1.02	0.86	1.08
	$	HK1	P19367	XCT_026	CytB	36		0.57	0.60	0.48	1.10	1.11	0.82
	X	no ID			P1	28		1.86	0.78	0.59	1.52	0.90	0.75
	*	ALDH2	P05091	QTOF_096	P1	57		0.75	0.79	0.59	1.29	0.92	0.89
	*	SIRT2	Q8IXJ6	QTOF_080	P1	83		0.46	0.74	0.81	1.24	0.77	1.03
	*	INA	Q16352	QTOF_092	P1	39		0.48	0.84	0.48	1.66	0.73	1.22
5	/	PRER / DPYSL2	P48147 / Q16555	QTOF_054	CytB	55		0.98	0.78	0.48	1.36	0.99	0.88
	*	TUBA1A	Q71U36		P2	17		0.73	0.54	0.56	1.11	0.92	0.98
	$	CRYM	Q14894	QTOF_025	CytA	185		0.73	1.46	0.62	0.80	0.97	0.53

Table S3 – continued

Cluster #	ID level	Gene name	Accesion #	MS file	2D map	spot #	t-test p-value/FC	Expression ration High/Low spike ep122	ep132	ep150	ep158	ep159	ep165
	$	GAPDH	P04406	QTOF_023	CytA	190		0.71	1.04	0.90	1.20	1.39	0.49
	/	ANXA6 / HSPA2	P08133 / P54652	QTOF_056	CytB	72		0.81	0.77	0.77	1.27	0.98	0.82
	X	no ID			CytB	223		0.79	0.94	0.71	1.29	0.88	0.76
	/	CALR / SYT1	P27797 / P21579	QTOF_060	CytA	109		0.80	1.02	0.69	1.02	1.54	0.89
	/	PYGB / ACO1	P11216 / P21399	QTOF_031	CytA	41		0.99	0.78	0.79	1.03	1.29	0.92
	$	HSP90B1	P14625	XCT_041	CytB	25		0.70	0.87	0.61	1.10	1.39	0.96
	/	RAD23B / VCAN	P54727 / P13611	QTOF_059	CytA	114		1.31	1.36	0.76	1.13	1.41	0.79
	$	ALDH2	P05091	QTOF_045	CytB	139	0.024/1.3	0.79	0.63	0.67	1.08	0.71	0.90
	/	MPI / PPME1	P34949 / Q9Y570	QTOF_052	CytA	175		0.78	1.00	0.59	1.12	0.73	0.81
5	*	PPP3R1	P63098	QTOF_010	CytA	232		0.80	0.98	0.74	1.27	1.29	0.85
	*	HSPH1	Q92598	QTOF_035	CytA	3		0.95	0.97	0.70	1.17	0.74	1.29
	*	ALDH1A1	P00352	QTOF_021	CytA	140		0.79	1.01	0.78	1.31	0.90	1.12
	$	SNCA	P37840	XCT_044	CytB	226		1.05	1.14	1.53	1.67	0.96	2.31
	*	SNCA	P37840		CytB	225	0.044/1.4	1.06	1.15	1.38	1.55	1.04	2.15
	/	ALDOC / PHYHIPL	P09972 / Q96FC7	QTOF_017	CytB	182		0.39	1.23	1.37	1.55	0.87	1.01
	$	HNRNPC	P07910	QTOF_088	P1	87		0.76	1.74	1.55	0.81	0.60	0.71
	$	STMN1	P16949	XCT_013	CytB	227	0.03/1.3	1.54	1.61	1.35	1.04	1.00	1.16
	$	VAMP2	P63027	XCT_045	CytA	230		0.65	1.18	1.28	1.07	0.85	1.61
	$	GOT2	P00505	QTOF_014	CytA	188		0.62	1.12	1.51	1.26	1.19	1.06
	*	PLCB1	Q9NQ66		CytA	5		1.20	0.99	1.92	1.23	1.81	0.56
	$	PLCB1	Q9NQ66	QTOF_037	CytA	4		0.96	1.02	1.76	1.07	1.86	0.69
	X	no ID			CytA	205		0.74	2.75	0.55	1.29	1.02	1.27
	*	NAPA	P54920	XCT_040	CytB	194		0.59	0.89	0.67	1.26	0.64	0.77
	*	PKM2	P14618	QTOF_024	CytA	142		0.59	0.77	1.42	1.20	0.90	1.04
6	*	HK1	P19367		CytB	35		0.78	0.53	0.58	1.32	1.03	0.75
	*	PKM2	P14618	XCT_051	CytA	143		0.71	0.66	0.79	1.22	0.88	0.77
	*	NAPB	Q9H115	XCT_068	CytB	195		0.57	0.79	0.39	1.43	1.11	0.99
	*	DNM1	Q05193	XCT_052	CytB	37		0.71	0.71	0.76	1.25	1.13	1.04
	*	DNM1	Q05193	QTOF_030	CytB	38		0.80	0.71	0.79	1.29	1.16	1.07
7	*	IGHG1	P01857		CytB	149		1.37	0.78	2.96	0.48	1.10	1.39

Table S3 – continued

Cluster #	ID level	Gene name	Accesion #	MS file	2D map	spot #	t-test p-value/FC	Expression ration High/Low spike ep122	ep132	ep150	ep158	ep159	ep165
7	*	IGHG1	P01857	XCT_031	CytB	148		1.11	0.86	4.10	0.51	0.99	1.71
	$	ACTR3	P61158	XCT_061	CytA	157		1.20	0.56	1.38	0.78	0.53	1.52
	$	ACTR3B	Q9P1U1	XCT_034	CytA	159		0.92	0.72	0.66	0.96	0.55	1.49
	$	ACTR3	P61158	QTOF_050	CytA	156		1.34	0.55	1.14	0.63	0.39	1.84
	*	ANXA11	P50995	XCT_049	CytA	141		0.86	0.56	1.77	0.84	0.71	1.14
	X	No ID			CytA	158		1.16	0.76	1.29	0.79	0.67	1.16
8	$	DPYSL2	Q16555	QTOF_104	P1	26		0.71	0.78	0.64	1.41	0.95	1.23
	/	EEF1G / ENO1	P26641 / P06733	QTOF_020	CytA	161		0.87	0.35	0.26	1.39	0.97	1.41
	$	GNAO1	P09471	QTOF_053	CytA	187		0.64	0.83	0.36	1.43	0.77	1.25
	*	CCT5	P48643	QTOF_058	CytB	120		0.76	0.73	0.44	1.18	1.03	1.19
	*	PSMC6	P62333	QTOF_015	CytA	163		0.79	0.75	0.73	1.32	1.00	1.28
	*	KIF5C	O60282	QTOF_038	CytB	28		0.85	0.77	0.46	1.48	0.94	1.06
	$	MAPRE3	Q9UPY8	XCT_038	CytA	196		0.45	0.54	0.70	1.47	1.06	1.20
	$	CDK5	Q00535	XCT_065	CytA	204		0.67	0.66	0.79	1.36	1.00	1.37
	$	CLTC	Q00610	QTOF_032	CytA	14		0.69	0.53	0.28	1.42	0.90	1.08
	$	SNAP91	O60641	XCT_017	CytA	1		0.75	0.59	0.45	1.51	0.98	1.29
	$	GNAO1	P09471	XCT_055	CytA	186		0.72	0.70	0.33	1.19	1.02	0.85
	/	DPYSL5 / CRMP1	Q9BPU6 / Q14194		CytB	107		0.81	0.76	0.61	1.39	0.94	1.03
9	$	DPYSL4	O14531	QTOF_149	CytA	130		0.81	0.90	2.06	1.32	1.10	1.27
	*	DNM1	Q05193	QTOF_033	CytA	40		0.84	0.66	0.70	1.48	1.29	1.29
	*	DNM1	Q05193	QTOF_034	CytA	39		0.81	0.64	0.74	1.41	1.27	1.12
	/	DPYSL5 / CRMP1	Q9BPU6 / Q14194	QTOF_063	CytB	108		0.62	0.57	0.74	1.23	1.05	0.85
	$	TPPP	O94811	XCT_064	CytB	211		0.66	1.07	0.84	1.52	0.51	0.76
	$	DPYSL5	Q9BPU6	XCT_070	CytB	128		0.62	0.72	1.48	1.35	1.00	1.14
	$	DPYSL4	O14531	QTOF_062	CytB	127		0.66	0.73	1.18	1.27	1.00	1.05
	*	CRMP1	Q14194	QTOF_051	CytA	129		0.74	0.93	1.34	1.28	0.90	1.12
	$	DNM1L	O00429	XCT_029	CytB	59		1.36	0.76	1.19	1.65	0.93	1.78
	X	no ID			CytA	131		0.69	0.78	1.03	1.39	1.06	1.38
10	$	GFAP	P14136		CytB	152	0.002/1.5	0.80	0.78	0.63	0.51	0.77	0.61
	$	GFAP	P14136	XCT_014	CytB	154		0.20	0.79	0.84	0.52	1.17	0.37

Table S3 – continued

Cluster #	ID level	Gene name	Accesion #	MS file	2D map	spot #	t-test p-value/FC	Expression ration High/Low spike ep122	ep132	ep150	ep158	ep159	ep165
10	$	GFAP	P14136	XCT_080	CytB	153	0.027/1.4	0.56	1.00	0.75	0.49	0.98	0.51
11	/	HNRNPK / CPNE6	P61978 / O95741	QTOF_135	P1	40	0.047/1.4	0.74	0.67	0.48	1.21	0.47	0.84
	*	TUBA1A	Q71U36		P2	21		0.68	0.16	0.48	1.19	0.96	0.92
	/	TUBA1A / TUBA1C	Q71U36 / Q9BQE3	QTOF_124	P2	20		0.66	0.11	0.47	1.22	0.94	0.91
	*	TUBA1A	Q71U36		P2	19		0.66	0.17	0.47	1.26	0.94	0.89
	*	TUBA1A	Q71U36		P2	22		0.70	0.29	0.49	1.15	0.94	0.94
	*	TUBA1A	Q71U36		P1	54		0.49	0.48	0.54	1.25	0.94	0.93
	*	TUBA1A	Q71U36		P1	53		0.44	0.52	0.58	1.34	0.93	0.94
	*	TUBA1A	Q71U36	QTOF_128	P1	52		0.45	0.55	0.61	1.34	0.91	0.96
	*	VDAC2	P45880	QTOF_117	P2	32		0.72	0.74	0.49	1.13	1.02	0.56
	$	SYN2	Q92777	QTOF_110	P2	16	0.034/1.7	1.48	3.01	2.23	1.15	1.09	1.22
12	$	ANXA2	P07355	QTOF_022	CytB	192		0.80	0.91	1.27	0.44	3.03	0.32
	*	ANXA2	P07355		CytB	191		0.78	1.35	1.27	0.46	2.92	0.50
	$	GFAP	P14136	XCT_035	CytA	170		0.80	0.58	0.91	0.51	2.83	0.72
	$	GFAP	P14136		CytA	169		1.30	0.67	1.37	0.54	1.82	0.84
13	*	GFAP	P14136		P1	61	0.001/1.8	0.73	0.51	0.35	0.61	0.59	0.55
	*	GFAP	P14136		P1	58	0.014/1.5	1.14	0.59	0.44	0.58	0.64	0.65
	*	GFAP	P14136		P1	60	0.001/1.6	0.94	0.55	0.52	0.57	0.59	0.56
	*	GFAP	P14136	XCT_077	P2	23	0.004/1.4	0.59	0.67	0.61	0.66	1.00	0.65
	*	GFAP	P14136		P2	24	0.038/1.4	0.60	0.58	0.44	0.95	1.06	0.74
	*	VDAC1	P21796	QTOF_116	P2	31		0.75	0.76	0.51	0.95	1.11	0.77
	*	LASP1	Q14847	QTOF_140	P1	91	0.026/1.3	0.50	0.83	0.57	0.91	0.87	0.87
	$	GNAO1	P09471	QTOF_129	P2	29	0.043/1.3	0.87	0.56	0.58	1.03	0.96	0.74
	/	NSF / STXBP1	P46459 / P61764	QTOF_109	P2	4		1.10	0.71	0.75	1.07	0.93	0.74
	*	GFAP	P14136		P1	59	0.011/1.5	1.02	0.60	0.40	0.62	0.70	0.65
	$	GFAP	P14136	QTOF_047	CytB	150	0.001/1.3	0.90	0.77	0.62	0.68	0.75	0.77
	$	GFAP	P14136		CytB	151	0.009/1.3	0.78	0.69	0.59	0.83	0.77	0.97
	$	GFAP	P14136	QTOF_043	CytA	173		0.76	1.20	1.10	0.80	1.31	0.64
	X	no ID			CytA	160		0.64	0.82	0.39	0.74	1.06	0.88
	$	KIF5C	O60282	XCT_071	CytB	29		0.70	0.83	0.76	0.87	1.07	0.76

Table S3 – continued

Cluster #	ID level	Gene name	Accession	MS file	2D map	spot #	t-test p-value/FC	Expression ration High/Low spike ep122	ep132	ep150	ep158	ep159	ep165
13	X	no ID			P1	112		0.81	0.74	1.07	1.02	0.73	0.46
	$	SYN1	P17600	QTOF_091	P1	29		0.68	0.88	0.63	1.13	0.77	1.07
	/	TUBA1A / TUBA1B	Q71U36 / P68363	XCT_074	P2	18		0.67	0.33	0.50	1.24	0.92	0.91
	$	GFAP	P14136	QTOF_150	CytA	168		1.69	0.99	1.03	0.72	1.31	1.05
	$	RAP1GDS1	P52306	QTOF_005	CytB	119		0.92	0.79	0.69	1.26	0.54	0.68
	X	no ID			CytA	197	0.025/1.3	0.90	0.72	0.55	0.78	1.03	0.63
14	*	SERPINA3	P01011		CytB	113		2.23	1.26	1.68	0.50	0.67	1.17
	*	SERPINA3	P01011		CytB	112		2.18	1.32	3.53	0.47	0.74	1.21
	$	SERPINA3	P01011	XCT_037	CytB	111		2.27	1.50	4.06	0.46	0.72	1.26
	*	SERPINA3	P01011		CytB	110		2.05	1.23	3.52	0.41	0.70	1.23
	X	no ID			P1	16		0.47	0.77	1.04	0.34	1.17	1.40
	X	no ID			P1	15		0.73	0.77	1.77	0.44	1.19	1.45
	$	CAPG	P40121	QTOF_019	CytB	180		0.89	1.08	0.87	0.42	0.28	2.75
	$	SERPINB9	P50453	XCT_067	CytB	179		0.80	1.21	0.84	0.47	0.45	3.46
15	*	HP	P00738		CytB	178		2.32	1.12	2.18	0.41	0.82	1.22
	*	HP	P00738	XCT_066	CytB	177		2.46	1.11	2.83	0.42	0.72	1.16
	*	HP	P00738	QTOF_046	CytB	176		1.99	1.08	3.24	0.46	0.76	1.12
	*	GNAQ	P50148	QTOF_083	P1	81		3.85	1.04	1.55	0.51	0.73	1.12
	$	CFL1	P23528	QTOF_121	P2	46		3.21	0.66	0.92	0.51	0.28	1.67
	*	ARF3	P61204	XCT_072	P2	45		2.36	0.81	0.65	0.40	0.44	1.30
	*	ARF3	P61204	QTOF_072	P1	110		3.43	1.15	0.81	0.42	0.62	0.83
	*	ARF3	P61204	XCT_032	CytA	228		2.92	1.10	1.76	0.42	0.51	1.13
	$	ARF3	P61204	QTOF_016	CytA	229		2.23	1.27	1.34	0.43	0.57	1.16
16	*	DPYSL5	Q9BPU6		CytA	103		2.32	1.13	1.77	0.55	0.91	0.94
	$	PRDX2	P32119	XCT_047	CytA	219		0.89	1.81	0.93	0.81	1.29	1.69
	$	GFAP	P14136		CytB	155		0.30	1.48	0.89	0.60	1.23	0.64
17	*	GFAP	P14136		P1	69		1.56	1.63	1.28	2.02	0.83	0.32
	*	GFAP	P14136		P1	68		2.12	1.30	2.77	0.47	1.09	0.56
	/	ACTB or ACTG1	P60709 or P63261		P1	74		1.48	1.28	1.95	0.63	1.40	0.60
	*	GFAP	P14136	QTOF_095	P1	72		2.24	1.56	1.81	0.47	1.38	0.35

Table S3 – continued

Cluster #	ID level	Gene name	Accesion #	MS file	2D map	spot #	t-test p-value/FC	Expression ration High/Low spike ep122	ep132	ep150	ep158	ep159	ep165
	/	ACTB or ACTG1	P60709 or P63261	QTOF_134	P1	75		2.03	1.33	1.56	0.45	3.25	0.53
	/	ACTB or ACTG1	P60709 or P63261		P1	76		1.39	1.36	1.72	0.61	1.85	0.49
	*	GFAP	P14136		P1	73		1.95	1.52	1.34	0.48	1.28	0.50
	/	ACTB or ACTG1	P60709 or P63261	QTOF_094	P1	80		1.26	1.42	1.93	0.68	2.73	0.68
17	/	ACTB or ACTG1	P60709 or P63261	QTOF_133	P1	79		1.26	1.22	1.44	0.78	1.45	0.78
	$	IDH3A	P50213	QTOF_081	P1	82		1.56	0.79	2.26	0.41	1.00	0.86
	$	DNM1	Q05193	QTOF_102	P1	14		1.29	1.18	1.43	0.85	0.78	0.97
	/	ACTB or ACTG1	P60709 or P63261		P1	77		1.24	1.10	1.73	0.63	1.75	0.69
	X	no ID			P1	92		1.49	0.68	0.87	0.39	1.50	0.88
	$	STMN1	P16949	QTOF_139	P1	109		1.34	1.68	1.07	1.30	1.08	1.51
	$	PRDX2	P32119	QTOF_070	P1	107		1.01	1.26	1.06	1.00	1.45	1.53
	*	GDI1	P31150	QTOF_114	P2	13		0.55	0.21	0.43	1.24	0.98	1.31
	*	STXBP1	P61764	QTOF_065	CytA	102		0.61	1.06	1.36	1.02	1.12	0.80
	/	HNRPDL / PHYHIP	O14979 / Q92561	QTOF_078	P1	90	0.015/1.3	0.76	0.73	0.77	1.03	0.69	0.87
	$	CRYM	Q14894	QTOF_087	P1	88		0.73	0.60	0.77	1.10	1.07	1.23
	$	CFL1	P23528	QTOF_123	P2	47		0.78	0.62	0.51	1.06	0.95	1.04
	*	GDI1	P31150	QTOF_093	P1	38		0.77	1.61	0.62	0.93	0.90	1.25
18	/	PKM2 / ALDH4A1	P14618 / P30038	QTOF_111	P2	15		0.79	0.78	0.73	1.01	1.08	1.27
	*	PPP3CA	Q08209		CytB	121		0.95	0.76	0.57	1.25	0.77	1.15
	*	RAP1GDS1	P52306	QTOF_061	CytA	136		1.01	1.19	0.71	1.17	1.66	1.28
	*	VAMP2	P63027	XCT_046	CytA	231		0.77	1.12	0.88	1.43	0.81	1.36
	/	DPYSL2 / CCT3	Q16555 / P49368	QTOF_097	P1	27		0.84	0.88	0.38	1.48	0.87	1.28
	$	ALDH1L1	O75891	QTOF_036	CytB	27		0.91	0.82	0.88	0.50	0.58	2.34
	$	LRSAM1	Q6UWE0	QTOF_041	CytA	45		0.87	1.36	1.35	0.63	0.75	2.81
	$	GAPDH	P04406	QTOF_077	P1	93	0.012/1.3	0.99	0.76	0.69	0.77	0.61	0.86
	*	GDI1	P31150	QTOF_115	P2	12		0.59	0.33	0.57	1.28	0.91	1.10
	*	GDI1	P31150		P2	11		0.58	0.34	0.66	1.28	0.88	1.13
	$	SNAP25	P60880	QTOF_119	P2	40		0.86	1.46	0.63	1.51	0.93	0.89
19	$	SNAP25	P60880	QTOF_118	P2	39		0.84	1.72	0.67	1.40	0.96	0.92
	*	PPP3CA	Q08209	XCT_033	CytB	122		0.99	0.59	0.60	1.72	0.90	1.28

Table S3 – continued

Cluster #	ID level	Gene name	Accesion #	MS file	2D map	spot #	t-test p-value/FC	Expression ration High/Low spike ep122	ep132	ep150	ep158	ep159	ep165
19	$	SNAP25	P60880	QTOF_069	P1	97		0.64	1.26	0.79	1.48	0.91	1.16
	*	ARF3	P61204		P1	111		3.56	1.39	0.56	0.53	0.64	0.74
	$	NEFL	P07196	QTOF_137	P1	18		0.51	0.99	0.51	0.90	0.72	0.96
20	*	A2M	P01023		CytA	9		2.61	0.78	3.17	0.42	0.61	0.79
	*	A2M	P01023		CytA	10		2.37	0.73	2.80	0.45	0.72	0.80
	$	A2M	P01023	QTOF_039	CytA	6		2.96	0.84	2.53	0.39	0.69	0.80
	*	A2M	P01023		CytA	7		2.93	0.75	3.26	0.37	0.63	0.77
	$	A2M	P01023	XCT_025	CytA	8		2.85	0.76	3.35	0.38	0.64	0.79
21	*	UGP2	Q16851	XCT_060	CytB	144	0.034/1.3	1.45	0.97	1.57	1.03	1.50	1.16
	$	DNM1	Q05193	QTOF_029	CytB	50		1.52	0.87	2.07	0.83	1.27	1.03
	*	DNM1	Q05193	QTOF_066	CytB	49		1.90	0.95	2.26	0.71	1.67	1.04
	X	no ID			CytA	15	0.03/1.6	2.32	1.02	2.11	1.38	1.06	1.44
	$	PPP2R4	Q15257	QTOF_018	CytB	181		1.74	1.00	1.50	0.74	1.24	1.94
	$	PRDX5	P30044	QTOF_073	P1	113		1.62	1.36	1.94	0.94	1.13	0.87
	$	EZR	P15311	XCT_043	CytB	52		1.65	0.90	2.07	0.80	0.86	0.75
	*	VCL	P18206		CytB	31		1.35	1.10	1.68	1.03	1.27	0.96
	*	CTNNA2	P26232	QTOF_108	P2	1		0.99	0.59	1.61	0.63	0.98	0.96
	$	EEF1G	P26641	XCT_053	CytA	164		2.78	1.90	1.27	1.07	1.43	0.61
	/	DPYSL2 / ALB	Q16555 / P02768	QTOF_151	CytB	57		1.57	1.05	1.39	0.94	1.28	0.75
	/	ARF3 or ARF1	P61204 or P84077	XCT_073	P2	44		2.30	0.52	0.61	0.56	0.66	1.34
	*	ALB	P02768		P2	9		2.12	0.23	1.63	0.45	0.81	1.31
	$	ALB	P02768	QTOF_127	P2	8		2.27	0.21	1.73	0.41	0.82	1.35
	*	ALB	P02768		P1	24		2.56	0.68	1.99	0.43	0.97	1.09
	*	ALB	P02768		P2	7		2.31	0.30	1.81	0.44	0.81	1.39
	*	ALB	P02768		P1	25		2.24	0.68	1.57	0.43	1.05	1.10
	*	ALB	P02768		P2	10		2.08	0.46	1.61	0.49	0.83	1.23
	$	DPYSL5	Q9BPU6	XCT_021	CytA	105		2.12	1.09	3.21	0.49	0.91	0.97
	X	no ID			CytA	104		1.87	1.09	1.53	0.69	0.91	0.91
22	*	DPYSL2	Q16555		CytA	125		1.46	0.88	1.34	1.35	0.59	1.42
	*	DPYSL2	Q16555	XCT_054	CytA	126		1.26	0.86	1.52	1.17	0.61	1.37

Table S3 – continued

Cluster #	ID level	Gene name	Accesion #	MS file	2D map	spot #	t-test p-value/FC	Expression ration High/Low spike ep122	ep132	ep150	ep158	ep159	ep165
	X	no ID			CytB	58		2.38	1.19	2.02	0.92	0.72	1.30
	/	DPYSL2 / HSPA12A	Q16555 / O43301	QTOF_064	CytB	56		2.20	1.06	1.62	0.86	0.80	0.96
	$	DPYSL2	Q16555	QTOF_057	CytA	124		1.64	1.01	1.91	1.10	0.54	1.47
	*	DPYSL2	Q16555		CytA	123		1.53	1.51	1.28	1.07	0.66	1.26
	*	TAGLN2	P37802	XCT_009	CytA	218		1.74	2.05	1.56	0.78	1.21	1.21
	$	USP5	P45974	QTOF_027	CytB	26		0.98	1.05	1.41	0.93	1.25	1.26
	*	GC	P02774	XCT_063	CytB	137		1.88	0.98	1.51	0.73	0.80	0.99
	$	SYN2	Q92777	QTOF_112	P2	14		1.61	0.66	1.29	0.77	1.00	1.12
	X	no ID			CytB	67		2.20	0.60	0.71	0.94	0.89	1.09
22	*	GC	P02774	XCT_062	CytB	138		1.75	0.99	1.51	0.72	0.79	0.90
	*	OGDHL	Q9ULD0		P2	2		1.46	0.66	1.60	1.06	1.07	0.94
	X	no ID			CytA	198	0.026/1.4	1.87	1.21	1.04	1.49	1.80	1.02
	/	CNTN1 / CP	Q12860 / P00450	XCT_042	CytA	2		2.95	1.40	2.03	0.70	1.17	1.04
	*	FABP5	Q01469	QTOF_008	CytB	234		1.22	1.52	1.55	0.70	1.46	1.22
	X	no ID			P1	78		1.59	1.24	1.73	0.44	0.97	0.95
	*	PCMT1	P22061	QTOF_075	P1	104		1.55	1.32	1.24	0.71	1.30	0.75
	$	MAP2	P11137	QTOF_026	CytB	24		1.38	1.42	1.30	1.16	0.73	2.11
	$	YWHAE	P62258	QTOF_084	P1	95		1.35	1.27	1.50	0.80	1.09	1.07
	/	YWHAZ / YWHAB	P63104 / P31946	QTOF_068	P1	96		1.92	1.40	1.74	0.71	1.06	1.08
	$	UBA1	P22314		P1	4		0.84	0.66	3.59	1.06	1.66	1.37
	*	UBA1	P22314		P1	5		0.82	0.68	3.93	0.94	1.77	1.44
	$	SYN2	Q92777	QTOF_098	P1	43		1.20	0.84	4.40	1.05	1.91	1.59
	*	UBA1	P22314		P1	2		0.80	0.65	3.48	0.91	1.95	1.73
	*	UBA1	P22314	QTOF_103	P1	3		0.85	0.65	4.12	0.87	2.11	1.61
23	$	ALDH6A1	Q02252	XCT_059	CytB	145		1.85	1.04	2.29	0.87	0.60	1.49
	$	CRMP1	Q14194	QTOF_132	P1	42		1.74	1.03	3.21	0.79	1.57	1.34
	$	DSP	P15924	QTOF_141	P1	41	0.025/1.4	1.73	1.14	1.90	1.05	1.27	1.21
	*	SOD1	P00441	QTOF_120	P2	48		1.41	1.97	2.06	1.01	0.70	0.53
	*	PRDX2	P32119		P1	106	0.036/1.4	1.43	1.72	1.83	1.15	0.94	1.14
	X	no ID			P1	45		0.76	0.69	1.99	1.06	1.58	1.08

Table S3 – continued

Cluster #	ID level	Gene name	Accesion #	MS file	2D map	spot #	t-test p-value/FC	Expression ration High/Low spike					
								ep122	ep132	ep150	ep158	ep159	ep165
	*	TF	P02787		CytA	61		2.41	1.08	2.32	1.01	1.04	1.28
	*	TF	P02787	XCT_027	CytA	60		2.36	0.92	1.89	0.70	1.02	1.38
	*	TF	P02787		CytA	62		2.83	0.86	2.02	0.62	0.95	1.21
	*	TF	P02787		CytA	63		2.67	0.82	1.66	0.68	1.01	1.18
	$	PKM2	P14618	QTOF_048	CytA	106		2.10	1.16	3.59	0.57	1.04	1.16
	X	no ID			CytB	30		2.54	0.77	2.13	1.42	1.12	1.34
	*	ALB	P02768		P1	23		2.96	0.78	2.30	0.42	0.98	1.12
	*	ALB	P02768		P2	6		2.38	0.36	1.94	0.45	0.82	1.40
	*	ALB	P02768	QTOF_131	P2	5		2.33	0.53	2.13	0.63	0.86	1.34
	*	ALB	P02768		P1	21		3.76	0.97	2.75	0.38	1.03	1.14
	*	ALB	P02768		P1	22		3.38	0.84	2.58	0.36	1.01	1.19
	*	A1BG	P04217	QTOF_028	CytA	42		3.68	1.24	2.14	0.36	0.81	1.31
	*	ORM1	P02763		CytA	166		3.34	1.23	2.55	0.45	0.92	0.98
	$	ALB	P02768	XCT_016	CytA	76		2.49	0.98	2.01	0.55	0.91	1.05
24	*	ALB	P02768		CytA	96		2.83	1.07	2.48	0.43	0.99	1.20
	*	ALB	P02768		CytA	75		2.80	1.06	2.05	0.43	0.88	1.09
	*	ALB	P02768		CytA	81		2.67	1.06	2.39	0.46	0.77	1.15
	$	ALB	P02768	XCT_001	CytA	97		2.84	0.98	2.19	0.45	0.93	1.10
	*	ALB	P02768		CytA	85		2.69	0.98	1.82	0.46	0.58	1.07
	*	ALB	P02768		CytA	82		2.70	1.03	2.40	0.43	0.70	1.06
	*	ALB	P02768	XCT_039	CytA	83		2.58	1.02	2.19	0.48	0.69	1.00
	*	ALB	P02768		CytA	74		3.11	1.11	2.10	0.42	0.88	1.12
	*	ALB	P02768		CytA	77		2.97	1.10	2.43	0.43	0.86	1.10
	*	ALB	P02768		CytA	79		3.12	1.14	2.63	0.38	0.92	1.05
	*	ALB	P02768		CytA	78		3.06	1.08	2.61	0.42	0.89	1.10
	*	ALB	P02768		CytA	80		2.76	1.03	2.58	0.41	0.79	1.08
	*	ALB	P02768		CytA	86		2.89	1.05	1.89	0.43	0.73	1.08
	*	ALB	P02768		CytA	73		2.67	1.38	2.48	0.42	0.97	1.17
	$	GFAP	P14136	QTOF_042	CytA	171		5.96	1.07	2.38	0.27	1.06	0.80
	*	ALB	P02768	XCT_024	CytB	21		2.65	0.97	3.31	0.51	0.60	0.82

Table S3 – continued

Cluster #	ID level	Gene name	Accesion #	MS file	2D map	spot #	t-test p-value/FC	Expression ration High/Low spike ep122	ep132	ep150	ep158	ep159	ep165
	$	ALB	P02768	QTOF_040	CytA	11		2.88	1.15	3.20	0.48	0.71	0.82
	*	ALB	P02768		CytA	84		2.69	1.09	1.78	0.48	0.67	0.84
	*	ALB	P02768		CytB	22		2.86	1.34	3.13	0.54	0.71	0.88
	*	ALB	P02768		CytA	16		2.88	1.18	2.68	0.58	0.69	0.85
	X	no ID			CytB	53		2.87	1.31	2.04	0.58	1.01	1.14
	*	ALB	P02768		CytA	87		2.87	1.14	1.95	0.59	0.97	0.85
	*	ALB	P02768		CytA	98		3.07	1.04	2.28	0.41	0.77	0.98
	*	TF	P02787		CytA	64		2.86	0.91	2.23	0.52	0.85	1.04
	X	no ID			CytA	48		2.02	1.19	2.88	0.71	1.15	1.10
24	$	ORM1	P02763	XCT_036	CytA	165		2.97	1.26	2.86	0.39	0.99	1.09
	X	no ID			CytA	46		2.80	1.47	2.94	0.69	1.20	1.15
	X	no ID			CytA	47		2.27	1.30	2.85	0.68	1.35	0.99
	*	VCL	P18206		CytB	33		2.08	1.42	5.07	0.88	1.81	0.74
	$	VCL	P18206	XCT_022	CytB	32		2.12	1.22	3.53	0.81	1.72	0.87
	*	ALB	P02768	XCT_023	CytA	18		2.52	1.12	2.07	0.80	0.73	0.93
	*	ALB	P02768		CytA	17		2.53	1.09	2.13	0.71	0.71	0.90
	*	ALB	P02768		CytA	20		2.35	1.17	2.23	0.64	0.71	0.93
	*	ALB	P02768		CytB	23		2.18	1.36	2.98	0.64	0.62	1.02
	*	ALB	P02768		CytA	19		2.14	1.37	2.26	0.81	0.66	0.87
	/	ATP6V1A / HSPA8	P38606 / P11142	QTOF_145	CytA	43		2.04	0.92	0.69	0.76	1.11	1.26
	$	SERPINA1	P01009	XCT_002	CytB	118		2.76	1.16	1.98	0.61	0.79	1.32
25	*	SERPINA1	P01009		CytB	115		2.48	1.32	1.35	0.51	0.81	0.91
	*	SERPINA1	P01009		CytB	116		2.72	1.36	1.79	0.41	0.77	1.01
	*	SERPINA1	P01009		CytB	117		2.70	1.32	1.97	0.46	0.75	1.03
	*	DPYSL2 / ALB	Q16555 / P02768		CytA	92		2.64	1.31	2.17	0.40	1.49	1.53
	*	ALB	P02768		CytA	94		2.71	1.23	2.32	0.43	1.35	1.41
	*	ALB	P02768		CytA	95		2.86	1.19	2.47	0.40	1.13	1.32
26	$	UBE2N	P61088	QTOF_009	CytB	233		2.34	1.15	1.58	0.79	0.97	1.15
	/	DPYSL2 / ALB	Q16555 / P02768	QTOF_148	CytA	89		2.46	1.06	1.46	0.53	0.91	1.32
	/	ATP6V1A / HSPA8	P38606 / P11142	QTOF_146	CytB	54		2.57	0.99	1.14	0.53	0.85	1.32

Table S3 – continued

Cluster #	ID level	Gene name	Accesion #	MS file	2D map	spot #	t-test p-value/FC	Expression ration High/Low spike ep122	ep132	ep150	ep158	ep159	ep165
26	$	ALB	P02768	XCT_010	CytA	91		2.44	1.44	1.71	0.52	1.35	1.49
	/	DPYSL2 / ALB	Q16555 / P02768		CytA	90		2.01	1.35	1.17	0.70	1.28	1.35
	$	DPYSL2	Q16555	QTOF_147	CytA	93	0.002/1.6	1.65	1.80	1.07	1.70	2.05	1.48
	*	DPYSL2	Q16555	QTOF_055	CytA	88		1.62	1.08	0.90	0.72	1.34	1.09
27	*	CA1	P00915	QTOF_142	CytA	199	0.021/1.6	1.24	2.00	2.17	0.90	1.38	1.88
	*	CA2	P00918	QTOF_143	CytB	207		0.89	1.71	2.54	0.75	1.31	1.74
	*	CA1	P00915		CytA	203		1.03	1.80	3.38	0.72	1.40	2.14
	*	CA1	P00915		CytA	202		0.91	1.77	5.15	0.61	1.46	2.19
	*	BLVRB	P30043	QTOF_067	CytA	215		0.90	1.56	4.00	0.55	1.49	1.91
	$	BLVRB	P30043	XCT_005	CytA	216		0.91	1.88	5.51	0.51	1.46	1.74
	*	CAT	P04040		CytB	135		0.90	2.02	9.70	0.47	1.47	1.62
	*	CAT	P04040	XCT_011	CytB	134		0.93	1.83	10.32	0.44	1.53	1.95
	*	CA1	P00915	XCT_003	CytA	201		0.86	2.06	9.78	0.61	1.55	2.19
	*	CA1	P00915		P1	99		0.93	1.28	3.23	0.52	1.45	1.85
	$	CA1	P00915	QTOF_126	P2	34		1.15	1.37	2.23	0.45	0.88	2.54
	*	CAT	P04040		CytB	132		0.88	2.04	5.16	0.73	1.47	1.87
	*	HBA	P69905	QTOF_013	CytB	206		0.81	2.16	2.65	0.73	1.27	1.73
	*	HBA	P69905		CytB	34		0.85	2.02	1.43	0.99	1.64	2.08
	*	CA1	P00915		P2	33		1.28	1.61	3.18	0.63	0.95	2.01
	*	CA1	P00915		P1	98		1.39	1.55	3.52	0.65	1.40	2.13
	*	CAT	P04040	XCT_012	CytB	133		0.76	1.77	7.44	0.50	1.41	1.76
	*	CA1	P00915		P1	100		0.85	1.19	5.81	0.53	1.39	1.69
	*	CA1	P00915	XCT_004	CytA	200		1.10	2.15	6.26	0.42	1.56	2.18
	$	HBB	P68871	QTOF_144	CytB	235		0.70	1.60	6.21	0.34	1.64	1.83
	$	HBA	P69905	XCT_030	CytA	13		0.73	2.18	10.43	0.84	1.50	2.22
	*	HBA	P69905		CytA	12		0.74	2.05	6.37	0.90	1.55	2.20
	*	APRT	P07741	XCT_020	CytA	221		0.96	1.79	2.49	0.80	1.52	2.01
28	X	no ID			CytB	209		3.31	1.16	1.66	0.62	1.08	1.26
	X	no ID			P1	31		2.03	0.64	2.12	0.84	2.33	1.01
	*	CA2	P00918	QTOF_076	P1	101		1.33	1.22	4.20	0.53	1.02	1.22

Table S3 – continued

Cluster #	ID level	Gene name	Accesion #	MS file	2D map	spot #	t-test p-value/FC	Expression ration High/Low spike ep122	ep132	ep150	ep158	ep159	ep165
	X	no ID			P2	38		1.43	0.55	1.99	0.77	0.88	1.16
	$	TMOD2	Q9NZR1	QTOF_089	P1	71		1.42	0.98	2.68	0.68	1.43	0.99
	X	no ID			P1	30		1.47	0.80	0.98	0.82	1.53	1.00
	*	NSF	P46459		CytA	66		2.81	1.34	1.37	0.74	0.74	1.02
	$	APOA1	P02647	XCT_007	CytB	214		3.00	1.13	2.85	0.56	0.89	0.74
	$	ATP5A1	P25705	XCT_058	CytB	146		2.31	0.94	3.10	0.52	0.97	1.39
	*	FGB	P02675		P1	44		2.20	0.75	3.30	0.72	3.59	2.64
	X	no ID			P1	32		3.05	0.77	1.30	0.95	2.10	0.81
	*	CKB	P12277	XCT_069	CytA	172		2.74	1.22	3.71	0.45	0.83	0.92
	*	FABP5	Q01469	QTOF_071	P1	114		1.99	1.53	9.06	0.61	1.13	1.12
	$	PRDX2	P32119	XCT_048	CytA	222		0.93	1.60	2.80	0.73	1.00	1.15
28	$	PRDX2	P32119	QTOF_004	CytA	220		0.53	1.99	1.87	0.78	1.13	1.34
	$	ANXA5	P08758	XCT_018	CytB	193		1.12	1.00	0.88	0.65	1.30	0.61
	*	ANXA1	P04083	QTOF_007	CytB	189		1.20	0.73	0.94	0.57	1.74	0.60
	$	APOA1	P02647	XCT_006	CytB	213		2.75	1.05	1.92	0.67	0.84	0.39
	*	CKB	P12277	QTOF_044	CytA	174		1.29	1.15	1.65	0.61	1.10	0.74
	$	BDH2	Q9BUT1	XCT_050	CytB	210		1.41	1.00	1.90	0.69	1.05	1.03
	*	CA1	P00915		P2	35		1.14	1.28	3.64	0.57	0.76	2.15
	/	ALDH6A1 / IGHG1	Q02252 / P01857	XCT_057	CytB	147		1.81	0.89	3.24	0.52	0.97	1.44
	*	CA2	P00918		P1	102		1.03	1.13	2.82	0.70	1.04	1.40
	$	CA2	P00918	XCT_079	P2	36		1.08	1.26	2.82	0.75	0.80	1.52
	*	ALDH1L1	O75891		CytA	44		0.76	0.91	0.80	0.75	0.87	1.02
	$	ATP5A1	P25705	QTOF_136	P1	50		1.58	1.11	1.95	0.81	1.35	1.12
	*	FGG	P02679		P1	6		0.80	0.61	2.35	1.04	1.63	1.56
29	X	no ID			CytB	71		0.32	2.15	0.57	1.14	1.18	2.85
	X	no ID			CytB	51		0.42	0.85	2.49	1.36	2.45	0.79
	X	no ID			P1	94		1.53	1.29	0.69	0.68	1.13	0.91
30	*	TMOD2	Q9NZR1		P1	70		1.70	0.97	5.65	0.43	2.87	1.02
	$	ATP5A1	P25705	QTOF_101	P1	51		1.18	1.22	1.87	0.73	2.67	0.89
31	X	no ID			P1	105		1.75	1.89	2.43	1.44	2.28	1.65

Table S3 – continued

Cluster #	ID level	Gene name	Accesion #	MS file	2D map	spot #	t-test p-value/FC	Expression ration High/Low spike ep122	ep132	ep150	ep158	ep159	ep165
32	*	GFAP	P14136		P2	28		3.65	1.82	2.18	0.61	1.72	1.01
	$	GFAP	P14136	XCT_076	P2	27		3.68	1.53	3.05	0.61	1.41	1.00
	*	GFAP	P14136	XCT_075	P2	26		4.31	1.62	3.67	0.72	1.16	1.14
	*	GFAP	P14136		P2	25		3.73	1.90	2.90	0.54	1.04	1.37
	*	NSF	P46459	XCT_028	CytA	65		2.82	1.10	2.34	0.57	0.86	1.02
	*	ALB	P02768		CytA	99		3.01	1.20	2.73	0.34	0.68	0.91
	*	ALB	P02768		CytA	100		2.75	1.35	2.94	0.44	0.65	0.88
	*	ALB	P02768		CytA	101		3.69	1.57	5.95	0.37	0.51	0.83
	*	ALB	P02768		P1	20		4.00	1.20	2.61	0.45	1.04	1.23
	*	ALB	P02768	QTOF_105	P1	19		3.21	1.24	1.79	0.59	1.12	1.15
33	$	GFAP	P14136	QTOF_090	P1	66		2.45	1.10	10.45	0.52	1.98	0.84
	*	GFAP	P14136		P1	65		3.21	1.31	8.62	0.61	1.63	0.80
	$	GFAP	P14136	QTOF_153	P1	67		2.25	1.02	7.61	0.46	1.94	0.71
	*	LASP1	Q14847	QTOF_079	P1	89		1.48	0.94	7.33	1.38	1.71	1.05
	$	APOD	P05090	QTOF_082	P1	84		0.91	1.26	1.68	0.63	1.63	1.15
34	*	TPM1	P09493		CytA	184		1.59	1.48	3.81	0.72	16.03	0.15
	$	TPM2	P07951	XCT_019	CytA	183		1.50	1.09	3.76	0.76	15.50	0.18
	$	TPM1	P09493	QTOF_085	P1	86		1.24	1.69	8.02	0.79	17.98	0.18
	$	TPM2	P07951	QTOF_086	P1	85		1.22	1.44	4.84	0.69	12.84	0.18
	*	TAGLN	Q01995	XCT_015	CytB	224		1.42	1.34	4.96	0.67	8.12	0.27
	*	TAGLN	Q01995	XCT_008	CytA	217		1.29	1.24	2.92	1.05	2.80	0.23
35	X	no ID			P1	37		0.47	0.60	1.10	0.81	5.39	0.93
	X	no ID			P1	35		1.62	0.69	4.63	1.36	10.94	1.35
	X	no ID			P1	36		1.26	0.58	1.68	0.82	3.82	1.28
	X	no ID			P1	34		3.35	0.56	2.20	1.12	8.26	1.14
	X	no ID			P1	33		2.29	0.56	1.36	1.14	4.13	1.11
36	*	FGG	P02679		P1	12		0.81	0.59	17.63	0.45	4.48	2.69
	*	FGG	P02679		P1	13		0.83	0.67	15.15	0.63	3.61	1.52
37	*	FGB	P02675	QTOF_099	P1	48		0.69	0.74	9.51	0.65	6.57	3.08
	*	FGB	P02675		P1	47		0.89	0.71	12.13	0.68	6.21	2.90

Table S3 – continue

Cluster #	ID level	Gene name	Accesion #	MS file	2D map	spot #	t-test p-value/FC	Expression ration High/Low spike ep122	ep132	ep150	ep158	ep159	ep165
	*	FGB	P02675		P1	49		0.73	0.73	11.50	0.75	5.68	4.79
	*	FGG	P02679	QTOF_003	P1	11		0.77	0.51	14.49	0.44	5.12	4.04
	$	FGB	P02675	QTOF_100	P1	46		0.93	0.74	12.93	0.75	4.56	4.20
37	*	FGG	P02679		P1	7		0.86	0.68	3.99	0.74	3.06	2.88
	*	FGG	P02679		P1	10		0.77	0.52	9.82	0.41	5.77	4.94
	*	FGG	P02679	QTOF_002	P1	9		0.79	0.56	10.43	0.41	5.47	5.35
	*	FGG	P02679		P1	8		0.85	0.62	7.29	0.49	4.62	4.66

ID levels: $ - Identification, * - Attribution, / - Ambiguous, X - unidentified, see appendix definitions for details

2D map	Spot #	Cluster #	ID level	Gene name	Accesion #	Protein description	MS file
CytA	1	8	$	SNAP91	O60641	Synaptosomal-associated protein, 91kDa homolog (mouse)	XCT_017
CytA	2	22	/	CNTN1	Q12860	Contactin 1	XCT_042
				CP	P00450	Ceruloplasmin (ferroxidase)	
CytA	3	5	*	HSPH1	Q92598	Heat shock 105kDa/110kDa protein 1	QTOF_035
CytA	4	6	$	PLCB1	Q9NQ66	Phospholipase C, beta 1 (phosphoinositide-specific)	QTOF_037
CytA	5	6	*	PLCB1	Q9NQ66	Phospholipase C, beta 1 (phosphoinositide-specific)	
CytA	6	20	$	A2M	P01023	Alpha-2-macroglobulin	QTOF_039
CytA	7	20	*	A2M	P01023	Alpha-2-macroglobulin	
CytA	8	20	$	A2M	P01023	Alpha-2-macroglobulin	XCT_025
CytA	9	20	*	A2M	P01023	Alpha-2-macroglobulin	
CytA	10	20	*	A2M	P01023	Alpha-2-macroglobulin	
CytA	11	24	$	ALB	P02768	Albumin	QTOF_040
CytA	12	27	*	HBA1	P69904	Hemoglobin, alpha 1	
CytA	13	27	$	HBA1	P69904	Hemoglobin, alpha 2	XCT_030
CytA	14	8	$	CLTC	Q00610	Clathrin, heavy chain (Hc)	QTOF_032
CytA	15	21	X	no ID	no ID		
CytA	16	24	*	ALB	P02768	Albumin	
CytA	17	24	*	ALB	P02768	Albumin	
CytA	18	24	*	ALB	P02768	Albumin	XCT_023
CytA	19	24	*	ALB	P02768	Albumin	
CytA	20	24	*	ALB	P02768	Albumin	
CytB	21	24	*	ALB	P02768	Albumin	XCT_024
CytB	22	24	*	ALB	P02768	Albumin	
CytB	23	24	*	ALB	P02768	Albumin	
CytB	24	22	$	MAP2	P11137	Microtubule-associated protein 2	QTOF_026
CytB	25	5	$	HSP90B1	P14625	Heat shock protein 90kDa beta (Grp94), member 1	XCT_041
CytB	26	22	$	USP5	P45974	Ubiquitin specific peptidase 5 (isopeptidase T)	QTOF_027
CytB	27	18	$	ALDH1L1	O75891	Aldehyde dehydrogenase 1 family, member L1	QTOF_036
CytB	28	8	*	KIF5C	O60282	Kinesin family member 5C	QTOF_038
CytB	29	13	$	KIF5C	O60282	Kinesin family member 5C	XCT_071

Table S4 – Spots of Interest by Fraction and Spot Number

Table S4 – continued

2D map	Spot #	Cluster #	ID level	Gene name	Accesion #	Protein description	MS file
CytB	30	24	X	no ID	no ID		
CytB	31	21	*	VCL	P18206	Vinculin	
CytB	32	24	$	VCL	P18206	Vinculin	XCT_022
CytB	33	24	*	VCL	P18206	Vinculin	
CytB	34	27	*	HBA1	P69904	Hemoglobin, alpha 1	
CytB	35	6	*	HK1	P19367	Hexokinase 1	
CytB	36	4	$	HK1	P19367	Hexokinase 1	XCT_026
CytB	37	6	*	DNM1	Q05193	Dynamin 1	XCT_052
CytB	38	6	*	DNM1	Q05193	Dynamin 1	QTOF_030
CytA	39	9	*	DNM1	Q05193	Dynamin 1	QTOF_034
CytA	40	9	*	DNM1	Q05193	Dynamin 1	QTOF_033
CytA	41	5	/	PYGB	P11216	Phosphorylase, glycogen; brain	QTOF_031
				ACO1	P21399	Aconitase 1, soluble	
CytA	42	24	*	A1BG	P04217	Alpha-1-B glycoprotein	QTOF_028
CytA	43	25	/	ATP6V1A	P38606	ATPase, H+ transporting, lysosomal 70kDa, V1 subunit A	QTOF_145
				HSPA8	P11142	Heat shock 70kDa protein 8	
CytA	44	28	*	ALDH1L1	O75891	Aldehyde dehydrogenase 1 family, member L1	
CytA	45	18	$	LRSAM1	Q6UWE0	Leucine rich repeat and sterile alpha motif containing 1	QTOF_041
CytA	46	24	X	no ID	no ID		
CytA	47	24	X	no ID	no ID		
CytA	48	24	X	no ID	no ID		
CytB	49	21	*	DNM1	Q05193	Dynamin 1	QTOF_066
CytB	50	21	$	DNM1	Q05193	Dynamin 1	QTOF_029
CytB	51	29	X	no ID	no ID		
CytB	52	21	$	EZR	P15311	Ezrin	XCT_043
CytB	53	24	X	no ID	no ID		
CytB	54	26	/	ATP6V1A	P38606	ATPase, H+ transporting, lysosomal 70kDa, V1 subunit A	QTOF_146
				HSPA8	P11142	Heat shock 70kDa protein 8	
CytB	55	5	/	PRER	P48147	Prolyl endopeptidase	QTOF_054
				DPYSL2	Q16555	Dihydropyrimidinase-like 2	

Table S4 – continued

2D map	Spot #	Cluster #	ID level	Gene name	Accesion #	Protein description	MS file
CytB	56	22	/	DPYSL2	Q16555	Dihydropyrimidinase-like 2	QTOF_064
				HSPA12A	O43301	Heat shock 70kDa protein 12A	
CytB	57	21	/	DPYSL2	Q16555	Dihydropyrimidinase-like 2	QTOF_151
				ALB	P02768	Albumin	
CytB	58	22	X	no ID	no ID		
CytB	59	9	$	DNM1L	O00429	Dynamin 1-like	XCT_029
CytA	60	24	*	TF	P02787	Transferrin	XCT_027
CytA	61	24	*	TF	P02787	Transferrin	
CytA	62	24	*	TF	P02787	Transferrin	
CytA	63	24	*	TF	P02787	Transferrin	
CytA	64	24	*	TF	P02787	Transferrin	
CytA	65	32	*	NSF	P46459	N-ethylmaleimide-sensitive factor	XCT_028
CytA	66	28	*	NSF	P46459	N-ethylmaleimide-sensitive factor	
CytB	67	22	X	no ID	no ID		
CytB	68	3	*	TF	P02787	Transferrin	
CytB	69	3	$	TF	P02787	Transferrin	QTOF_049
CytB	70	3	*	TF	P02787	Transferrin	
CytB	71	29	X	no ID	no ID		
CytB	72	5	/	ANXA6	P08133	Annexin A6	QTOF_056
				HSPA2	P54652	Heat shock 70kDa protein 2	
CytA	73	24	*	ALB	P02768	Albumin	
CytA	74	24	*	ALB	P02768	Albumin	
CytA	75	24	*	ALB	P02768	Albumin	
CytA	76	24	$	ALB	P02768	Albumin	XCT_016
CytA	77	24	*	ALB	P02768	Albumin	
CytA	78	24	*	ALB	P02768	Albumin	
CytA	79	24	*	ALB	P02768	Albumin	
CytA	80	24	*	ALB	P02768	Albumin	
CytA	81	24	*	ALB	P02768	Albumin	
CytA	82	24	*	ALB	P02768	Albumin	

Table S4 – continued

2D map	Spot #	Cluster #	ID level	Gene name	Accesion #	Protein description	MS file
CytA	83	24	*	ALB	P02768	Albumin	XCT_039
CytA	84	24	*	ALB	P02768	Albumin	
CytA	85	24	*	ALB	P02768	Albumin	
CytA	86	24	*	ALB	P02768	Albumin	
CytA	87	24	*	ALB	P02768	Albumin	
CytA	88	26	*	DPYSL2	Q16555	Dihydropyrimidinase-like 2	QTOF_055
CytA	89	26	/	DPYSL2	Q16555	Dihydropyrimidinase-like 2	QTOF_148
				ALB	P02768	Albumin	
CytA	90	26	/	DPYSL2	Q16555	Dihydropyrimidinase-like 2	
				ALB	P02768	Albumin	
CytA	91	26	$	ALB	P02768	Albumin	XCT_010
CytA	92	26	/	DPYSL2	Q16555	Dihydropyrimidinase-like 2	
				ALB	P02768	Albumin	
CytA	93	26	$	DPYSL2	Q16555	Dihydropyrimidinase-like 2	QTOF_147
CytA	94	26	*	ALB	P02768	Albumin	
CytA	95	26	*	ALB	P02768	Albumin	
CytA	96	24	*	ALB	P02768	Albumin	
CytA	97	24	$	ALB	P02768	Albumin	XCT_001
CytA	98	24	*	ALB	P02768	Albumin	
CytA	99	32	*	ALB	P02768	Albumin	
CytA	100	32	*	ALB	P02768	Albumin	
CytA	101	32	*	ALB	P02768	Albumin	
CytA	102	18	*	STXBP1	P61764	Syntaxin binding protein 1	QTOF_065
CytA	103	16	*	DPYSL5	Q9BPU6	Dihydropyrimidinase-like 5	
CytA	104	21	X	no ID	no ID		
CytA	105	21	$	DPYSL5	Q9BPU6	Dihydropyrimidinase-like 5	XCT_021
CytA	106	24	$	PKM2	P14618	Pyruvate kinase, muscle	QTOF_048
CytB	107	8	/	DPYSL5	Q9BPU6	Dihydropyrimidinase-like 5	
				CRMP1	Q14194	Collapsin response mediator protein 1	

Table S4 – continued

2D map	Spot #	Cluster #	ID level	Gene name	Accesion #	Protein description	MS file
CytB	108	9	/	DPYSL5	Q9BPU6	Dihydropyrimidinase-like 5	QTOF_063
				CRMP1	Q14194	Collapsin response mediator protein 1	
CytA	109	5	/	CALR	P27797	Calreticulin	QTOF_060
				SYT1	P21579	Synaptotagmin I	
CytB	110	14	*	SERPINA3	P01011	Serpin peptidase inhibitor, clade A (alpha-1 antiproteinase, antitrypsin), member 3	
CytB	111	14	$	SERPINA3	P01011	Serpin peptidase inhibitor, clade A (alpha-1 antiproteinase, antitrypsin), member 3	XCT_037
CytB	112	14	*	SERPINA3	P01011	Serpin peptidase inhibitor, clade A (alpha-1 antiproteinase, antitrypsin), member 3	
CytB	113	14	*	SERPINA3	P01011	Serpin peptidase inhibitor, clade A (alpha-1 antiproteinase, antitrypsin), member 3	
CytA	114	5	/	RAD23B	P54727	RAD23 homolog B (S. cerevisiae)	QTOF_059
				VCAN	P13611	Versican	
CytB	115	25	*	SERPINA1	P01009	Serpin peptidase inhibitor, clade A (alpha-1 antiproteinase, antitrypsin), member 1	
CytB	116	25	*	SERPINA1	P01009	Serpin peptidase inhibitor, clade A (alpha-1 antiproteinase, antitrypsin), member 1	
CytB	117	25	*	SERPINA1	P01009	Serpin peptidase inhibitor, clade A (alpha-1 antiproteinase, antitrypsin), member 1	
CytB	118	25	$	SERPINA1	P01009	Serpin peptidase inhibitor, clade A (alpha-1 antiproteinase, antitrypsin), member 1	XCT_002
CytB	119	13	$	RAP1GDS1	P52306	RAP1, GTP-GDP dissociation stimulator 1	QTOF_005
CytB	120	8	*	CCT5	P48643	Chaperonin containing TCP1, subunit 5 (epsilon)	QTOF_058
CytB	121	18	*	PPP3CA	Q08209	Protein phosphatase 3 (formerly 2B), catalytic subunit, alpha isoform	
CytB	122	19	*	PPP3CA	Q08209	Protein phosphatase 3 (formerly 2B), catalytic subunit, alpha isoform	XCT_033
CytA	123	22	*	DPYSL2	Q16555	Dihydropyrimidinase-like 2	
CytA	124	22	$	DPYSL2	Q16555	Dihydropyrimidinase-like 2	QTOF_057

Table S4 – continued

2D map	Spot #	Cluster #	ID level	Gene name	Accesion #	Protein description	MS file
CytA	125	22	*	DPYSL2	Q16555	Dihydropyrimidinase-like 2	
CytA	126	22	*	DPYSL2	Q16555	Dihydropyrimidinase-like 2	XCT_054
CytB	127	9	$	DPYSL4	O14531	Dihydropyrimidinase-like 4	QTOF_062
CytB	128	9	$	DPYSL5	Q9BPU6	Dihydropyrimidinase-like 5	XCT_070
CytA	129	9	*	CRMP1	Q14194	Collapsin response mediator protein 1	QTOF_051
CytA	130	9	$	DPYSL4	O14531	Dihydropyrimidinase-like 4	QTOF_149
CytA	131	9	X	no ID	no ID		
CytB	132	27	*	CAT	P04040	Catalase	
CytB	133	27	*	CAT	P04040	Catalase	XCT_012
CytB	134	27	*	CAT	P04040	Catalase	XCT_011
CytB	135	27	*	CAT	P04040	Catalase	
CytA	136	18	*	RAP1GDS1	P52306	RAP1, GTP-GDP dissociation stimulator 1	QTOF_061
CytB	137	22	*	GC	P02774	Group-specific component (vitamin D binding protein)	XCT_063
CytB	138	22	*	GC	P02774	Group-specific component (vitamin D binding protein)	XCT_062
CytB	139	5	$	ALDH2	P05091	Aldehyde dehydrogenase 2 family (mitochondrial)	QTOF_045
CytA	140	5	*	ALDH1A1	P00352	Aldehyde dehydrogenase 1 family, member A1	QTOF_021
CytA	141	7	*	ANXA11	P50995	Annexin A11	XCT_049
CytA	142	6	*	PKM2	P14618	Pyruvate kinase, muscle	QTOF_024
CytA	143	6	*	PKM2	P14618	Pyruvate kinase, muscle	XCT_051
CytB	144	21	*	UGP2	Q16851	UDP-glucose pyrophosphorylase 2	XCT_060
CytB	145	23	$	ALDH6A1	Q02252	Aldehyde dehydrogenase 6 family, member A1	XCT_059
CytB	146	28	$	ATP5A1	P25705	ATP synthase, H+ transporting, mitochondrial F1 complex, alpha subunit 1, cardiac muscle	XCT_058
CytB	147	28	/	ALDH6A1	Q02252	Aldehyde dehydrogenase 6 family, member A1	XCT_057
				IGHG1	P01857	Immunoglobulin heavy constant gamma 1 (G1m marker)	
CytB	148	7	*	IGHG1	P01857	Immunoglobulin heavy constant gamma 1 (G1m marker)	XCT_031
CytB	149	7	*	IGHG1	P01857	Immunoglobulin heavy constant gamma 1 (G1m marker)	
CytB	150	13	$	GFAP	P14136	Glial fibrillary acidic protein	QTOF_047
CytB	151	13	$	GFAP	P14136	Glial fibrillary acidic protein	
CytB	152	10	$	GFAP	P14136	Glial fibrillary acidic protein	

Table S4 – continued

2D map	Spot #	Cluster #	ID level	Gene name	Accesion #	Protein description	MS file
CytB	153	10	$	GFAP	P14136	Glial fibrillary acidic protein	XCT_080
CytB	154	10	$	GFAP	P14136	Glial fibrillary acidic protein	XCT_014
CytB	155	16	$	GFAP	P14136	Glial fibrillary acidic protein	
CytA	156	7	$	ACTR3	P61158	ARP3 actin-related protein 3 homolog (yeast)	QTOF_050
CytA	157	7	$	ACTR3	P61158	ARP3 actin-related protein 3 homolog (yeast)	XCT_061
CytA	158	7	X	No ID	no ID		
CytA	159	7	$	ACTR3B	Q9P1U1	ARP3 actin-related protein 3 homolog B (yeast)	XCT_034
CytA	160	13	X	no ID	no ID		
CytA	161	8	/	EEF1G	P26641	Eukaryotic translation elongation factor 1 gamma	QTOF_020
				ENO1	P06733	Enolase 1, (alpha)	
CytA	162	3	$	ENO1	P06733	Enolase 1, (alpha)	QTOF_006
CytA	163	8	*	PSMC6	P62333	Proteasome (prosome, macropain) 26S subunit, ATPase, 6	QTOF_015
CytA	164	21	$	EEF1G	P26641	Eukaryotic translation elongation factor 1 gamma	XCT_053
CytA	165	24	$	ORM1	P02763	Orosomucoid 1	XCT_036
CytA	166	24	*	ORM1	P02763	Orosomucoid 1	
CytB	167	3	$	NSFL1C	Q9UNZ2	NSFL1 (p97) cofactor (p47)	XCT_056
CytA	168	13	$	GFAP	P14136	Glial fibrillary acidic protein	QTOF_150
CytA	169	12	$	GFAP	P14136	Glial fibrillary acidic protein	
CytA	170	12	$	GFAP	P14136	Glial fibrillary acidic protein	XCT_035
CytA	171	24	$	GFAP	P14136	Glial fibrillary acidic protein	QTOF_042
CytA	172	28	*	CKB	P12277	Creatine kinase, brain	XCT_069
CytA	173	13	$	GFAP	P14136	Glial fibrillary acidic protein	QTOF_043
CytA	174	28	*	CKB	P12277	Creatine kinase, brain	QTOF_044
CytA	175	5	/	MPI	P34949	Mannose phosphate isomerase	QTOF_052
				PPME1	Q9Y570	Protein phosphatase methylesterase 1	
CytB	176	15	*	HP	P00738	Haptoglobin	QTOF_046
CytB	177	15	*	HP	P00738	Haptoglobin	XCT_066
CytB	178	15	*	HP	P00738	Haptoglobin	
CytB	179	14	$	SERPINB9	P50453	Serpin peptidase inhibitor, clade B (ovalbumin), member 9	XCT_067
CytB	180	14	$	CAPG	P40121	Capping protein (actin filament), gelsolin-like	QTOF_019

Table S4 – continued

2D map	Spot #	Cluster #	ID level	Gene name	Accesion #	Protein description	MS file
CytB	181	21	$	PPP2R4	Q15257	Protein phosphatase 2A activator, regulatory subunit 4	QTOF_018
CytB	182	5	/	ALDOC	P09972	Aldolase C, fructose-bisphosphate	QTOF_017
				PHYHIPL	Q96FC7	Phytanoyl-CoA 2-hydroxylase interacting protein-like	
CytA	183	34	$	TPM2	P07951	Tropomyosin 2 (beta)	XCT_019
CytA	184	34	*	TPM1	P09493	Tropomyosin 1 (alpha)	
CytA	185	5	$	CRYM	Q14894	Crystallin, mu	QTOF_025
CytA	186	8	$	GNAO1	P09471	Guanine nucleotide binding protein (G protein), alpha activating activity polypeptide O	XCT_055
CytA	187	8	$	GNAO1	P09471	Guanine nucleotide binding protein (G protein), alpha activating activity polypeptide O	QTOF_053
CytA	188	5	$	GOT2	P00505	Glutamic-oxaloacetic transaminase 2, mitochondrial (aspartate aminotransferase 2)	QTOF_014
CytB	189	28	*	ANXA1	P04083	Annexin A1	QTOF_007
CytA	190	5	$	GAPDH	P04406	Glyceraldehyde-3-phosphate dehydrogenase	QTOF_023
CytB	191	12	*	ANXA2	P07355	Annexin A2	
CytB	192	12	$	ANXA2	P07355	Annexin A2	QTOF_022
CytB	193	28	$	ANXA5	P08758	Annexin A5	XCT_018
CytB	194	6	*	NAPA	P54920	N-ethylmaleimide-sensitive factor attachment protein, alpha	XCT_040
CytB	195	6	*	NAPB	Q9H115	N-ethylmaleimide-sensitive factor attachment protein, beta	XCT_068
CytA	196	8	$	MAPRE3	Q9UPY8	Microtubule-associated protein, RP/EB family, member 3	XCT_038
CytA	197	13	X	no ID	no ID		
CytA	198	22	X	no ID	no ID		
CytA	199	27	*	CA1	P00915	Carbonic anhydrase I	QTOF_142
CytA	200	27	*	CA1	P00915	Carbonic anhydrase I	XCT_004
CytA	201	27	*	CA1	P00915	Carbonic anhydrase I	XCT_003
CytA	202	27	*	CA1	P00915	Carbonic anhydrase I	
CytA	203	27	*	CA1	P00915	Carbonic anhydrase I	
CytA	204	8	$	CDK5	Q00535	Cyclin-dependent kinase 5	XCT_065
CytA	205	6	X	no ID	no ID		
CytB	206	27	*	HBA2	P69905	Hemoglobin, alpha 1	QTOF_013

Table S4 – continued

2D map	Spot #	Cluster #	ID level	Gene name	Accesion #	Protein description	MS file
CytB	207	27	*	CA2	P00918	Carbonic anhydrase II	QTOF_143
CytB	208	3	*	QDPR	P09417	Quinoid dihydropteridine reductase	QTOF_011
CytB	209	28	X	no ID	no ID		
CytB	210	28	$	BDH2	Q9BUT1	3-hydroxybutyrate dehydrogenase, type 2	XCT_050
CytB	211	9	$	TPPP	O94811	Tubulin polymerization promoting protein	XCT_064
CytB	212	3	$	GSTM2	P28161	Glutathione S-transferase M2 (muscle)	QTOF_012
CytB	213	28	$	APOA1	P02647	Apolipoprotein A-I	XCT_006
CytB	214	28	$	APOA1	P02647	Apolipoprotein A-I	XCT_007
CytA	215	27	*	BLVRB	P30043	Biliverdin reductase B (flavin reductase (NADPH))	QTOF_067
CytA	216	27	$	BLVRB	P30043	Biliverdin reductase B (flavin reductase (NADPH))	XCT_005
CytA	217	34	*	TAGLN	Q01995	Transgelin	XCT_008
CytA	218	22	*	TAGLN2	P37802	Transgelin 2	XCT_009
CytA	219	16	$	PRDX2	P32119	Peroxiredoxin 2	XCT_047
CytA	220	28	$	PRDX2	P32119	Peroxiredoxin 2	QTOF_004
CytA	221	27	*	APRT	P007741	Adenine phosphoribosyltransferase	XCT_020
CytA	222	28	$	PRDX2	P32119	Peroxiredoxin 2	XCT_048
CytB	223	5	X	no ID	no ID		
CytB	224	34	*	TAGLN	Q01995	Transgelin	XCT_015
CytB	225	5	*	SNCA	P37840	Synuclein, alpha (non A4 component of amyloid precursor)	
CytB	226	5	$	SNCA	P37840	Synuclein, alpha (non A4 component of amyloid precursor)	XCT_044
CytB	227	5	$	STMN1	P16949	Stathmin 1/oncoprotein 18	XCT_013
CytA	228	15	*	ARF3	P61204	ADP-ribosylation factor 3	XCT_032
CytA	229	15	$	ARF3	P61204	ADP-ribosylation factor 3	QTOF_016
CytA	230	5	$	VAMP2	P63027	Vesicle-associated membrane protein 2 (synaptobrevin 2)	XCT_045
CytA	231	18	*	VAMP2	P63027	Vesicle-associated membrane protein 2 (synaptobrevin 2)	XCT_046
CytA	232	5	*	PPP3R1	P63098	Protein phosphatase 3 (formerly 2B), regulatory subunit B, alpha isoform	QTOF_010
CytB	233	26	$	UBE2N	P61088	Ubiquitin-conjugating enzyme E2N	QTOF_009
CytB	234	22	*	FABP5	Q01469	Fatty acid binding protein 5 (psoriasis-associated)	QTOF_008
CytB	235	27	$	HBB	P68871	Hemoglobin, beta	QTOF_144

Table S4 – continued

2D map	Spot #	Cluster #	ID level	Gene name	Accesion #	Protein description	MS file
P1	1	4	$	NEFM	P07197	Neurofilament, medium polypeptide	QTOF_001
P1	2	23	*	UBA1	P22314	Ubiquitin-like modifier activating enzyme 1	
P1	3	23	*	UBA1	P22314	Ubiquitin-like modifier activating enzyme 1	QTOF_103
P1	4	23	$	UBA1	P22314	Ubiquitin-like modifier activating enzyme 1	
P1	5	23	*	UBA1	P22314	Ubiquitin-like modifier activating enzyme 1	
P1	6	28	*	FGG	P02679	Fibrinogen gamma chain	
P1	7	37	*	FGG	P02679	Fibrinogen gamma chain	
P1	8	37	*	FGG	P02679	Fibrinogen gamma chain	
P1	9	37	*	FGG	P02679	Fibrinogen gamma chain	QTOF_002
P1	10	37	*	FGG	P02679	Fibrinogen gamma chain	
P1	11	37	*	FGG	P02679	Fibrinogen gamma chain	QTOF_003
P1	12	36	*	FGG	P02679	Fibrinogen gamma chain	
P1	13	36	*	FGG	P02679	Fibrinogen gamma chain	
P1	14	17	$	DNM1	Q05193	Dynamin 1	QTOF_102
P1	15	14	X	no ID	no ID		
P1	16	14	X	no ID	no ID		
P1	17	2	$	NEFL	P07196	Neurofilament, light polypeptide 68kDa	QTOF_107
P1	18	19	$	NEFL	P07196	Neurofilament, light polypeptide 68kDa	QTOF_137
P1	19	32	*	ALB	P02768	Albumin	QTOF_105
P1	20	32	*	ALB	P02768	Albumin	
P1	21	24	*	ALB	P02768	Albumin	
P1	22	24	*	ALB	P02768	Albumin	
P1	23	24	*	ALB	P02768	Albumin	
P1	24	21	*	ALB	P02768	Albumin	
P1	25	21	*	ALB	P02768	Albumin	
P1	26	8	$	DPYSL2	Q16555	Dihydropyrimidinase-like 2	QTOF_104
P1	27	18	/	DPYSL2	Q16555	Dihydropyrimidinase-like 2	QTOF_097
				CCT3	P49368	Chaperonin containing TCP1, subunit 3 (gamma)	
P1	28	4	X	no ID	no ID		
P1	29	13	$	SYN1	P17600	Synapsin I	QTOF_091

Table S4 – continued

2D map	Spot #	Cluster #	ID level	Gene name	Accesion #	Protein description	MS file
P1	30	28	X	no ID	no ID		
P1	31	28	X	no ID	no ID		
P1	32	28	X	no ID	no ID		
P1	33	35	X	no ID	no ID		
P1	34	35	X	no ID	no ID		
P1	35	35	X	no ID	no ID		
P1	36	35	X	no ID	no ID		
P1	37	35	X	no ID	no ID		
P1	38	18	*	GDI1	P31150	GDP dissociation inhibitor 1	QTOF_093
P1	39	4	*	INA	Q16352	Internexin neuronal intermediate filament protein, alpha	QTOF_092
P1	40	11	/	HNRNPK	P61978	Heterogeneous nuclear ribonucleoprotein K	QTOF_135
				CPNE6	O95741	Copine VI (neuronal)	
P1	41	23	$	DSP	P15924	Desmoplakin	QTOF_141
P1	42	23	$	CRMP1	Q14194	Collapsin response mediator protein 1	QTOF_132
P1	43	23	$	SYN2	Q92777	Synapsin II	QTOF_098
P1	44	28	*	FGB	P02675	Fibrinogen beta chain	
P1	45	23	X	no ID	no ID		
P1	46	37	$	FGB	P02675	Fibrinogen beta chain	QTOF_100
P1	47	37	*	FGB	P02675	Fibrinogen beta chain	
P1	48	37	*	FGB	P02675	Fibrinogen beta chain	QTOF_099
P1	49	37	*	FGB	P02675	Fibrinogen beta chain	
P1	50	28	$	ATP5A1	P25705	ATP synthase, H+ transporting, mitochondrial F1 complex, alpha subunit 1, cardiac muscle	QTOF_136
P1	51	30	$	ATP5A1	P25705	ATP synthase, H+ transporting, mitochondrial F1 complex, alpha subunit 1, cardiac muscle	QTOF_101
P1	52	11	*	TUBA1A	Q71U36	Tubulin, alpha 1a	QTOF_128
P1	53	11	*	TUBA1A	Q71U36	Tubulin, alpha 1a	
P1	54	11	*	TUBA1A	Q71U36	Tubulin, alpha 1a	
P1	55	1	*	TUBA1A	Q71U36	Tubulin, alpha 1a	
P1	56	1	*	TUBA1A	Q71U36	Tubulin, alpha 1a	QTOF_138

Table S4 – continued

2D map	Spot #	Cluster #	ID level	Gene name	Accesion #	Protein description	MS file
P1	57	4	*	ALDH2	P05091	Aldehyde dehydrogenase 2 family (mitochondrial)	QTOF_096
P1	58	13	*	GFAP	P14136	Glial fibrillary acidic protein	
P1	59	13	*	GFAP	P14136	Glial fibrillary acidic protein	
P1	60	13	*	GFAP	P14136	Glial fibrillary acidic protein	
P1	61	13	*	GFAP	P14136	Glial fibrillary acidic protein	
P1	62	1	$	GFAP	P14136	Glial fibrillary acidic protein	QTOF_152
P1	63	2	$	GFAP	P14136	Glial fibrillary acidic protein	QTOF_106
P1	64	2	$	GFAP	P14136	Glial fibrillary acidic protein	QTOF_154
P1	65	33	*	GFAP	P14136	Glial fibrillary acidic protein	
P1	66	33	$	GFAP	P14136	Glial fibrillary acidic protein	QTOF_090
P1	67	33	$	GFAP	P14136	Glial fibrillary acidic protein	QTOF_153
P1	68	17	*	GFAP	P14136	Glial fibrillary acidic protein	
P1	69	17	*	GFAP	P14136	Glial fibrillary acidic protein	
P1	70	30	*	TMOD2	Q9NZR1	Tropomodulin 2 (neuronal)	
P1	71	28	$	TMOD2	Q9NZR1	Tropomodulin 2 (neuronal)	QTOF_089
P1	72	17	*	GFAP	P14136	Glial fibrillary acidic protein	QTOF_095
P1	73	17	*	GFAP	P14136	Glial fibrillary acidic protein	
P1	74	17	/	ACTB	P60709	Actin, beta	
				ACTG1	P63261	Actin, gamma 1	
P1	75	17	/	ACTB	P60709	Actin, beta	QTOF_134
				ACTG1	P63261	Actin, gamma 1	
P1	76	17	/	ACTB	P60709	Actin, beta	
				ACTG1	P63261	Actin, gamma 1	
P1	77	17	/	ACTB	P60709	Actin, beta	
				ACTG1	P63261	Actin, gamma 1	
P1	78	22	X	no ID	no ID		
P1	79	17	/	ACTB	P60709	Actin, beta	QTOF_133
				ACTG1	P63261	Actin, gamma 1	
P1	80	17	/	ACTB	P60709	Actin, beta	QTOF_094
				ACTG1	P63261	Actin, gamma 1	

Table S4 – continued

2D map	Spot #	Cluster #	ID level	Gene name	Accesion #	Protein description	MS file
P1	81	15	*	GNAQ	P50148	Guanine nucleotide binding protein (G protein), q polypeptide	QTOF_083
P1	82	17	$	IDH3A	P50213	Isocitrate dehydrogenase 3 (NAD+) alpha	QTOF_081
P1	83	4	*	SIRT2	Q8IXJ6	Sirtuin 2	QTOF_080
P1	84	33	$	APOD	P05090	Apolipoprotein D	QTOF_082
P1	85	34	$	TPM2	P07951	Tropomyosin 2 (beta)	QTOF_086
P1	86	34	$	TPM1	P09493	Tropomyosin 1 (alpha)	QTOF_085
P1	87	5	$	HNRNPC	P07910	Heterogeneous nuclear ribonucleoprotein C (C1/C2)	QTOF_088
P1	88	18	$	CRYM	Q14894	Crystallin, mu	QTOF_087
P1	89	33	*	LASP1	Q14847	LIM and SH3 protein 1	QTOF_079
P1	90	18	/	HNRPDL	O14979	Heterogeneous nuclear ribonucleoprotein D-like	QTOF_078
				PHYHIP	Q92561	Phytanoyl-CoA 2-hydroxylase interacting protein	
P1	91	13	*	LASP1	Q14847	LIM and SH3 protein 1	QTOF_140
P1	92	17	X	no ID	no ID		
P1	93	18	$	GAPDH	P04406	Glyceraldehyde-3-phosphate dehydrogenase	QTOF_077
P1	94	30	X	no ID	no ID		
P1	95	22	$	YWHAE	P62258	Tyrosine 3-monooxygenase/tryptophan 5-monooxygenase activation protein, epsilon polypeptide	QTOF_084
P1	96	22	/	YWHAZ	P63104	Tyrosine 3-monooxygenase/tryptophan 5-monooxygenase activation protein, zeta polypeptide	QTOF_068
				YWHAB	P31946	Tyrosine 3-monooxygenase/tryptophan 5-monooxygenase activation protein, beta polypeptide	
P1	97	19	$	SNAP25	P60880	Synaptosomal-associated protein, 25kDa	QTOF_069
P1	98	27	*	CA1	P00915	Carbonic anhydrase I	
P1	99	27	*	CA1	P00915	Carbonic anhydrase I	
P1	100	27	*	CA1	P00915	Carbonic anhydrase I	
P1	101	28	*	CA2	P00918	Carbonic anhydrase II	QTOF_076
P1	102	28	*	CA2	P00918	Carbonic anhydrase II	
P1	103	4	$	TPPP	O94811	Tubulin polymerization promoting protein	QTOF_074
P1	104	22	*	PCMT1	P22061	Protein-L-isoaspartate (D-aspartate) O-methyltransferase	QTOF_075
P1	105	31	X	no ID	no ID		

Table S4 – continued

2D map	Spot #	Cluster #	ID level	Gene name	Accession	Protein description	MS file
P1	106	23	*	PRDX2	P32119	Peroxiredoxin 2	
P1	107	18	$	PRDX2	P32119	Peroxiredoxin 2	QTOF_070
P1	108	4	*	CRYAB	P02511	Crystallin, alpha B	
P1	109	18	$	STMN1	P16949	Stathmin 1/oncoprotein 18	QTOF_139
P1	110	15	*	ARF3	P61204	ADP-ribosylation factor 3	QTOF_072
P1	111	19	*	ARF3	P61204	ADP-ribosylation factor 3	
P1	112	13	X	no ID	no ID		
P1	113	21	$	PRDX5	P30044	Peroxiredoxin 5	QTOF_073
P1	114	28	*	FABP5	Q01469	Fatty acid binding protein 5 (psoriasis-associated)	QTOF_071
P2	1	21	*	CTNNA2	P26232	Catenin (cadherin-associated protein), alpha 2	QTOF_108
P2	2	22	*	OGDHL	Q9ULD0	Oxoglutarate dehydrogenase-like	
P2	3	4	$	NEFL	P07196	Neurofilament, light polypeptide 68kDa	QTOF_113
P2	4	13	/	NSF	P46459	N-ethylmaleimide-sensitive factor	QTOF_109
				STXBP1	P61764	Syntaxin binding protein 1	
P2	5	24	*	ALB	P02768	Albumin	QTOF_131
P2	6	24	*	ALB	P02768	Albumin	
P2	7	21	*	ALB	P02768	Albumin	
P2	8	21	$	ALB	P02768	Albumin	QTOF_127
P2	9	21	*	ALB	P02768	Albumin	
P2	10	21	*	ALB	P02768	Albumin	
P2	11	18	*	GDI1	P31150	GDP dissociation inhibitor 1	
P2	12	18	*	GDI1	P31150	GDP dissociation inhibitor 1	QTOF_115
P2	13	18	*	GDI1	P31150	GDP dissociation inhibitor 1	QTOF_114
P2	14	22	$	SYN2	Q92777	Synapsin II	QTOF_112
P2	15	18	/	PKM2	P14618	Pyruvate kinase, muscle	QTOF_111
				ALDH4A1	P30038	Aldehyde dehydrogenase 4 family, member A1	
P2	16	11	$	SYN2	Q92777	Synapsin II	QTOF_110
P2	17	5	*	TUBA1A	Q71U36	Tubulin, alpha 1a	
P2	18	13	/	TUBA1A	Q71U36	Tubulin, alpha 1a	XCT_074
				TUBA1B	P68363	Tubulin, alpha 1b	

Table S4 – continued

2D map	Spot #	Cluster #	ID level	Gene name	Accesion #	Protein description	MS file
P2	19	11	*	TUBA1A	Q71U36	Tubulin, alpha 1a	
P2	20	11	/	TUBA1A	Q71U36	Tubulin, alpha 1a	QTOF_124
				TUBA1C	Q9BQE3	Tubulin, alpha 1c	
P2	21	11	*	TUBA1A	Q71U36	Tubulin, alpha 1a	
P2	22	11	*	TUBA1A	Q71U36	Tubulin, alpha 1a	
P2	23	13	*	GFAP	P14136	Glial fibrillary acidic protein	XCT_077
P2	24	13	*	GFAP	P14136	Glial fibrillary acidic protein	
P2	25	32	*	GFAP	P14136	Glial fibrillary acidic protein	
P2	26	32	*	GFAP	P14136	Glial fibrillary acidic protein	XCT_075
P2	27	32	$	GFAP	P14136	Glial fibrillary acidic protein	XCT_076
P2	28	32	*	GFAP	P14136	Glial fibrillary acidic protein	
P2	29	13	$	GNAO1	P09471	Guanine nucleotide binding protein (G protein), alpha activating activity polypeptide O	QTOF_129
P2	30	1	$	GNAO1	P09471	Guanine nucleotide binding protein (G protein), alpha activating activity polypeptide O	QTOF_130
P2	31	13	*	VDAC1	P21796	Voltage-dependent anion channel 1	QTOF_116
P2	32	11	*	VDAC2	P45880	Voltage-dependent anion channel 2	QTOF_117
P2	33	27	*	CA1	P00915	Carbonic anhydrase I	
P2	34	27	$	CA1	P00915	Carbonic anhydrase I	QTOF_126
P2	35	28	*	CA1	P00915	Carbonic anhydrase I	
P2	36	28	$	CA2	P00918	Carbonic anhydrase II	XCT_079
P2	37	4	*	QDPR	P09417	Quinoid dihydropteridine reductase	QTOF_125
P2	38	28	X	no ID	no ID		
P2	39	19	$	SNAP25	P60880	Synaptosomal-associated protein, 25kDa	QTOF_118
P2	40	19	$	SNAP25	P60880	Synaptosomal-associated protein, 25kDa	QTOF_119
P2	41	2	X	no ID	no ID		
P2	42	2	$	CRYAB	P02511	Crystallin, alpha B	QTOF_122
P2	43	2	$	CRYAB	P02511	Crystallin, alpha B	XCT_078
P2	44	21	/	ARF3	P61204	ADP-ribosylation factor 3	XCT_073
				ARF1	P84077	ADP-ribosylation factor 1	

Table S4 – continued

2D map	Spot #	Cluster #	ID level	Gene name	Accesion #	Protein description	MS file
P2	45	15	*	ARF3	P61204	ADP-ribosylation factor 3	XCT_072
P2	46	15	$	CFL1	P23528	Cofilin 1 (non-muscle)	QTOF_121
P2	47	18	$	CFL1	P23528	Cofilin 1 (non-muscle)	QTOF_123
P2	48	23	*	SOD1	P00441	Superoxide dismutase 1, soluble (amyotrophic lateral sclerosis 1 (adult))	QTOF_120

ID levels: $ - Identification, * - Attribution, / - Ambiguous, X - unidentified, see appendix definitions for details

Table S5 – Spots of Interest Mascot Search Information

MS file	2D map	spot #	ID level	Gene assigned	Gene MS found	Accession #	unique pep'	% covrage	Mowse score
QTOF_001	P1	1	$	NEFM	NEFM	P07197	4	5	185
QTOF_002	P1	9	*	FGG	FGG	P02679	3	10	60
QTOF_003	P1	11	*	FGG	FGG	P02679	6	17	228
QTOF_004	CytA	220	$	PRDX2	PRDX2	P32119	2	9	63
QTOF_005	CytB	119	$	RAP1GDS1	RAP1GDS1	P52306	5	7	137
QTOF_006	CytA	162	$	ENO1	ENO1	P06733	7	19	173
QTOF_007	CytB	189	*	ANXA1	AKR7A2	O43488	5	12	257
					ANXA1	P04083	6	20	255
					MDH1	P40925	3	11	119
QTOF_008	CytB	234	*	FABP5	HBB	P68871	5	36	113
					FABP5	Q01469	1	6	52
QTOF_009	CytB	233	$	UBE2N	UBE2N	P61088	5	27	172
QTOF_010	CytA	232	*	PPP3R1	PPP3R1	P63098	3	22	75
					SNCA	P37840	2	25	50
QTOF_011	CytB	208	*	QDPR	QDPR	P09417	5	35	251
					HBB	P68871	3	21	50
QTOF_012	CytB	212	$	GSTM2	GSTM2	P28161	7	33	227
QTOF_013	CytB	206	*	HBA	HBA	P69905	2	14	57
					NIPSNAP2	O075323	2	4	34
QTOF_014	CytA	188	$	GOT2	GOT2	P00505	5	14	227
QTOF_015	CytA	163	*	PSMC6	CKMT1B	P12532	4	12	171
					PSMC6	P62333	5	16	116
					IDH2	P48735	2	6	69
QTOF_016	CytA	229	$	ARF3	ARF3	P61204	6	33	179
QTOF_017	CytB	182	/	ALDOC / PHYHIPL	ALDOC	P09972	5	21	176
					PHYHIPL	Q96FC7	4	9	60
QTOF_018	CytB	181	$	PPP2R4	PPP2R4	Q15257	2	6	34
QTOF_019	CytB	180	$	CAPG	CAPG	P40121	3	10	69
QTOF_020	CytA	161	/	EEF1G / ENO1	EEF1G	P26641	4	10	167
					ENO1	P06733	4	14	143

Table S5 – continued

MS file	2D map	spot #	ID level	Gene assigned	Gene MS found	Accession #	unique pep'	% covrage	Mowse score
QTOF_021	CytA	140	*	ALDH1A1	GLUD1 or GLUD2	P00367 or P49448	2	3	77
					ALDH1A1	P00352	4	10	66
QTOF_022	CytB	192	$	ANXA2	ANXA2	P07355	9	30	360
QTOF_023	CytA	190	$	GAPDH	GAPDH	P04406	4	17	87
QTOF_024	CytA	142	*	PKM2	PKM2	P14618	4	9	132
					FARSA	Q9Y285	3	7	101
					UGP2	Q16851	3	6	55
QTOF_025	CytA	185	$	CRYM	CRYM	Q14894	4	17	127
QTOF_026	CytB	24	$	MAP2	MAP2	P11137	3	2	124
QTOF_027	CytB	26	$	USP5	USP5	P45974	4	5	162
QTOF_028	CytA	42	*	A1BG	A1BG	P04217	3	6	81
					TUBA1C or TUBA1A or TUBA1B	Q9BQE3 or Q71U36 or P68363	3	7	56
QTOF_029	CytB	50	$	DNM1	DNM1	Q05193	11	13	382
QTOF_030	CytB	38	*	DNM1	DNM1	Q05193	18	21	576
					ACO1	P21399	5	5	105
					PYGB	P11216	4	5	89
QTOF_031	CytA	41	/	PYGB / ACO1	PYGB	P11216	9	11	233
					ACO1	P21399	9	12	187
QTOF_032	CytA	14	$	CLTC	CLTC	Q00610	5	3	51
QTOF_033	CytA	40	*	DNM1	DNM1	Q05193	8	9	228
					EEF2	P13639	5	5	91
QTOF_034	CytA	39	*	DNM1	DNM1	Q05193	11	13	316
					EEF2	P13639	4	4	83
QTOF_035	CytA	3	*	HSPH1	HSPH1	Q92598	6	8	171
					UBA1	P22314	4	5	95
					PSMD1	Q99460	4	4	70
QTOF_036	CytB	27	$	ALDH1L1	ALDA1L1	O75891	10	12	237
QTOF_037	CytA	4	$	PLCB1	PLCB1	Q9NQ66	10	8	169

Table S5 – continued

MS file	2D map	spot #	ID level	Gene assigned	Gene MS found	Accession #	unique pep'	% covrage	Mowse score
QTOF_038	CytB	28	*	KIF5C	CAND1	Q86VP6	4	4	132
					KIF5C	O60282	7	8	119
QTOF_039	CytA	6	$	A2M	A2M	P01023	14	12	340
QTOF_040	CytA	11	$	ALB	ALB	P02768	5	8	131
QTOF_041	CytA	45	$	LRSAM1	LRSAM1	Q6UWE0	5	8	50
QTOF_042	CytA	171	$	GFAP	GFAP	P14136	2	4	51
QTOF_043	CytA	173	$	GFAP	GFAP	P14136	3	9	170
					ACTB or ACTG1	P60709 or P63261	2	5	47
QTOF_044	CytA	174	*	CKB	CKB	P12277	4	11	102
					ACTB or ACTG1	P60709 or P63261	3	9	100
					GFAP	P14136	3	9	91
QTOF_045	CytB	139	$	ALDH2	ALDH2	P05091	7	17	240
QTOF_046	CytB	176	*	HP	HP	P00738	4	10	127
					SH3GL2	Q99963	2	6	127
QTOF_047	CytB	150	$	GFAP	GFAP	P14136	7	21	392
					RNH1	P13489	3	8	164
					CDC37	Q16543	3	11	142
QTOF_048	CytA	106	$	PKM2	PKM2	P14618	9	22	287
QTOF_049	CytB	69	$	TF	TF	P02787	8	12	202
QTOF_050	CytA	156	$	ACTR3	ACTR3	P61158	5	13	80
QTOF_051	CytA	129	*	CRMP1	CRMP1	Q14194	11	23	587
					YARS	P54577	7	12	213
					DPYSL4	O14531	4	7	143
					DPYS	Q14117	3	6	104
QTOF_052	CytA	175	/	MPI / PPME1	MPI	P34943	5	12	161
					PPME1	Q9Y570	3	6	111
QTOF_053	CytA	187	$	GNAO1	GNAO1	P09471	6	21	215
QTOF_054	CytB	55	/	PRER / DPYSL2	PRER	P48147	13	23	445
					DPYSL2	Q16555	8	17	167
					NCDN	Q9UBB6	4	8	87

Table S5 – continued

MS file	2D map	spot #	ID level	Gene assigned	Gene MS found	Accession #	unique pep'	% covrage	Mowse score
QTOF_055	CytA	88	*	DPYSL2	DPYSL2	Q16555	12	29	244
					RNPEP	Q9H4A4	4	6	91
QTOF_056	CytB	72	/	ANXA6 / HSPA2	ANXA6	P08133	15	21	345
					HSPA2	P54652	9	20	321
					DPYSL2	Q16555	4	7	80
QTOF_057	CytA	124	$	DPYSL2	DPYSL2	Q16555	12	26	397
QTOF_058	CytB	120	*	CCT5	CCT5	P48643	12	24	481
					PPP3CA	Q08209	6	12	170
					CCT8	P50990	5	9	110
					PPP3CB	P16298	5	11	95
QTOF_059	CytA	114	/	RAD23B / VCAN	RAD23B	P54727	3	8	90
					VCAN	P13611	3	0	48
QTOF_060	CytA	109	/	CALR / SYT1	CALR	P27797	5	11	188
					SYT1	P21579	2	5	64
QTOF_061	CytA	136	*	RAP1GDS1	RAP1GDS1	P52306	8	15	355
					RUFY3	Q7L099	3	7	106
					CAP2	P40123	3	7	71
QTOF_062	CytB	127	$	DPYSL4	DPYSL4	O14531	10	20	402
QTOF_063	CytB	108	/	DPYSL5 / CRMP1	DPYSL5	Q9BPU6	9	17	197
					CRMP1	Q14194	7	14	196
					DPYSL4	O14531	3	6	58
QTOF_064	CytB	56	/	DPYSL2 / HSPA12A	DPYSL2	Q16555	10	23	424
					HSPA12A	O43301	10	20	313
QTOF_065	CytA	102	*	STXBP1	STXBP1	P61764	8	13	246
					DPYSL2	Q16555	3	5	37
QTOF_066	CytB	49	*	DNM1	DNM1	Q05193	13	17	436
					PDCD6IP	Q8WUM4	9	11	256
QTOF_067	CytA	215	*	BLVRB	BLVRB	P30043	1	7	62
QTOF_068	P1	96	/	YWHAZ / YWHAB	YWHAZ	P63104	6	33	222
					YWHAB	P31946	4	19	153

Table S5 – continued

MS file	2D map	spot #	ID level	Gene assigned	Gene MS found	Accession #	unique pep'	% covrage	Mowse score
QTOF_069	P1	97	$	SNAP25	SNAP25	P60880	5	31	214
QTOF_070	P1	107	$	PRDX2	PRDX2	P32119	4	22	164
QTOF_071	P1	114	*	FABP5	FABP5	Q01469	1	6	47
QTOF_072	P1	110	*	ARF3	ARF3 or ARF1	P61204 or P84077	4	27	182
					CFL1	P23528	3	22	105
QTOF_073	P1	113	$	PRDX5	PRDX5	P30044	5	28	209
QTOF_074	P1	103	$	TPPP	TPPP	O94811	2	12	146
QTOF_075	P1	104	*	PCMT1	PCMT1	P22061	1	4	46
QTOF_076	P1	101	*	CA2	CA2	P00918	1	3	32
QTOF_077	P1	93	$	GAPDH	GAPDH	P04406	3	12	104
QTOF_078	P1	90	/	HNRPDL / PHYHIP	HNRPDL	O14979	5	11	156
					PHYHIP	Q92561	2	5	63
QTOF_079	P1	89	*	LASP1	LASP1	Q14847	1	4	35
QTOF_080	P1	83	*	SIRT2	SIRT2	Q8IXJ6	7	23	310
					IDH3A	P50213	5	15	133
					GNB5	O14775	3	7	40
QTOF_081	P1	82	$	IDH3A	IDH3A	P50213	2	6	77
QTOF_082	P1	84	$	APOD	APOD	P05090	2	12	50
QTOF_083	P1	81	*	GNAQ	GNAQ	P50148	7	20	215
					GNAO1	P09471	3	8	39
QTOF_084	P1	95	$	YWHAE	YWHAE	P62258	6	26	215
QTOF_085	P1	86	$	TPM1	TPM1	P09493	5	10	143
QTOF_086	P1	85	$	TPM2	TPM2	P07951	4	7	127
QTOF_087	P1	88	$	CRYM	CRYM	Q14894	6	25	270
QTOF_088	P1	87	$	HNRNPC	HNRNPC	P07910	2	6	74
QTOF_089	P1	71	$	TMOD2	TMOD2	Q9NZR1	5	16	118
QTOF_090	P1	66	$	GFAP	GFAP	P14136	7	20	341
QTOF_091	P1	29	$	SYN1	SYN1	P17600	9	23	292
QTOF_092	P1	39	*	INA	INA	Q16352	13	29	559
					HASPD1	P10809	9	22	205

Table S5 – continued

MS file	2D map	spot #	ID level	Gene assigned	Gene MS found	Accession #	unique pep'	% covrage	Mowse score
QTOF_093	P1	38	*	GDI1	HSPD1	P10809	9	25	231
					GDI1	P31150	8	26	210
					INA	Q16352	7	16	210
					SYT1	P21579	3	8	108
QTOF_094	P1	80	/	ACTB or ACTG1	CKB	P12277	8	29	289
					ACTA2 or ACTG2 or ACTC1	P62736 or P63267 or P68032	8	27	240
					ACTB or ACTG1	P60709 or P63261	7	22	220
QTOF_095	P1	72	*	GFAP	GFAP	P14136	7	21	265
					ACTB	P60709	4	14	92
					CKB	P12277	3	9	76
QTOF_096	P1	57	*	ALDH2	ALDH2	P05091	8	22	306
					SEPT8	Q92599	6	15	196
					DLST	P36957	6	13	192
					SELENBP1	Q13228	5	10	104
					CNDP2	Q96KP4	4	11	100
QTOF_097	P1	27	/	DPYSL2 / CCT3	DPYSL2	Q16555	17	44	694
					CCT3	P49368	5	10	115
QTOF_098	P1	43	$	SYN2	SYN2	Q92777	6	13	131
QTOF_099	P1	48	*	FGB	ATP5A1	P25705	6	13	217
					ALDH6A1	Q02252	6	15	169
					FGB	P02675	6	17	134
QTOF_100	P1	46	$	FGB	FGB	P02675	5	14	107
QTOF_101	P1	51	$	ATP5A1	ATP5A1	P25705	6	13	222
QTOF_102	P1	14	$	DNM1	DNM1	Q05193	7	8	211
QTOF_103	P1	3	*	UBA1	UBA1	P22314	13	18	534
QTOF_104	P1	26	$	DPYSL2	DPYSL2	Q16555	11	25	364
					HSPA12A	O43301	8	17	284
QTOF_105	P1	19	*	ALB	ALB	P02768	6	10	160
					DPYSL2	Q16555	3	5	90

Table S5 – continued

MS file	2D map	spot #	ID level	Gene assigned	Gene MS found	Accession	unique pep'	% covrage	Mowse score
QTOF_106	P1	63	$	GFAP	GFAP	P14136	9	26	431
QTOF_107	P1	17	$	NEFL	NEFL	P07196	11	26	548
QTOF_108	P2	1	*	CTNNA2	CTNNA2	P26232	12	17	419
					GANAB	Q14697	5	5	66
					HSPA4L	O95757	3	4	49
					CTNNB1	P35222	2	1	49
QTOF_109	P2	4	/	NSF / STXBP1	NSF	P46459	23	31	642
					STXBP	P61764	2	3	46
QTOF_110	P2	16	$	SYN2	SYN2	Q92777	5	10	88
QTOF_111	P2	15	/	PKM2 / ALDH4A1	PKM2	P14618	8	19	298
					ALDH4A1	P30038	5	11	139
QTOF_112	P2	14	$	SYN2	SYN2	Q92777	7	15	166
QTOF_113	P2	3	$	NEFL	NEFL	P07196	10	21	545
QTOF_114	P2	13	*	GDI1	GDI1	P31150	14	40	557
					TUBA1C	Q9BQE3	7	20	153
QTOF_115	P2	12	*	GDI1	GDI1	P31150	14	42	445
					PPP2R1A	P30153	7	15	189
QTOF_116	P2	31	*	VDAC1	VDAC1	P21796	12	53	443
					VDAC2	P45880	5	21	150
QTOF_117	P2	32	*	VDAC2	VDAC2	P45880	6	24	206
					VDAC1	P21796	3	15	112
QTOF_118	P2	39	$	SNAP25	SNAP25	P60880	3	21	121
QTOF_119	P2	40	$	SNAP25	SNAP25	P60880	3	21	141
QTOF_120	P2	48	*	SOD1	SOD1	P00441	1	9	37
QTOF_121	P2	46	$	CFL1	CFL1	P23528	2	15	66
QTOF_122	P2	42	$	CRYAB	CRYAB	P02511	2	10	60
QTOF_123	P2	47	$	CFL1	CFL1	P23528	5	43	201
QTOF_124	P2	20	/	TUBA1A / TUBA1C	TUBA1A	Q71U36	5	14	148
					TUBA1C	Q9BQE3	5	14	130

Table S5 – continued

MS file	2D map	spot #	ID level	Gene assigned	Gene MS found	Accession #	unique pep'	% covrage	Mowse score
QTOF_125	P2	37	*	QDPR	QDPR	P09417	6	40	159
					TUBA8	Q9NY65	2	6	84
					TUBA3E	Q6PEY2	2	6	61
QTOF_126	P2	34	$	CA1	CA1	P00915	4	25	137
					PGAM1	P18669	4	27	35
QTOF_127	P2	8	$	ALB	ALB	P02768	10	15	263
QTOF_128	P1	52	*	TUBA1A	TUBA1A or TUBA1B	Q71U36 or P68363	8	23	225
					TUBA4A	P68366	6	17	163
QTOF_129	P2	29	$	GNAO1	GNAO1	P09471	5	18	179
QTOF_130	P2	30	$	GNAO1	GNAO1	P09471	2	7	36
QTOF_131	P2	5	*	ALB	ALB	P02768	6	9	225
					DPYSL2	Q16555	5	10	150
QTOF_132	P1	42	$	CRMP1	CRMP1	Q14194	2	2	66
QTOF_133	P1	79	/	ACTB or ACTG1	ACTB or ACTG1	P60709 or P63261	4	14	151
					ACTA2 or ACTG2 or ACTC1 or ACTA1	P62736 or P63267 or P68032 or P68133	4	14	132
QTOF_134	P1	75	/	ACTB or ACTG1	ACTB or ACTG1	P60709 or P63261	2	6	38
QTOF_135	P1	40	/	HNRNPK / CPNE6	HNRNPK	P61978	3	10	106
					CPNE6	O95741	2	3	39
QTOF_136	P1	50	$	ATP5A1	ATP5A1	P25705	5	11	231
QTOF_137	P1	18	$	NEFL	NEFL	P07196	2	4	51
QTOF_138	P1	56	*	TUBA1A	TUBA1A or TUBA1B	Q71U36 or P68363	11	30	441
					TUBA4A	P68366	9	23	279
QTOF_139	P1	109	$	STMN1	STMN1	P16949	2	14	96
QTOF_140	P1	91	*	LASP1	LASP1	Q14847	2	10	44
					GAPDH	P04406	2	8	37
QTOF_141	P1	41	$	DSP	DSP	P15924	5	1	136
QTOF_142	CytA	199	*	CA1	CA1	P00915	1	3	35
QTOF_143	CytB	207	*	CA2	CA2	P00918	3	11	153
					HBB	P68871	3	23	139

Table S5 – continued

MS file	2D map	spot #	ID level	Gene assigned	Gene MS found	Accession #	unique pep'	% covrage	Mowse score
QTOF_144	CytB	235	$	HBB	HBB	P68871	3	23	127
QTOF_145	CytA	43	/	ATP6V1A / HSPA8	ATP6V1A	P38606	4	7	110
					HSPA8	P11142	2	3	101
QTOF_146	CytB	54	/	ATP6V1A / HSPA8	ATP6V1A	P38606	4	7	110
					HSPA8	P11142	2	3	101
					DPYSL2	Q16555	2	3	40
QTOF_147	CytA	93	$	DPYSL2	DPYSL2	Q16555	7	16	292
QTOF_148	CytA	89	/	DPYSL2 / ALB	DPYSL2	Q16555	9	21	315
					ALB	P02768	6	9	272
QTOF_149	CytA	130	$	DPYSL4	DPYSL4	O14531	2	3	46
QTOF_150	CytA	168	$	GFAP	GFAP	P14136	4	11	221
QTOF_151	CytB	57	/	DPYSL2 / ALB	DPYSL2	Q16555	10	22	380
					ALB	P02768	6	10	127
QTOF_152	P1	62	$	GFAP	GFAP	P14136	15	37	598
QTOF_153	P1	67	$	GFAP	GFAP	P14136	8	21	350
QTOF_154	P1	64	$	GFAP	GFAP	P14136	11	29	508
XCT_001	CytA	97	$	ALB	ALB	P02768	33	53	1208
XCT_002	CytB	118	$	SERPINA1	SERPINA1	P01009	19	52	915
XCT_003	CytA	201	*	CA1	CA1	P00915	6	29	344
					HBB	P68871	2	23	141
XCT_004	CytA	200	*	CA1	CA1	P00915	7	33	305
					HBB	P68871	3	23	132
XCT_005	CytA	216	$	BLVRB	BLVRB	P30043	4	23	230
XCT_006	CytB	213	$	APOA1	APOA1	P02647	7	23	233
XCT_007	CytB	214	$	APOA1	APOA1	P02647	5	19	252
XCT_008	CytA	217	*	TAGLN	TAGLN	Q01995	6	33	302
					AK1	P00568	3	16	164
XCT_009	CytA	218	*	TAGLN2	TAGLN2	P37802	2	11	134
					HBA	P69905	4	29	119
XCT_010	CytA	91	$	ALB	ALB	P02768	9	14	365

Table S5 – continued

MS file	2D map	spot #	ID level	Gene assigned	Gene MS found	Accession #	unique pep'	% covrage	Mowse score
XCT_011	CytB	134	*	CAT	CAT	P04040	13	26	639
					PKM2	P14618	5	10	197
					ALDH4A1	P30038	3	6	73
XCT_012	CytB	133	*	CAT	CAT	P04040	14	28	613
					ALDH4A1	P30038	6	12	296
					PKM2	P14618	6	13	264
XCT_013	CytB	227	$	STMN1	STMN1	P16949	3	22	117
XCT_014	CytB	154	$	GFAP	GFAP	P14136	18	46	894
					ACTB or ACTG1	P60709 or P63261	9	28	303
XCT_015	CytB	224	*	TAGLN	TAGLN	Q01995	1	5	66
XCT_016	CytA	76	$	ALB	ALB	P02768	5	8	248
XCT_017	CytA	1	$	SNAP91	SNAP91	O60641	8	9	433
XCT_018	CytB	193	$	ANXA5	ANXA5	P08758	11	35	482
XCT_019	CytA	183	$	TPM2	TPM2	P07951	3	11	165
XCT_020	CytA	221	*	APRT	APRT	P07741	3	17	153
					PRDX2	P32119	4	19	150
					RAB2A	P61019	2	12	74
XCT_021	CytA	105	$	DPYSL5	DPYSL5	Q9BPU6	9	22	271
XCT_022	CytB	32	$	VCL	VCL	P18206	10	9	436
XCT_023	CytA	18	*	ALB	ALB	P02468	7	11	269
					CLTC	Q00610	5	4	109
XCT_024	CytB	21	*	ALB	ALB	P02768	1	1	70
XCT_025	CytA	8	$	A2M	A2M	P01023	2	1	67
XCT_026	CytB	36	$	HK1	HK1	P19367	11	11	400
XCT_027	CytA	60	*	TF	TF	P02787	8	12	297
					NSF	P46459	2	3	96
XCT_028	CytA	65	*	NSF	NSF	P46459	4	5	173
					WASF1	Q92558	2	4	88
					TF	P02787	2	3	51
XCT_029	CytB	59	$	DNM1L	DNM1L	O00429	6	10	208

Table S5 – continued

MS file	2D map	spot #	ID level	Gene assigned	Gene MS found	Accession #	unique pep'	% covrage	Mowse score
XCT_030	CytA	13	$	HBA	HBA1	P69904	6	42	254
XCT_031	CytB	148	*	IGHG1	IGHG1	P01857	4	14	146
					IGHG3	P01860	4	10	108
XCT_032	CytA	228	*	ARF3	ARF3 or ARF1	P61204 or P84077	3	15	137
					CFL1	P23528	3	19	112
XCT_033	CytB	122	*	PPP3CA	PPP3CA	Q08209	7	14	268
					PPP3CB	P16298	5	11	179
					CCT8	P50990	5	9	149
XCT_034	CytA	159	$	ACTR3B	ACTR3B	Q9P1U1	6	15	261
XCT_035	CytA	170	$	GFAP	GFAP	P14136	5	14	349
					ASNA1	O43681	5	12	170
XCT_036	CytA	165	$	ORM1	ORM1	P02763	4	14	148
XCT_037	CytB	111	$	SERPINA3	SERPINA3	P01011	3	6	177
XCT_038	CytA	196	$	MAPRE3	MAPRE3	Q9UPY8	9	27	263
XCT_039	CytA	83	*	ALB	ALB	P02768	12	14	458
					IRGQ	Q8WZA9	5	9	202
					TUBB2B or TUBB2A	Q9BVA1 or Q13885	4	11	131
					TUBB8 or TUBB4A	Q3ZCM7 or P04350	3	7	82
					NRBP1	Q9UHY1	2	4	74
XCT_040	CytB	194	*	NAPA	NAPB	Q9H115	4	13	188
					APOE	P02649	3	14	171
					NAPA	P54920	3	11	99
XCT_041	CytB	25	$	HSP90B1	HSP90B1	P14625	11	15	580
XCT_042	CytA	2	/	CNTN1 / CP	CNTN1	Q12860	5	5	181
					CP	P00450	3	3	129
XCT_043	CytB	52	$	EZR	EZR	P15311	9	14	288
XCT_044	CytB	226	$	SNCA	SNCA	P37840	7	45	479
XCT_045	CytA	230	$	VAMP2	VAMP2	P63027	2	28	153
XCT_046	CytA	231	*	VAMP2	VAMP2 or VAMP3	P63027 or Q15836	1	14	103
XCT_047	CytA	219	$	PRDX2	PRDX2	P32119	4	23	222

Table S5 – continued

MS file	2D map	spot #	ID level	Gene assigned	Gene MS found	Accession #	unique pep'	% covrage	Mowse score
XCT_048	CytA	222	$	PRDX2	PRDX2	P32119	4	16	150
XCT_049	CytA	141	*	ANXA11	FGB	P02675	7	19	294
					ANXA11	P50995	6	12	255
XCT_050	CytB	210	$	BDH2	BDH2	Q9BUT1	4	20	219
XCT_051	CytA	143	*	PKM2	CCT7	Q99832	14	30	677
					PKM2	P14618	11	28	615
XCT_052	CytB	37	*	DNM1	DNM1	Q05193	7	7	335
					DLG3	Q92796	4	6	120
XCT_053	CytA	164	$	EEF1G	EEF1G	P26641	7	15	318
XCT_054	CytA	126	*	DPYSL2	DPYSL2	Q16555	9	20	299
					PPP3CB	P16298	5	12	299
					PPP3CA	Q08209	3	6	167
					PSMC1	P62191	3	10	155
XCT_055	CytA	186	$	GNAO1	GNAO1	P09471	7	24	371
XCT_056	CytB	167	$	NSFL1C	NSFL1C	Q9UNZ2	9	36	566
XCT_057	CytB	147	/	ALDH6A1 / IGHG1	ALDH6A1	Q02252	2	2	78
					IGHG1	P01857	3	11	76
XCT_058	CytB	146	$	ATP5A1	ATP5A1	P25705	8	17	455
XCT_059	CytB	145	$	ALDH6A1	ALDH6A1	Q02252	8	18	323
XCT_060	CytB	144	*	UGP2	UGP2	Q16851	9	20	366
					NAMPT	P43490	5	9	198
					DNPEP	P51649	3	7	115
XCT_061	CytA	157	$	ACTR3	ACTR3	P61158	8	20	335
XCT_062	CytB	138	*	GC	SELENBP1	Q13228	5	11	202
					GC	P02774	5	10	175
					CNDP2	Q96KP4	5	15	152
					HARS	P12081	5	9	148
XCT_063	CytB	137	*	GC	GC	P02774	5	10	208
					TUBA4A	P68366	5	9	194
XCT_064	CytB	211	$	TPPP	TPPP	O94811	3	16	205

Table S5 – continued

MS file	2D map	spot #	ID level	Gene assigned	Gene MS found	Accession #	unique pep'	% covrage	Mowse score
XCT_065	CytA	204	$	CDK5	CDK5	Q00535	8	28	277
XCT_066	CytB	177	*	HP	HP	P00738	7	18	345
					UBFD1	O14562	3	13	156
XCT_067	CytB	179	$	SERPINB9	SERPINB9	P50453	2	6	105
XCT_068	CytB	195	*	NAPB	NAPB	Q9H115	8	32	503
					NAPA	P54920	5	20	245
XCT_069	CytA	172	*	CKB	CKB	P12277	4	16	249
					SH3GL3	Q99963	4	14	231
					HP	P00738	5	11	209
					ACTB or ACTG1	P60709 or P63261	4	12	150
					ACTA2	P62736	5	17	125
					NDRG2	Q9UN36	2	6	110
					GFAP	P14136	2	5	102
XCT_070	CytB	128	$	DPYSL5	DPYSL5	Q9BPU6	13	28	474
XCT_071	CytB	29	$	KIF5C	KIF5C	O60282	13	16	641
XCT_072	P2	45	*	ARF3	ARF3 or ARF1	P61204 or P84077	6	35	324
					CFL1	P23528	2	15	90
					ARF4	P18085	2	14	89
XCT_073	P2	44	/	ARF3 or ARF1	ARF3 or ARF1	P61204 or P84077	4	26	227
					ARPC5L	Q9BPX5	3	21	164
XCT_074	P2	18	/	TUBA1A / TUBA1B	TUBA1A	Q71U36	12	35	697
					TUBA1B	P68363	12	35	657
					TUBA4A	P68366	11	31	532
XCT_075	P2	26	*	GFAP	GFAP	P14136	10	25	482
					TUBA1B	P68363	5	18	235
					TUBA4A	P68366	4	16	174
					ALB	P02768	3	4	113
XCT_076	P2	27	$	GFAP	GFAP	P14136	8	20	471
XCT_077	P2	23	*	GFAP	GFAP	P14136	20	55	1057
					ACTG	P63261	7	24	329

MS file	2D map	spot #	ID level	Gene assigned	Gene MS found	Accession #	unique pep'	% covrage	Mowse score
XCT_078	P2	43	$	CRYAB	CRYAB	P02511	4	22	189
XCT_079	P2	36	$	CA2	CA2	P00918	6	22	227
XCT_080	CytB	153	$	GFAP	GFAP	P14136	19	46	846
					ACTB or ACTG1	P60709 or P63261	8	25	249

ID levels: $ - Identification, * - Attribution, / - Ambiguous, X - unidentified, see appendix definitions for details

Table S5 – continued

Table S6 – MS information for protein identified by a single peptide (OHW)

Gene	Note	Accession	MS file	m/z meas.	z	Δ m/z [ppm]	Score	Sequence	Modifications	expected MW/pI
FABP5	* †	Q01469	QTOF_008	464.2837	2	-2.16	52.2	K.ELGVGIALR.K		15.8/6.6
BLVRB	* †	P30043	QTOF_067	756.9396	2	-1.66	62.4	K.TVAGQDAVIVLLGTR.N		22.3/7.1
FABP5	* †	Q01469	QTOF_071	464.2852	2	1.06	47.4	K.ELGVGIALR.K		15.8/6.6
PCMT1	*	P22061	QTOF_075	598.8040	2	2.31	46.2	K.VFEVMLATDR.S	Oxidation: 5	24.9/6.7
CA2	* †	P00918	QTOF_076	494.2900	2	0.72	32.4	K.VVDVLDSIK.T		29.3/6.8
LASP1	* †	Q14847	QTOF_079	709.8690	2	2.35	35	K.GFSVVADTPELQR.I		30.4/6.6
SOD1	*	P00441	QTOF_120	751.3895	2	4.74	37.5	K.GDGPVQGIINFEQK.E		16.3/5.7
CA1	* †	P00915	QTOF_142	485.7981	2	-4.37	34.8	K.VLDALQAIK.T		29.0/6.6
TAGLN	†	Q01995	XCT_015	610.7700	2	-130.3	67.6	R.TLMALGSLAVTK.N	Oxidation: 3	22.7/8.9
ALB	†	P02768	XCT_024	679.7400	2	-115.45	69.6	K.AVMDDFAAFVEK.C	Oxidation: 3	73.0/5.9
VAMP2 or VAMP3	†	P63027 or Q15836	XCT_046	834.5200	2	153.88	104.8	R.ADALQAGASQFETSAAK.L	Deamidated: 5, 10	12.8/7.9

Note: ID further information - (*) indicate matching observed and expected 2D-PAGE MW/pI. (†) indicate identification of 2D-PAGE proximal spot as the same protein.

FABP5, Q01469, QTOF_008

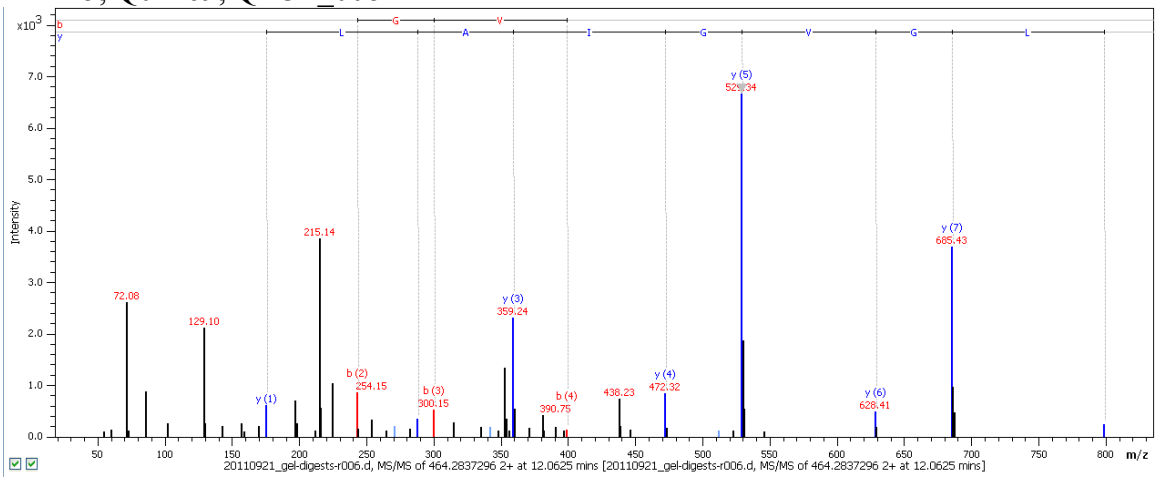

BLVRB, P30043, QTOF_067

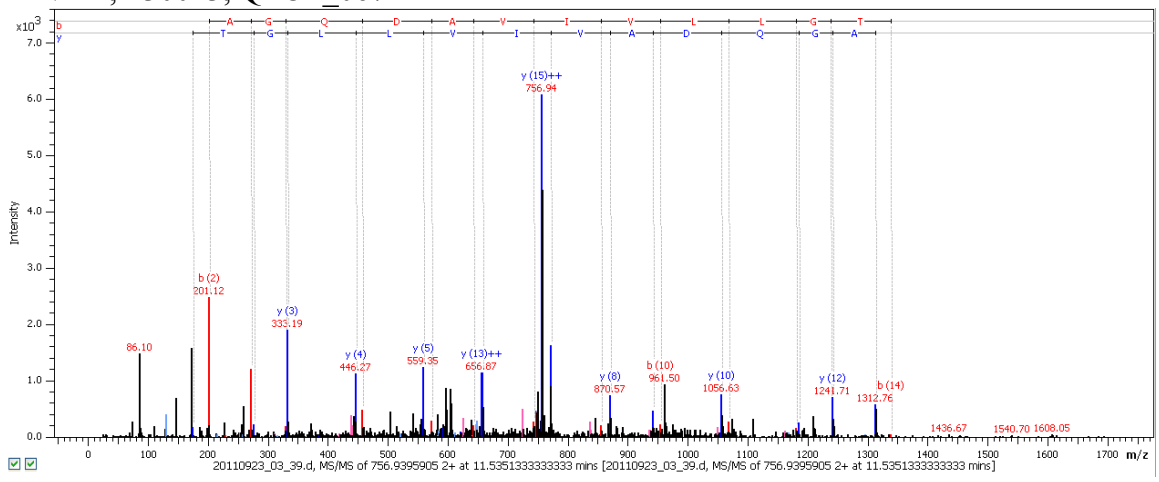

FABP5, Q01469, QTOF_071

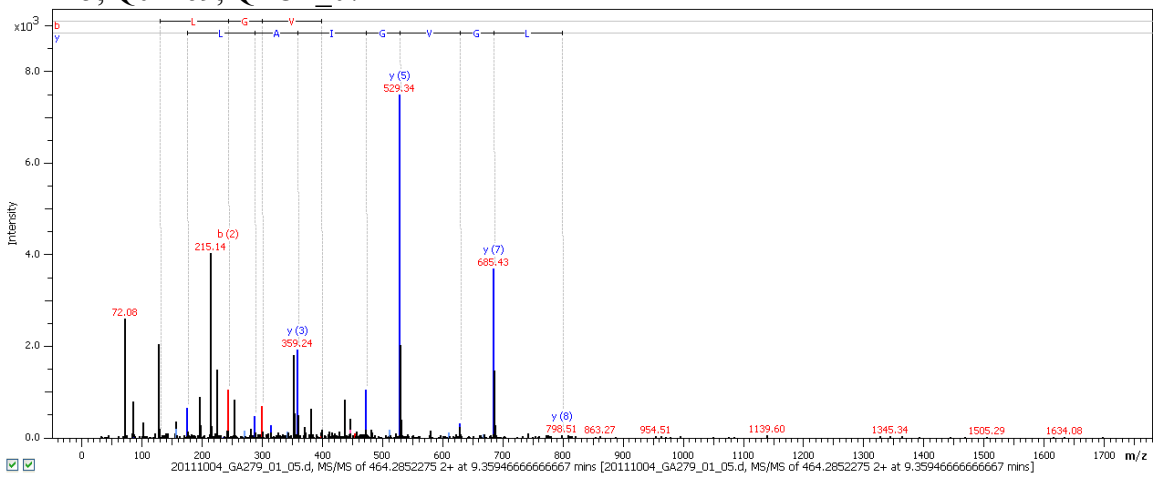

PCMT1, P22061, QTOF_075

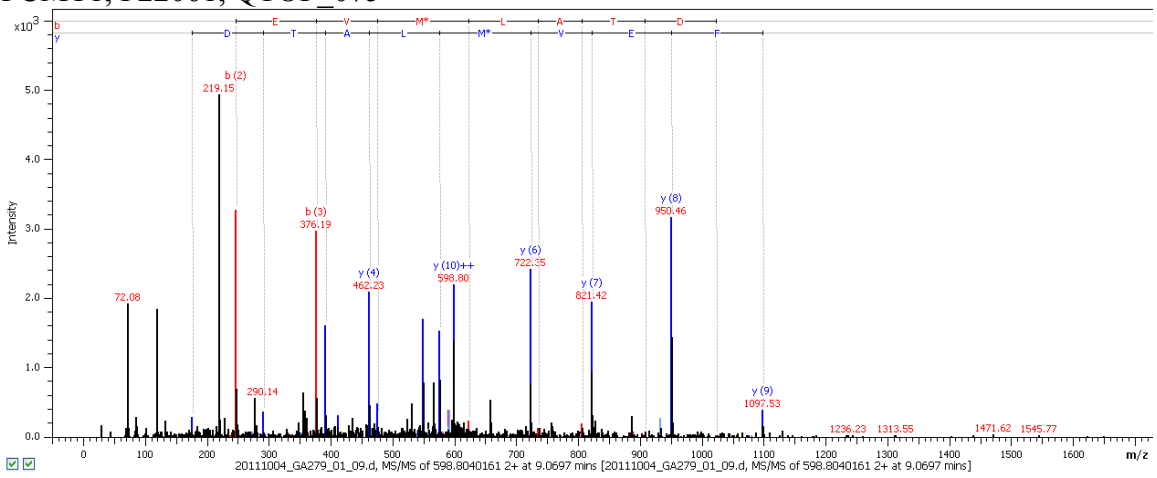

CA2, P00918, QTOF_076

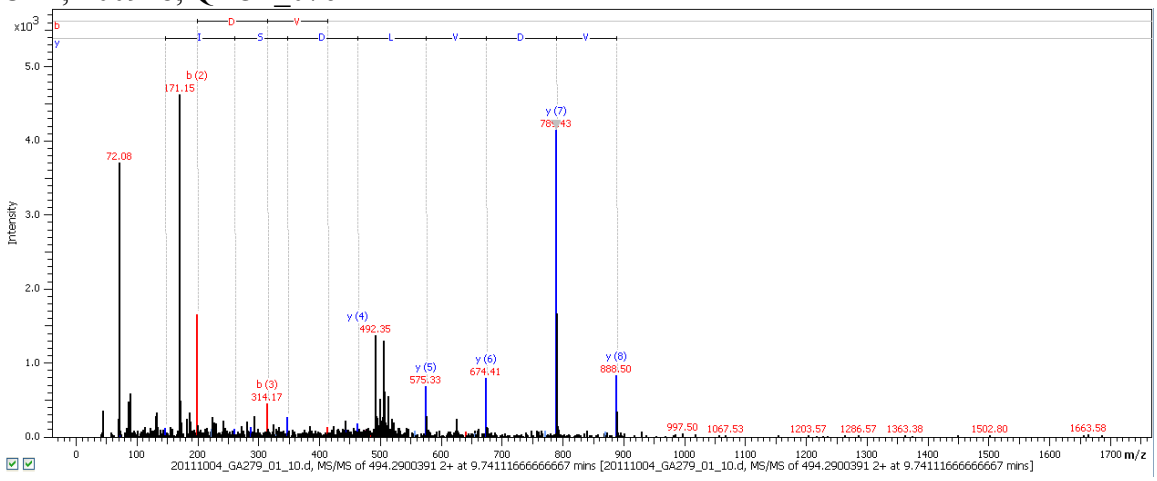

LASP1, Q14847, QTOF_079

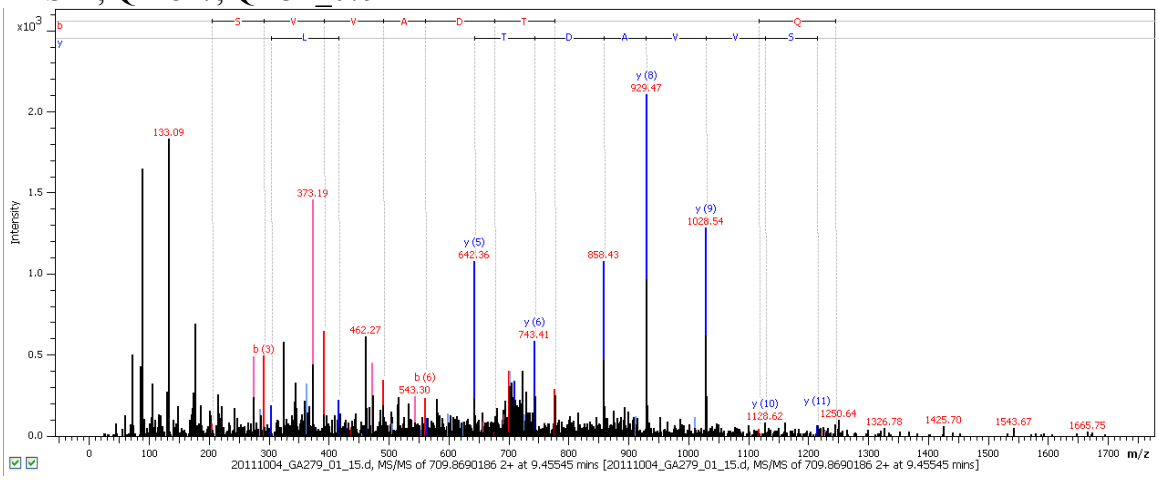

SOD1, P00441, QTOF_120

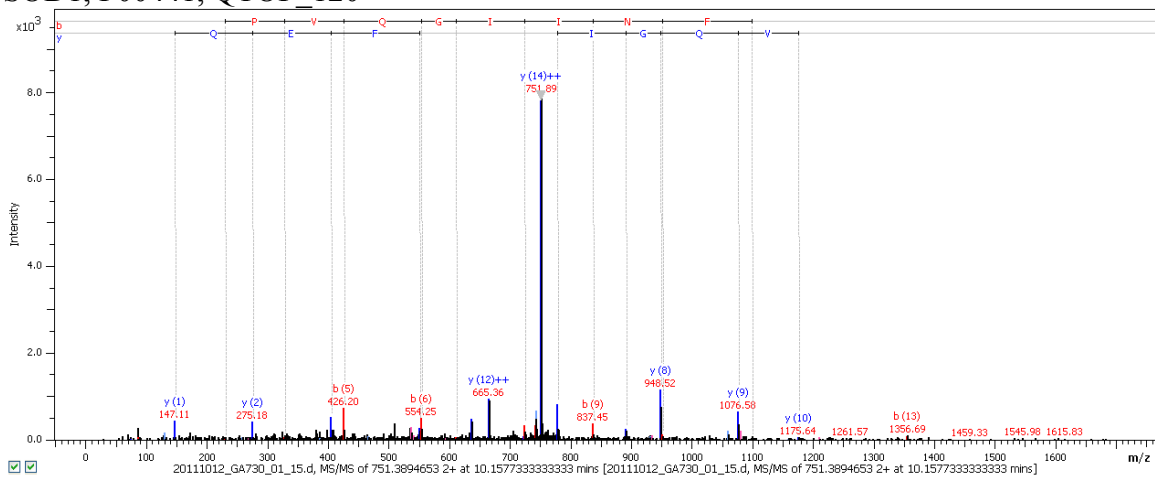

CA1, P00915, QTOF_142

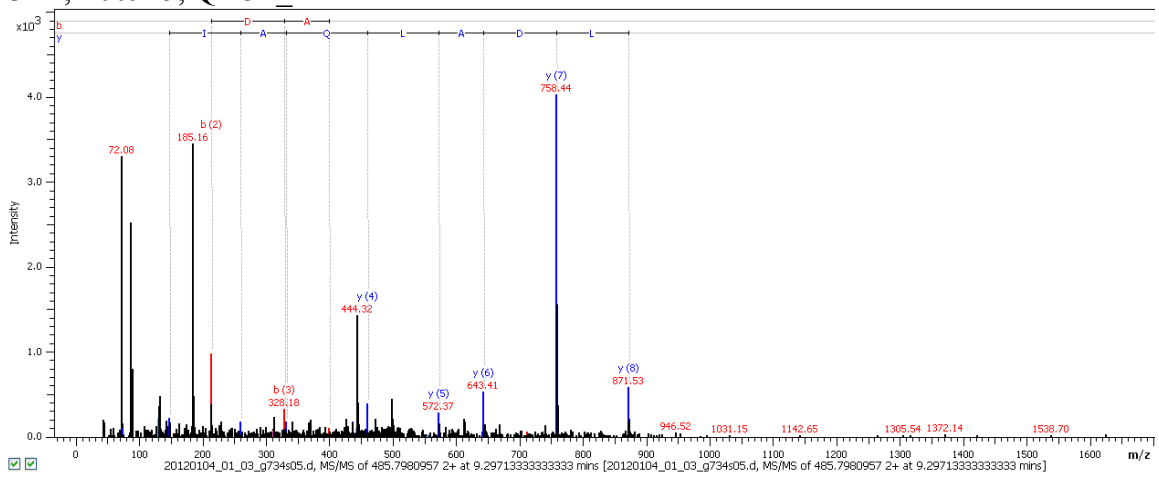

TAGLN, Q01995, XCT_015

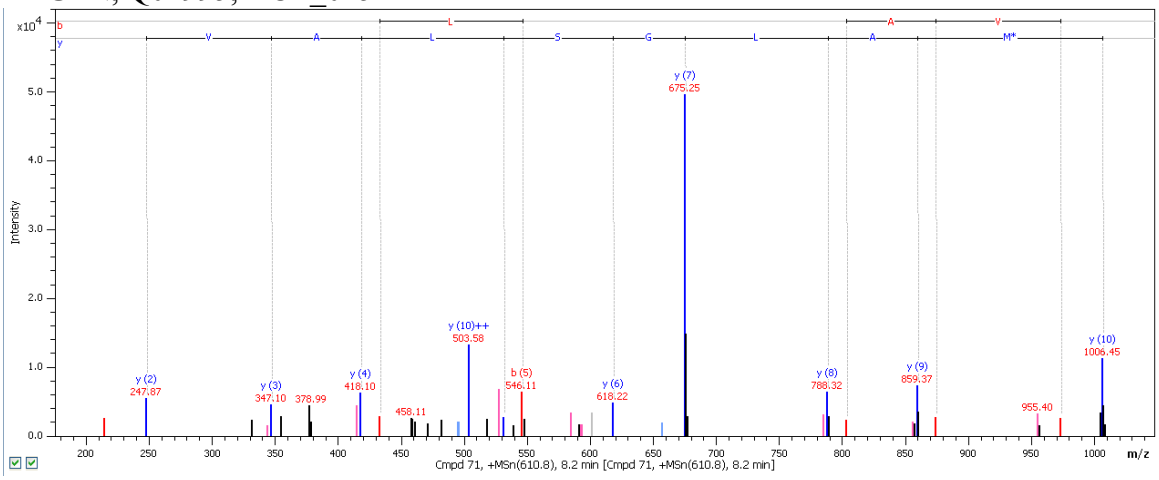

ALB, P02768, XCT_024

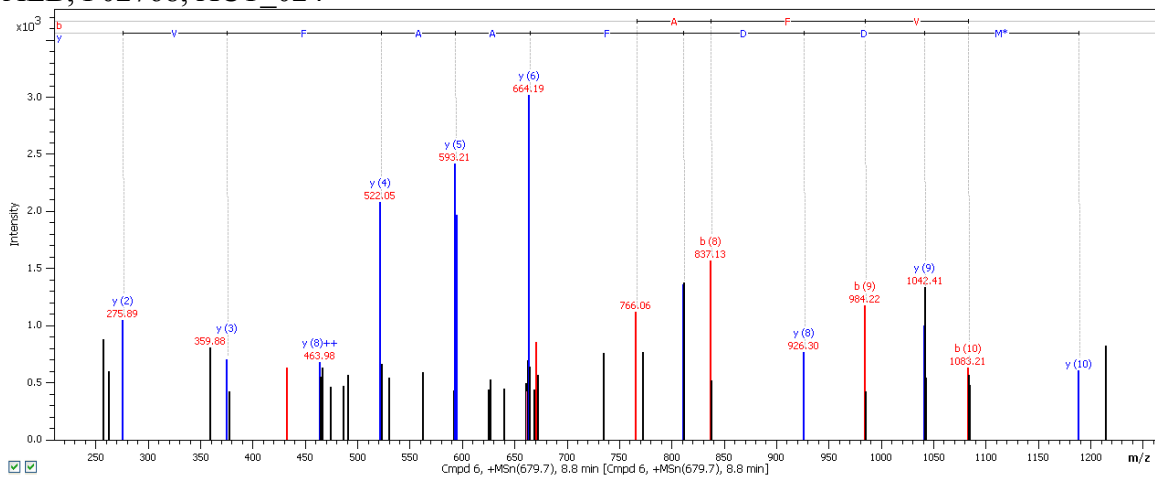

VAMP2 or VAMP3, P63027 or Q15836, XCT_046